School of Medicine
Oregon Health & Science University

CERTIFICATE OF APPROVAL

This is to certify that the Ph.D. dissertation of

Clare J. Wilhelm

has been approved

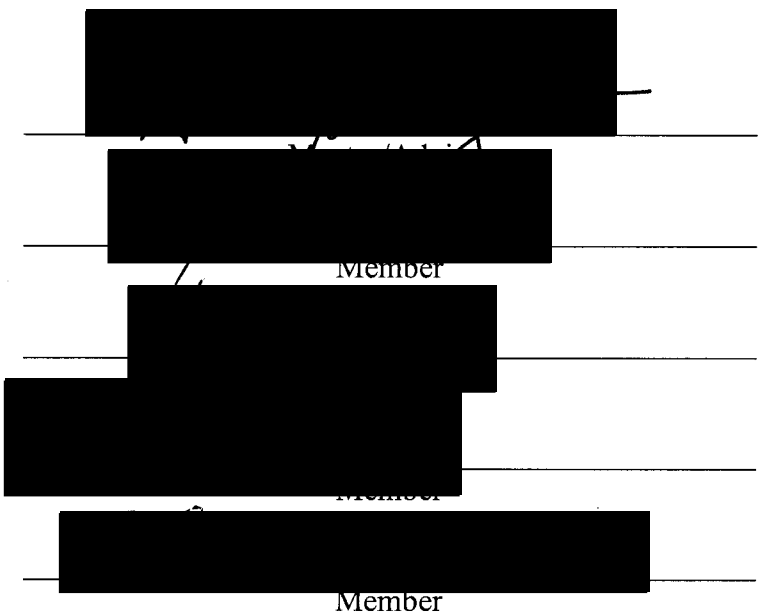

Member

Member

Methamphetamine-induced disruption of dopamine homeostasis: the ins and outs of transport

by

Clare Jon Wilhelm

A DISSERTATION

Presented to the Department of Physiology and Pharmacology
And Oregon Health & Science University
School of Medicine
In partial fulfillment of
The requirements of the degree of
Doctor of Philosophy
February 2006

Table of Contents

LIST OF FIGURES AND TABLES

ABBREVIATIONS

AMPH	Amphetamine
ANOVA	Analysis of Variance
B_{max}	Maximal number of binding sites
DA	Dopamine
DAT	Dopamine transporter
DHTB	Dihydrotetrabenazine
DMEM	Dulbecco's modified Eagle's medium
DMSO	Dimethylsulfoxide
GPCR	G protein-coupled receptor
HEK	Human embryonic kidney cells
HEPES	4-(2-hydroxyethyl)-1-piperazineethanesulfonic acid
IC_{50}	Half-maximal inhibitory concentration
K_d	Equilibrium dissociation constant
K_m	Michaelis-Menten constant (dissociation constant)
MDMA	Methylenedioxymethamphetamine
METH	Methamphetamine
MSR	Macrophage scavenger receptor
RTI-55	3β-(4-iodophenyl)tropane-2β-carboxylic acid methyl ester
SNARF	5-and 6-carboxyseminapthorhodofluor-1 acetoxymethyl ester
VMAT2	Vesicular monoamine transporter-2
V_{max}	Maximal rate of transport

ACKNOWLEDGEMENTS

I would like to thank my mentor, Aaron Janowsky, for his time, our always fruitful discussions and for giving me the opportunity to work for him.

Thank you to my committee members: Charles Allen, Paul Berger, Amy Eshleman and Kim Neve.

Thank you to the members of the Janowsky/Neve labs, for providing me with an enjoyable atmosphere to work and study. Thank you to Robert Johnson, for taking the brunt of my frustration.

Finally, a special thank you to my wife Laura, and my boys Jacob and Noah.

I dedicate this thesis to my family, Laura, Jake and Noah, because this would mean nothing without them.

Abstract

The psychostimulant and drug of abuse methamphetamine (METH) disrupts dopamine (DA) homeostasis through a number of distinct and related mechanisms. The cell surface DA transporter (DAT) is responsible for reuptake of DA. METH is also transported by the DAT and competes directly with DA for reuptake. Studies by Sonders et al. (1997) demonstrate that METH is a substrate and is thus actively accumulated by the DAT. In addition, METH causes reversal of transport by the DAT through a mechanism consistent with facilitated exchange (one METH molecule transported in exchange for one DA molecule released) and/or through a channel-like release of DA (one METH molecule leads to the loss of multiple DA molecules) (Kahlig et al. 2005). Inside of the cell, METH interacts with the vesicular monoamine transporter (VMAT2), which concentrates neurotransmitters into vesicles. METH inhibits binding of [^{3}H]reserpine with an IC_{50} of ~3 μM, which demonstrates a direct interaction of METH with the VMAT2 (Peter et al. 1994). METH also inhibits uptake of [^{3}H]serotonin (5-HT) by the VMAT2 (Peter et al. 1994). In addition, METH may be a substrate of the VMAT2 and act as a "false transmitter", by displacing endogenous neurotransmitter from vesicles. This study examines the interactions of METH with the DAT and VMAT2 using human embryonic kidney (HEK-293) cells stably transfected with the DAT and VMAT2.

HEK-293 cells coexpressing the human (h) isoforms of the VMAT2 and DAT were developed and characterized. Studies by Eshleman et al. (2002) demonstrate that the VMAT2 in transfected HEK-293 cells is expressed on early endosomes, an acidic intracellular compartment that would provide the proton gradient required for VMAT2 function. The DAT antagonist RTI-55 was used to measure DAT density in cells

expressing the DAT alone, or coexpressing the DAT and VMAT2. Saturation [^{125}I]RTI-55 binding curves demonstrated both DAT and DAT-VMAT2 cell lines expressed the DAT with similar densities (B_{max} ~5.5 pmol/mg protein) (Wilhelm et al. 2004). Binding of [^{125}I]RTI-55 was of high affinity (~3 nM) and consistent with the affinity of [^{125}I]RTI-55 at the DAT in native tissue. Saturation [^{3}H]dihydrotetrabenazine (DHTB; VMAT2 antagonist) binding to cotransfected DAT-VMAT2 cells with a K_d of 9 nM, consistent with the potency of DHTB binding to the VMAT2 in native tissue (Thiriot and Ruoho, 2001), and a B_{max} of 2.8 pmol/mg protein. Specific binding of [^{3}H]DHTB to DAT cells was also detected, however it was significantly ($p<0.05$) lower in affinity than the K_d found in DAT-VMAT2 cells.

Cells coexpressing the DAT and VMAT2 took up more [^{3}H]DA than cells expressing only the DAT. Pretreatment of DAT-VMAT2 cells with the VMAT2 antagonist DHTB decreased [^{3}H]DA accumulation to a level not different from [^{3}H]DA uptake by DAT cells. Likewise, [^{3}H]DA uptake time course and saturation curves demonstrated that blockade of the VMAT2 with DHTB in DAT-VMAT2 cells decreased [^{3}H]DA uptake.

Cells coexpressing the VMAT2 also retained [^{3}H]DA more effectively than cells expressing only the DAT. This was in contrast to retention of [^{3}H]METH which was unaffected by expression of the VMAT2. Unlike [^{3}H]DA which remained in both DAT and DAT-VMAT2 cells in both static and superfusion release assays, [^{3}H]METH was not effectively retained. At pH 7.4, 18-28% of the total [^{3}H]DA recovered remained in DAT or DAT-VMAT2 cells at the end of a superfusion release experiment. At pH 7.4, 1% of the total [^{3}H]METH was recovered at the end of a superfusion release experiment.

Retention of [^{3}H]DA was decreased at pH 8.6 compared with pH 7.4, with 7-15% of the total [^{3}H]DA recovered remaining in DAT or DAT-VMAT2 cells at the end of the experiment. The pH-induced [^{3}H]DA release could be attenuated by the DAT antagonists cocaine (10 μM) and GBR-12935 (30 nM). Thus, a pH-sensor may exist on the DAT, which could mediate DA release following changes in extracellular pH. In contrast, retention of [^{3}H]METH was slightly improved by elevated extracellular pH, with 2% of the total [^{3}H]METH recovered present in cells at the end of superfusion experiments.

RTI-55, nomifensine, and lobeline inhibited both [^{3}H]METH uptake and METH-induced [^{3}H]DA release. The concentration of each drug required to block METH-induced [^{3}H]DA release was significantly higher than the concentration required to inhibit [^{3}H]METH accumulation. This suggests that DAT-mediated uptake of METH is not required for METH to elicit [^{3}H]DA release.

PREFACE

In accordance with the guidelines set forth by the Graduate Program of the School of Medicine, Oregon Health and Science University of Portland, Oregon, I have prepared my dissertation consisting of a general introduction, five chapters of original data, and a discussion and conclusion chapter. Each data chapter includes an abstract, introduction, materials and methods, results, and discussion section. References are listed alphabetically, and follow the format of the *Journal of Neurochemistry*.

Chapter 2 contains data, figures, and text as they appear in an original paper that has been published previously (Wilhelm et al. 2004). Chapter 3 contains data, figures,

and text as they appear in an original paper that has been published previously (Wilhelm et al. 2006). Chapter 4 contains data, figures and text as they appear in an original paper that is in preparation. Chapter 5 and Chapter 6 represent data that were collected during the project.

Papers representative of this work

Wilhelm, C.J., Johnson R.A., Lysko P.G., Eshleman A.J., & Janowsky A. (2004) Effects of methamphetamine and lobeline on vesicular monoamine and dopamine transporter-mediated dopamine release in a co-transfected model system. *J Pharm. Exp Ther.* Sept; 310(3): 1142-51,

Wilhelm, C.J., Johnson R.A., Eshleman, A.J., & Janowsky A. (2006) Hydrogen ion concentration differentiates effects of methamphetamine and dopamine on transporter-mediated efflux. *J Neurochem* 96(4): 1149-1159.

Wilhelm, C.J., Johnson R.A., Eshleman, A.J., & Janowsky A. Mechanisms of methamphetamine action: diffusion versus transpoter-mediated uptake. *In preparation*

Abstracts representative of this work

Wilhelm, C.J., Johnson R.A., Lysko P.G., Eshleman A.J., & Janowsky A. (2003) Blockade of hVMAT2 in HEK-hDAT-hVMAT2 cells results in altered [^{3}H]DA uptake kinetics. Society for Neuroscience, New Orleans, LA.

Wilhelm, C.J., Johnson R.A., Eshleman, A.J., & Janowsky A. (2005) Methamphetamine: one curious transporter substrate. Experimental Biology, San Diego, CA

INTRODUCTION

MONOAMINE NEUROTRANSMITTERS

Dopamine (DA), norepinephrine (NE), and serotonin (5-HT) are chemical messengers that mediate signals within the brain. DA and NE are synthesized from tyrosine, while 5-HT is synthesized from tryptophan. In the brain, synthesis of these neurotransmitters occurs within the respective DA, NE, or 5-HT neurons where they are concentrated into vesicles by the vesicular monoamine transporter (VMAT2) (Peter et al. 1994). For NE neurons, DA is synthesized and concentrated into vesicles, where the enzyme dopamine β-hydroxylase converts DA into NE (Menniti and Diliberto 1989, Rush and Geffen 1980). Following stimulation, vesicles fuse to the plasma membrane, where they release their contents into the synapse (von Gersdorff and Mathews 1994). In the synapse, neurotransmitters may interact with pre- and postsynaptic receptors (Benoit-Marand et al. 2001, Sesack et al. 1994). Cell surface transporters are expressed along the periphery of the synapse and recover released neurotransmitter as it diffuses away from the synapse (Nirenberg et al. 1996, Hersch et al. 1997). For each of the monoamine transmitters (DA, NE and 5-HT), there is a specific cell surface transporter (DA, NE, and 5-HT transporters DAT, NET, and SERT respectively). Hertting and Axelrod provided the first evidence of neurotransmitter transport in 1961, though the concept was theorized many years earlier. They discovered that administered [^{3}H]NE was concentrated in sympathetic nerve endings. In March of 1991, the cDNA of the NET was cloned (Pacholczyk et al. 1991). Shortly thereafter, cDNA for both the DAT and SERT were also cloned (Kilty et al. 1991, Hoffman et al. 1991).

The dopaminergic system mediates reward, motivation, attention, and movement (Jaber et al. 1997, Dayan and Belleine 2002, Nass and Blakely 2003). Parkinson's disease is the specific degeneration of dopaminergic neurons in the substrantia nigra and results in a severe movement disorder (Miller et al. 1999, Nass and Blakely 2003). The rewarding effects of abusable substances are also often mediated by the DA system (Eshleman et al. 1994, Jaber et al. 1997, Jones et al. 1998). Specifically, methamphetamine (METH), amphetamine, and cocaine all interact directly with the DAT to increase DA neurotransmission (Bradberry and Roth 1989, Eshleman et al. 1994). Insight into the mechanisms and proteins that maintain DA homeostasis are essential to finding new and effective treatments for Parkinson's disease and drug abuse.

The Dopamine Transporter and other Na^+/Cl^- dependent monoamine transporters

Although a high-resolution structure has not been solved for the DAT, experimental findings verify that the DAT is a member of a family of twelve-transmembrane domain spanning Na^+/Cl^- dependent proteins (Hersch SM 1997 and Vaugh and Kuhar 1996). Members of this gene family include four γ-aminobutyric acid (GABA) transporters (GAT1, GAT2, GAT3, and GAT4), the NET, DAT and SERT and at least two glycine transporters (GLYT1 and GLYT2) (Zahniser and Doolen 2001). Also included in this gene family are amino acid transporters for betaine, creatine, proline and taurine (Zahniser and Doolen 2001). This transporter family possesses intracellular amino and carboxyl termini (Nelson 1998). Many of these proteins also possess a large glycosylated extracellular loop between transmembrane domains 3 and 4 (Nelson 1998). These proteins are expressed on the cell surface and use Na^+ and Cl^- gradients to transport their respective substrates (Nelson 1998). The DAT cotransports two Na^+ and

one Cl^- for each DA molecule translocated from outside to inside of the cell (Krueger 1990, Gu et al. 1994). Recent work suggests that the DAT may also exhibit channel-like properties that "uncouple" the fixed two Na+ and one Cl- stoichiometry (Sonders et al. 1997). In general, monoamine neurotransmitters interact with G-protein coupled receptors (GPCRs)(Zahniser and Doolen 2001). GPCRs transmit chemical signals much more slowly, compared to receptors coupled to ion channels in the postsynaptic cell (Beckman and Quick 1998). The relatively slow transmission of signals by GPCRs means that DA can diffuse away from the synapse and be recovered by the DAT, which is expressed along the periphery of the synapse (Nirenberg et al. 1996, Hersch et al. 1997).

A great deal of scientific effort has been expended to create drugs that are specific for the DAT, NET, and SERT. The high degree of amino acid homology among these transporters translates into structural similarities that make this task difficult. Cocaine, amphetamine (AMPH), and methamphetamine (METH) inhibit reuptake by the DAT, NET, and SERT (Eshleman et al. 1999). In contrast, 3,4-methylenedioxymethamphetamine (MDMA, ecstasy) is somewhat selective for the SERT. Popular antidepressants

FIGURE 1-1

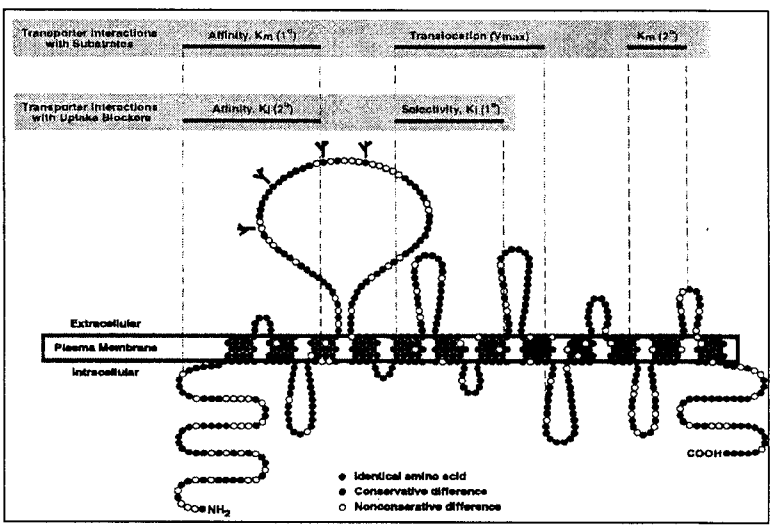

such as fluoxetine (Prozac) and paroxetine (paxil) (selective serotonin reuptake inhibitors (SSRIs)) exhibit a high degree of specificity for blocking the SERT. Nisoxetine is a relatively selective compound for blocking the NET and GBR-12935 is selective for the DAT. The DAT is only expressed in dopaminergic neurons. Surprisingly, however, the NET has a higher affinity for DA than does the DAT (Eshleman et al. 1999). Evidence also suggests that the NET may take up DA *in vivo* (Jones et al. 1998). The monoamine transporters exhibit specific rank order of potency profiles that are often used to identify each individual transporter (Eshleman et al. 1999).

A high degree of homology, particularly within the transmembrane domains, is found in the monoamine transporters (Torres et al. 2003). This, coupled with the distinctive rank order of potency profiles for the individual monoamine transporters, made chimeras a useful tool to evaluate the specific binding and interaction sites for compounds that exhibit transporter specificity (Buck and Amara 1994, 1995, Giros et al. 1994). Some subtle differences were found between the initial DAT-NET chimera studies. Figure 1-1 (Buck and Amara 1995) depicts the putative 12 transmembrane domains of the DAT and identifies the amino terminus as important for both substrate and inhibitor affinity. In contrast, Figure 1-2 (Giros et al. 1994) identifies the carboxyl terminal region as important for substrate affinity and identifies transmembrane domains 5 through 8 as important for interactions with inhibitors. Other discrepancies between

FIGURE 1-2

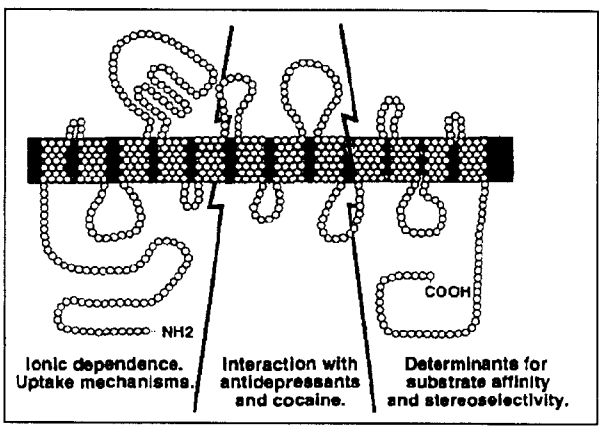

these models also exist. Buck and Amara (1995) suggest that the region between transmembrane domains 5 through 8 is involved in substrate translocation, whereas Giros et al. (1994) attribute this function to a region from the amino terminus through transmembrane domain 5. To further elucidate the structure of the DAT and the function of specific residues of the DAT, numerous site-directed mutagenesis studies have been conducted (for review see Volz and Schenk 2005). This review identified numerous residues on the DAT that appear to affect either binding or substrate efflux exclusively. The residues are scattered throughout the DAT molecule, however, not implicating specific DAT region(s) as important for interactions with substrates or inhibitors. Instead, results of mutagenesis studies suggest that even single amino acid substitutions can significantly alter the secondary and tertiary structure of the DAT, thereby affecting substrate translocation, antagonist binding, and surface expression of the protein.

The DAT is densely expressed in the dendrites and cell bodies of neurons located in the substantia nigra pars compacta and ventral tegmental area (Ciliax et al. 1999). High levels of DAT protein are also found in the striatum and nucleus accumbens (Ciliax et al. 1999). Giros et al. (1996) created a DAT knockout mouse that exhibited spontaneous hyperlocomotion. This was in spite of lower levels of neurotransmitter and DA receptor expression. Extracellular DA remained for ~100 times longer in $DAT^{-/-}$ mice than in mice with normal DAT expression. Thus, the DAT is crucial for coordinating DA signaling within dopaminergic neurons.

Vesicular Transporters

Vesicular monoamine transporters are also putative twelve-transmembrane domain proteins (Peter et al. 1996). Liu et al. (1992) cloned the first such transporter by

using the neurotoxin 1-methyl-4-phenylpyridinium (MPP^+) to select for cells that were resistant to MPP^+ toxicity. Expression of the VMAT1 protects cells from the toxic effects of MPP^+ (Liu et al. 1992). Unlike the cell surface monoamine transporters, however, energy for the uptake of neurotransmitter by vesicular transporters is derived from counter transport of protons concentrated within acidic vesicles by the H^+-ATPase (Knoth et al. 1981). Vesicular monoamine transporters have a large loop between transmembrane domains 1 and 2 that is predicted to lie in the vesicular lumen (Peter et al. 1996). This configuration suggests that the amino- and carboxyl termini of the protein are in the cytosol.

Two highly related vesicular monoamine transporters have been identified, VMAT1 and VMAT2. The VMAT1 and VMAT2 have distinctive pharmacological profiles, which allow them to be easily distinguished. In general, the VMAT2 exhibits a higher affinity for endogenous substrates than the VMAT1 (Peter et al. 1994). Histamine has a more than 100-fold higher affinity for VMAT2 than for VMAT1 (Peter et al. 1994). Other endogenous substrates, such as 5-HT, DA, NE and epinephrine have about a 5-fold higher affinity for the VMAT2 (Peter et al. 1994, Finn et al. 1998). Tetrabenazine is a VMAT inhibitor, but exhibits a 10-fold higher affinity at the VMAT2 than at the VMAT1 (Peter et al. 1996). In contrast, reserpine has a similar affinity for the VMAT1 and VMAT2. The VMAT2 is primarily expressed in the central nervous

FIGURE 1-3

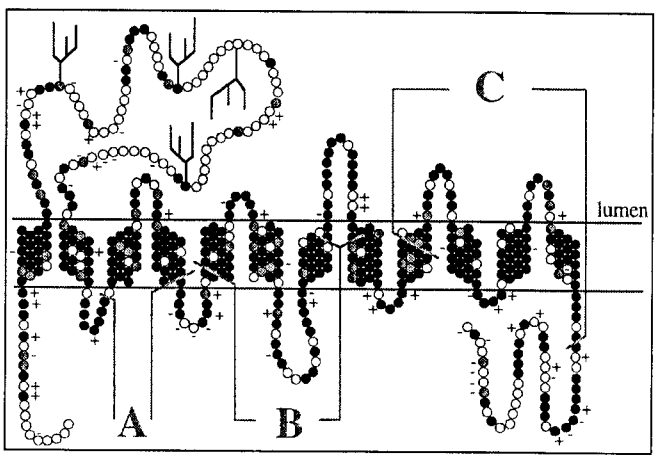

system, while the VMAT1 is associated with the adrenal gland (Edwards 1992, Peter et al. 1995).

The primary function of the VMAT2 is to concentrate neurotransmitter into vesicles in preparation for their release (Fon et al. 1997, Fumagalli et al. 1999). Since the VMAT2 confers protection against the neurotoxic compound MPP^+, the VMAT2 may also act as a molecular scavenger and collect potentially harmful compounds from within the cell (Liu et al. 1992). These may include AMPH-like compounds, MPP^+, and antibiotics (Liu et al. 1992, Sulzer et al. 2005). Like the monoamine transporters, the high degree of homology between VMAT1 and VMAT2 proteins allowed for the creation of functional chimeras (Peter et al. 1996). Figure 1-3 (Peter et al. 1996) is a topological plot of the VMAT2 (black circles represent residues conserved between VMAT1 and VMAT2, grey circles represent residues that are similar between VMAT1 and VMAT2, and open circles represent residues that are not conserved between VMAT1 and VMAT2). A high degree of homology is observed between the VMAT1 and VMAT2, particularly within transmembrane domain regions. Three key VMAT regions are identified: Region A, transmembrane domains 3 and 4, is important for high affinity serotonin (substrate) recognition. Region B (transmembrane domains 5 through 8) and region C (transmembrane domains 8 through 12) are important for high affinity interactions with histamine and tetrabenazine. Regions B and C are also important for high affinity serotonin uptake, but only if other more amino-terminal VMAT2 sequences are present.

Dopamine Homeostasis

In order to maintain DA homeostasis, DA is synthesized, degraded and recycled within dopaminergic neurons (Elsworth and Roth 1997, Jones et al. 1999). In the brain, DA is synthesized within the cytosol by an enzymatic process beginning with the primary amino acid tyrosine (Elsworth and Roth 1997). Tyrosine is converted into dihydroxyphenylalanine (L-DOPA) by tyrosine hydroxylase (Elsworth and Roth 1997). This is the rate-limiting step in the synthesis process and the site of feedback inhibition by DA (Elsworth and Roth 1997). Interestingly, both reserpine and AMPH also affect activity of tyrosine hydroxylase (Bower et al. 1998, Ellison et al. 1978, Mueller et al. 1969, Reis et al. 1975). L-DOPA is converted to DA by the enzyme L-aromatic amino acid decarboxylase (Elsworth and Roth 1997). Once synthesized, DA is concentrated into vesicles by the VMAT2 (Elsworth and Roth 1997). Following excitation, vesicles fuse with the plasma membrane and release DA into the synapse (Fon and Edwards 2001). DA interacts with postsynaptic receptors and diffuses out of the synapse where it is recovered by the DAT and may also interact with presynaptic autoreceptors such as the DA D_2 receptor (Zahniser and Doolen 2001). Following uptake, DA is then either repackaged into vesicles by the VMAT2, or degraded by the enzyme monoamine oxidase (MAO)(Elsworth and Roth 1997). Another metabolic enzyme, catechol-o-methyltransferase (COMT) resides primarily outside of the cell and may be responsible for the degradation of DA as well (Elsworth and Roth 1997). Studies using DAT null mutant mice suggest that recycling of DA is a greater part of DA homeostasis than *de novo* synthesis (Jones et al. 1998). Therefore, the cell surface DAT is particularly important in maintaining DA homeostasis.

Transport versus binding to the DAT

Pharmacologically, the cell surface DAT interacts with numerous molecules (Eshleman et al. 1999). Typically, these molecules are either transported by the DAT, or bind to the DAT and inhibit its function. DA and NE are endogenous substrates of the DAT (Eshleman et al. 1999). Other substrates include the drugs of abuse AMPH, METH, and MDMA, as well as numerous other AMPH-like compounds (Sonders et al. 1997). These compounds, like the endogenous substrates, are transported by the DAT into the cell. Some neurotoxins such as MPP^+ are transported by the DAT as well (Kilbourn et al. 2000). In contrast, other compounds such as mazindol, are not transported by the DAT, but simply bind to the surface of the DAT molecule and inhibit substrate transport (Sonders et al. 1997). Other compounds that bind to the DAT include methyphenidate (Ritalin), RTI-55, nomifensine, mazindol and cocaine (Sonders et al. 1997). The high degree of homology among the monoamine transporters (DAT, NET and SERT) translates into a relative lack of specificity for the majority of compounds that interact with these transporters (Eshleman et al. 1999). Therefore, a compound such as fluoxetine (prozac), a selective serotonin reuptake inhibitor (SSRI), which is frequently prescribed for depression, interacts with both the DAT and the NET when concentrations are high enough (Eshleman et al. 1999). Differentiating between substrates and non-substrates of cell surface transporters can be difficult. Comparing inhibition of [^{125}I] 2 β -carbomethoxy-3 β -(4-iodophenyl)tropane (RTI-55, β-CIT) binding and inhibition of [^{3}H]DA uptake is sometimes useful. RTI-55 is a cocaine analog that binds with high affinity to the DAT, NET, and SERT (Eshleman et al. 1999). In general, non-substrates have similar potencies for both inhibition of [^{125}I]RTI-55 and inhibition of [^{3}H]DA

uptake (Eshleman et al. 1999). In contrast, substrates, such as DA and METH more potently inhibit [^{3}H]DA uptake than [^{125}I]RTI-55 binding. Both DA and METH are ~100-fold more potent inhibitors of [^{3}H]DA uptake than inhibitors of [^{125}I]RTI-55 binding (Eshleman et al. 1999). Perhaps the most discriminating method for determining whether a drug is a substrate is the use of current-voltage plots derived from electrophysiology experiments. Sonders et al. (1997) used DAT-expressing *Xenopus* oocytes to measure the steady-state current generated by the application of numerous substrate and non-substrate drugs. The resulting current-voltage plots could be characterized as DA-like or cocaine-like, based on the distinctive shape of the substrate (DA) and inhibitor (cocaine) curves. The results suggest that DA, p-tyramine, AMPH, METH, MPP^{+}, norepinephrine, metariminol, m-tyramine, and β-phenethylamine are substrates of the DAT. Cocaine, GBR 12909, methylphenidate, amfonelic acid, aminorex, indatraline, mazindol, pemoline, phendimetrazine, and RTI-55 had current-voltage plots similar to cocaine.

Transport versus binding to the VMAT2

Unlike the DAT, which can easily be evaluated using electrophysiological techniques (Sitte et al. 1998, Sonder et al. 1997, Scarponi et al. 1999), the VMAT2 is not expressed on the cell surface, making it much more difficult to study electrophysiologically. Whitley et al. (2004) found that *Xenopus* oocytes injected with a rat VMAT2 mutant retained functional VMAT2 molecules on the plasma membrane. This model may be useful to perform electrophysiological studies. Currently, only pharmacological methods have been used to determine whether drugs are substrates or inhibitors.

Regulation of DAT expression

Initially, cell surface transporters were theorized to be relatively one-dimensional molecules in terms of their overall function, i.e. the DAT is expressed at a constant level on the cell surface and its sole function is to recover released DA (Zahniser and Doolen 2001). Expression of the DAT, however, is highly regulated. The endogenous substrate DA can cause down-regulation of the DAT (Gulley et al. 2002, Chi and Reith 2003). Likewise, Fleckenstein et al (1997) found that one hour after a single METH treatment, rat striatal synaptosomes exhibit significantly reduced [^{3}H]DA uptake compared with saline-injected animals. This study, however, did not differentiate between a decrease in the function of the DAT and a decrease in the cell surface expression of the DAT. Using HEK-293 cells stably expressing DAT, Saunders et al. (2000) found that DAT immunofluorescence on the cell surface was reduced following exposure to either DA or AMPH. Treatment with both AMPH and a DAT antagonist such as mazindol or cocaine blocked internalization of the DAT (Saunders et al. 2000). Mutation of dynamin I, a protein involved in endocytosis, also blocked the AMPH-induced internalization of DAT, suggesting that DAT internalization is mediated through an endocytotic process (Saunders et al. 2000). Conversely, some drugs actually increase expression of the DAT; Mayfield et al. (2001) found that following ethanol treatment, *Xenopus oocytes* expressing the DAT exhibited greater [^{3}H]DA uptake and [^{3}H]WIN 35,428 binding. Thus, alcohol increased DA uptake by increasing the cell surface expression of the DAT, as opposed to increasing the function of the transporters already on the cell surface. Following in utero cocaine exposure, DAT protein is upregulated in fetal rhesus monkey

brain as measured by [^{125}I]RTI-121 binding, and mRNA expression (Fang and Rønnekleiv, 1999).

The DAT also contains numerous consensus phosphorylation sites for protein kinase A (PKA), protein kinase C (PKC), and Ca^{2+}-calmodulin-dependent kinase II (CaM kinase II) (Zahniser and Doolen 2001). Activation of PKC by phorbol 12-myristate 13-acetate (PMA) results in a decrease in surface expression of the DAT, as measured by a decrease in the maximal rate of [^{3}H]DA transport (V_{max}) and a decrease in DAT biotinylation (Melikian and Buckley 1999). Interestingly, although numerous PKC sites are present on the DAT, phosphorylation of these sites does not appear to be a critical component of DAT trafficking. Chang et al. (2001) reported that a DAT with mutated PKC phosphorylation sites still exhibits PMA-induced decreases in DA uptake and cell surface expression, as measured by confocal microscopy. These results clearly suggest that regulated expression of the DAT is controlled by a number of mechanisms that are important for DAT function.

Regulation of VMAT2 expression

Recent studies have shown that trafficking of vesicular transporters, such as the VMAT2, plays a major role in neurotransmitter homeostasis. Using a rat model, Brown et al. (2000) demonstrated that following multiple METH administrations, both DA uptake and DHTB binding were reduced in a vesicle preparation from striatum. Follow-ups to this study found that the METH-induced decreases in VMAT2 activity can be blocked by post-treatment with methylphenidate (Hanson et al. 2004, Sandoval et al. 2003). Purified vesicles from the striatum of rats administered MDMA show decreases in [^{3}H]DA uptake and [^{3}H]DHTB binding, indicating a decrease in VMAT2 expression

(Hansen et al. 2002). The persistence of VMAT2 deficits differed slightly between MDMA and METH, however, in that no recovery of VMAT2 expression was observed 24 hours after treatment with METH, whereas VMAT2 expression had recovered 24 hours after treatment with MDMA (Brown et al. 2000, Hansen et al. 2001). In contrast, phencyclidine, cocaine, and methylphenidate increase activity of the VMAT2 as measured by [^{3}H]DA uptake and [^{3}H]DHTB binding to purified striatal vesicles (Riddle et al. 2002, Crosby et al. 2002, Sandoval et al. 2002). The effects of these drugs on VMAT2 activity occur rapidly (approximately 1 hour after treatment regimen) suggesting that the increases in VMAT2 expression are not due to synthesis of new transporters. Riddle et al. (2002) found differences in the subcellular localization of the VMAT2 following treatment with either METH or cocaine. Treatment with cocaine increased VMAT2 immunoreactivity in vesicle-enriched fractions, whereas treatment with METH decreased VMAT2 immunoreactivity in vesicle-enriched fractions. Regulation of the VMAT2 could have a significant impact on cellular homeostasis. Inhibition of VMAT2 activity, as observed following METH treatment, could result in the accumulation of DA in the cytosol due to decreased uptake of DA into the vesicles. High levels of DA within the cytosol or synapse can result in DA oxidation and formation of harmful reactive oxygen species (LaVoie and Hastings 1999). Compromised expression of the VMAT2, as in VMAT2$^{+/-}$ (mice with one VMAT2 gene disrupted) mice, led to increased METH-induced neurotoxicity as evidenced by deficits in DA and DA metabolites, as well as DAT expression (Fumagalli et al. 1999). Proper function and expression of the VMAT2 is essential to properly maintain DA homeostasis.

The role of pH in dopamine homeostasis

DA exists in multiple ionic forms, including anion, cation, neutral, and zwitterions (Berfield et al. 1999, Wilhelm et al. 2006). The abundance of each form is dependent upon the prevailing pH (Berfield et al. 1999, Wilhelm et al. 2006). Like AMPH and METH, DA is a weak base. The zwitterionic form of DA occurs when the amine group has accepted a proton and one of the hydroxyl groups has donated a proton, thus giving DA both a positive and negative charge, with the net molecular charge still neutral. The amine group of DA can accept a proton, while the two aromatic hydroxyl groups can be proton donors. Compared with pH 7.4, uptake of [^{3}H]DA at pH 6.0 has a lower affinity (K_m) in HEK-293 (human embryonic kidney cells) expressing the DAT. No effect on the maximal rate of transport (V_{max}) was observed. Increasing the pH from 7.4 to 8.0 did not effect either the affinity or maximal rate of [^{3}H]DA uptake (Berfield et al. 1999). Based on their analysis of [^{3}H]DA uptake kinetics at different pH's, Berfield et al. (1999) concluded that the cationic and zwitterionic forms of DA were the forms of DA transported by the DAT. Furthermore, their calculations suggest that the combined proportion of cationic and zwitterionic forms of DA remained relatively constant over the pH range of 6.0 to 8.2. This study also demonstrated the stability of the DAT over this pH range. Aside from a decrease in affinity (K_m) at pH 6.0, uptake of [^{3}H]DA by the DAT remained largely unaffected by changes in extracellular pH (no observed differences in V_{max}). This is somewhat surprising since single amino acid residue changes can exert profound effects on transport or expression of the DAT (Volz and Schenk 2005). Altering the extracellular pH will affect ionizable amino acid residues present in the extracellular loops of the DAT, which could cause changes to the

secondary or tertiary structure of the molecule, thereby interfering with substrate translocation (Berfield et al. 1999).

The VMAT2 requires a pH gradient for its function, so alterations in pH have a more profound and direct effect on the VMAT2 than on the DAT (Eiden et al. 2004). Like the DAT, the VMAT2 also has positive and negatively charged amino acid moieties present in loops that reside in the vesicle lumen or the cytoplasm (Figure 1-3) (Peter et al. 1996). Thus, changes in intracellular pH, or intravesicular pH could effect the conformation of the transporter. The coupling of protons to the transport of substrate by the VMAT2 confounds the effect of pH on the structure of the transporter.

Transporter Multimers

Cross-linking experiments done by Hastrup et al. (2001) demonstrate an interaction between cysteines present at residue 306 near the end of the 6^{th} transmembrane domain of neighboring DAT molecules. The results of these experiments suggest that two DAT molecules form a homodimer, with a molecular mass of 195 kDa. This compares with 85 kDa for a single glycosylated DAT molecule. Further studies by Hastrup et al. (2003) using a cysteine-deficient DAT molecule suggest that the DAT may exist as a tetramer, or dimer of dimers. Interestingly, some DAT inhibitors (mazindol, benztropine, and a cocaine analog), but no DAT substrates (tyramine or DA), were able to inhibit cross-linking of Cys^{243}, an additional site of cross-linking, thereby indicating a direct interaction of inhibitors with this residue (Hastrup et al. 2003). Other transporters in the Na^+/Cl^- dependent superfamily also display oligomerization, including the SERT and GABA1 transporters (Schmid et al. 2001). In contrast to the DAT, no data is available on the oligomerization of vesicular monoamine transporters. The

oligomerization of transporters may have implications for function, regulation, and recycling and thus will be important in further studies.

Amphetamine and amphetamine-like compounds: History

Plants of the genus *Ephedra* and the tree *Catha edulis* produce AMPH-like compounds naturally. Uses of the naturally occurring forms of AMPH date back thousands of years. An early Chinese book of medicine (written in the first century) discusses the use of these herbs for treating asthma and upper respiratory infections. In 1887, Nagajoshi Nagai isolated the active compound in *Ephedra* plants (ephedrine). Likewise, cathinone and norpseudoephedrine (AMPH-like compounds) were isolated from the tree *Catha edulis*. Lazar Edeleanu first synthesized AMPH in 1887. In 1978, J.H. Biel and B.A. Bopp defined the structural components of AMPH as an unsubstituted phenyl ring, a two-carbon side chain between the phenyl ring and nitrogen, an α-methyl group, and a primary amino group. The stimulant effects of AMPH were first identified in 1933 (Alles, 1933). In 1936, Benzedrine (AMPH) was made commercially available by the pharmaceutical firm Smith, Kline and French and did not require a prescription. AMPH became popular, especially among college campuses, selling over 50 million 10 mg tablets within the first three years of release (Sulzer et al. 2005). Bear in mind that the total population of the US was just under 131 million people according to the 1940 US Census. AMPH was deemed a "wonder drug" and was used to treat more than 30 conditions ranging from schizophrenia to persistent hiccups. In 1937, Guttmann and Sargeant suggested that AMPH may be addictive. Unfortunately, this study was widely overlooked until the 1960s. In 1939, over the counter sales of AMPH were halted and purchase of AMPH was by prescription only. Today, AMPH and AMPH-like

compounds are still used clinically for treatment of attention-deficit hyperactivity disorder and as appetite suppressants, as well as by the military to increase alertness in soldiers involved in long missions. Many AMPH-like compounds including AMPH, METH, and methylenedioxymethamphetamine (MDMA, ecstasy) are also used illegally. The widespread abuse and addiction to AMPH-like compounds has led to increasing efforts to more clearly understand the underlying actions of these drugs.

Methamphetamine: An epidemic

Abuse of METH is increasing across the United States (Lineberry and Bostwick 2006). METH is highly addictive, inexpensive to produce, and readily available (Lineberry and Bostwick 2006). Chronic users of METH exhibit impairments in psychomotor speed, information processing, learning, and memory (Meredith et al. 2005). METH is neurotoxic and can permanently damage the brain (Xie et al. 2000). Treatment for METH abuse consists primarily of cognitive behavior therapy, which is occasionally combined with an antidepressant (Cretzmeyer et al. 2003). To design and develop effective treatments for METH abuse, it is imperative to understand the drug's underlying mechanisms of actions.

Mechanisms of action and effects of Amphetamine-like compounds

Within the central nervous system, AMPH-like compounds cause an accumulation of DA within the synapse (Jones et al. 1999). This phenomenon occurs through a number of distinct mechanisms. AMPH and similar compounds are substrates of the DAT and thus compete directly with DA for reuptake by the DAT (Sonders et al. 1997, Zaczek et al. 1991a & b, Wilhelm et al. 2006). AMPH also causes reversal of transport at the DAT (Eshleman et al. 1994, Falkenburger et al. 2001). When the DAT reverses, intracellular

DA that is in the cytosol is transported out of the cell (Pifl et al. 1995, Wilhelm et al. 2004, Falkenburger et al. 2001). Falkenburger et al. (2001) suggested that a tonic "leak" of DA by the DAT provides an underlying inhibitory tone. This could be achieved through an interaction of leaked DA with presynaptic D2 receptors, which are coupled to inhibitory G-proteins that decrease vesicular release of DA. Additional leakage of DA, as caused by treatment with an AMPH-like compound, would result in added inhibition of dopaminergic neuronal activity.

Once inside the cell, AMPH-like compounds interfere with vesicular storage (Sulzer et al. 1990 and 1995). It is unclear precisely how AMPH-like compounds interact with the VMAT2. One possibility is that AMPH-like compounds are VMAT2 substrates, just like they are for the cell surface DAT. Structurally, AMPH-like compounds strongly resemble DA and NE, further supporting this hypothesis. AMPH displaces both reserpine and tetrabenazine from the VMAT2 (Gonzalez et al. 1994, Peter et al. 1994). Reserpine and tetrabenazine are VMAT2 antagonists (Finn and Edwards 1998). It cannot be assumed that displacement of these compounds by AMPH is an indication of uptake by the VMAT2. Sulzer and Rayport (1990) found that AMPH destroys the intravesicular pH gradients required for the proper function of the VMAT2. On the basis of this finding, the weak base hypothesis was formed, which proposes that regardless of the specific interaction of AMPH with the VMAT2, AMPH dissipates the acidic vesicular pH, leading to decreased activity of the VMAT2. Based on these findings, Sulzer and Rayport (1990) suggested that AMPH becomes protonated within vesicles, thereby dissipating the pH gradient. Once AMPH becomes protonated, it is less likely to diffuse across membranes, thereby allowing it to be stored inside the vesicle for subsequent

release. If AMPH-like compounds become trapped in the vesicle, then these compounds should be effectively retained within the cells, in a manner similar to DA. There have been no studies to this point that have explored the retention of AMPH-like compounds by the DAT and VMAT2.

AMPH-like compounds may also interfere with DA degradation. One study suggests AMPH, though not degraded by MAO, inhibits its activity (Blaschko et al. 1937, Leitz and Stefano 1971). Inhibition of MAO activity will result in accumulation of DA within the cytosol. Free cellular DA may be oxidized and cause damage to the cell (Filloux and Townsend 1993). Cubells et al. (1994) showed that METH neurotoxicity is dependent upon oxidative stress induced by intracellular DA. Yamamoto and Zhu (1998) also found that METH treatment led to increased production of free radicals and oxidative stress in dopaminergic neurons.

AMPH also exerts effects on DA synthesis. AMPH increases the rate of DA synthesis by increasing the activity of tyrosine hydroxylase, the rate-limiting enzyme in DA synthesis (Kuczenski 1975). DA synthesis increased 70% at concentrations of 15 μM AMPH (Kuczenski 1975). Although AMPH-induced increases in tyrosine hydroxylase activity are dependent on calcium (Fung and Uretsky, 1982), the precise mechanism of action is unclear. One hypothesis is that AMPH may block or bind to tyrosine hydroxylase at the site of feedback inhibition by DA, resulting in increased activity of the enzyme (Haycock 1993). Long-term administration of AMPH results in decreased DA and tyrosine hydroxylase levels in the striatum, but unchanged levels in the midbrain (Bower et al. 1998). Thus, long-term abuse of AMPH leads to dopaminergic deficits (Nordahl et al. 2003).

Global Hypothesis

Uptake and retention of DA and METH will be similar in a model system expressing the DAT and VMAT2.

Specific Aims

1. Create and characterize an immortalized cell line expressing both the DAT and VMAT2. A cell line that expresses both of the key transporters involved in DA homeostasis will provide a valuable tool to study the specific contributions of each of these proteins to DA homeostasis.
2. Test the hypothesis that DA and METH are stored similarly. DA and METH share highly analogous structures. Therefore, it is likely that METH and DA are stored similarly in cells expressing the DAT and VMAT2. Some theories suggest that METH may act as a "false transmitter" and be released from vesicles like DA. Understanding the storage of METH has significant implications for effective treatment of METH overdoses and abuse, and may help to identify potential targets for therapeutic treatment of treat METH abuse.
3. Identify compounds that effectively block METH-induced [^{3}H]DA release. The net release of DA following METH exposure is one of the primary mechanisms of METH action. A molecule that specifically blocks this effect would be an excellent candidate for a pharmacotherapeutic to treat METH addiction.

II. Effects of methamphetamine and lobeline on vesicular monoamine and dopamine transporter-mediated dopamine release in a co-transfected model system

As published in the Journal of Pharmacology and Experimental Therapeutics with minor modifications September 2004

ABSTRACT

Dopamine (DA) retention and drug-induced release kinetics were characterized in HEK-293 cells stably coexpressing the human DA transporter (hDAT) and human vesicular monoamine transporter (hVMAT2). Co-function of hDAT and hVMAT2 caused greater retention of [^{3}H]DA at 20 minutes (37°C), or 45 minutes (22°C) as compared to cells that were treated with dihydrotetrabenazene (DHTB) to block the hVMAT2. In hDAT and hVMAT2 coexpressing cells treated with DHTB during [^{3}H]DA loading, methamphetamine (METH)-induced efflux was only 20% of preloaded [^{3}H]DA, as compared with 50-60% efflux in the absence of DHTB. Interestingly, the presence of DHTB (during release only) increased the potency and efficacy of METH at inducing [^{3}H]DA release (without DHTB: EC_{50}=33.8 μM, maximal release 51%; release with DHTB: EC_{50}=3.2 μM, maximal release 61%), suggesting that the effects of METH and DHTB on vesicular storage are additive. High concentrations of lobeline induced a statistically significant release of [^{3}H]DA from HEK-hDAT-hVMAT2 cells, but only in the absence of DHTB, suggesting an hVMAT2-mediated effect. Likewise, lobeline did not induce a significant release of [^{3}H]DA from HEK-hDAT cells. The substrates DA and p-tyramine induced robust release of preloaded [^{3}H]DA from cotransfected cells. Cocaine was somewhat effective at blocking substrate-induced [^{3}H]DA efflux. These results suggest that coexpression of the hDAT and hVMAT2 can be used as a model system to distinguish functional pools of DA, and to quantify differences in drug effects on DA disposition. In addition, cotransfected cells can be used to determine mechanisms of simultaneous drug interactions at multiple sites.

Introduction

All drugs of abuse, including METH, either directly or indirectly increase DA neurotransmission (Grace 2000; DiChiara 2002). The DAT and VMAT2 terminate neurotransmission following stimulated release by reuptake and repackaging of DA into vesicles. The interaction of these proteins in a simple, stable system has not been described in detail. However, Pifl et al. (1995), using a superfusion apparatus, reported increases in DA uptake and amphetamine-induced release of [^{3}H]DA in cells coexpressing the hDAT and rat (r)VMAT2, as compared to cells expressing only the hDAT. There was also an apparent decrease in the potency and efficacy of amphetamine-induced release from DAT cells versus hDAT/rVMAT2 cells, although no direct comparisons were made.

METH is an efficacious and relatively potent releaser of DA and preloaded 1-methyl-4-phenylpyridinium (MPP^+) *via* the hDAT (Eshleman et al. 1994; Sulzer et al. 1995; Johnson et al. 1998; Dwoskin and Crooks 2002). The amphetamines exert their actions through a number of mechanisms including inhibition of reuptake, redistribution of DA between vesicle stores and cytoplasm, reversal of transport and possibly by collapsing proton gradients driving vesicular uptake (Cubells et al. 1994, Sabol & Seiden 1998; Jones et al. 1999; Schmitz et al. 2001). METH also exerts regulatory effects on both the DAT and VMAT2, affecting long-term DA homeostasis (Fleckenstein et al. 1997; Brown et al. 2000; Gulley et al. 2002; Ugarte et al. 2003). Other drugs, such as lobeline, a potential pharmacotherapeutic, also affect DA release, but their mechanisms of action may differ from those of METH (Dwoskin and Crooks 2002). Recently,

Dwoskin and Crooks (2002) suggested that lobeline interacts with the VMAT2 and affects DA homeostasis.

There are no reports describing effects of METH and other substrates, or lobeline on DA efflux in cells stably expressing both hDAT and hVMAT2. To further explore the possible shift in affinity during drug-induced release (Pifl et al., 1995) and to examine in more detail DA homeostasis and drug potency and efficacy, HEK-293 cells stably expressing hDAT and hVMAT2 were developed.

We now report that retention of [^{3}H]DA within stably transfected hDAT cells is increased by the presence of the hVMAT2, and that blockade of hVMAT2 (during drug-induced DA release only) increases the apparent potency and efficacy of METH-induced release. Importantly, blockade of hVMAT2 during [^{3}H]DA loading results in a decrease in the magnitude of METH-induced release. The differences in [^{3}H]DA retention between HEK-hDAT and HEK-hDAT-hVMAT2 cells suggest that the expressed hVMAT2 is functional and that nonneuronal cotransfected cells possess the biochemical intermediates necessary to provide the proton-gradient required for hVMAT2 function (Erickson et al. 1992; Merickel et al. 1995). In neurons, vesicles make use of an ATP-dependent proton pump to create a pH gradient that is used by the hVMAT2 to concentrate neurotransmitter. In the model system used here, the hVMAT2 is likely associated with early endosomes (Eshleman et al. 2002) that have an acidic internal pH that aids in the dissociation of receptor-ligand complexes (Sheff et al. 1999). Likewise Liu and Edwards (1997), using transfected Chinese hamster ovary cells, reported the comigration of a vesicular monoamine transporter (VMAT1) with transferrin receptor, a commonly used early endosomal marker, in western blots following differential

centrifugation. The acidic pH of early endosomes could drive the uptake of neurotransmitter by the hVMAT2. Our results indicate that lobeline induces [^{3}H]DA release and appears to exert its effects exclusively through interaction with the hVMAT2. DHTB, a drug that binds with high affinity to the hVMAT2 (Sievert et al. 1998; Thiriot and Ruoho 2001), completely blocks the effect of lobeline on [^{3}H]DA release, and blocks 60-70% of the effect of METH. Thus, similarly to METH effects on efflux, the majority of the lobeline effect is on [^{3}H]DA that is sequestered by the hVMAT2. Unlike METH, the endogenous substrate DA and the trace amine, p-tyramine, do not exhibit a shift in potency or efficacy in response to hVMAT2 blockade during release. These drugs also have the largest maximal effect (about 75% release), as compared to that of METH (50-60%). This simple model system can be used to quantify the drug-induced disposition of DA into two sequestered compartments within the cell and to determine the specific mechanism of action of abused drugs and potential pharmacotherapeutics.

Materials and Methods

Materials

[^{3}H]DA (3,4-[7-^{3}H]dihydroxyphenylethylamine, 5.8–9.7 Ci/mmol) was purchased from Amersham Biosciences (Piscataway, NJ). Eco-Lume scintillation fluid was purchased from ICN biochemicals, inc. (Aurora, OH). DHTB and [^{3}H]DHTB were purchased from American Radiolabeled Chemicals, Inc. (St. Louis, MO). All water used in these experiments was purified by a Milli-Q system (Millipore Corp., Bedford, MA, U.S.A.). Methamphetamine, lobeline, pargyline, tropolone and most other chemicals were purchased from Sigma-Aldrich (St. Louis, MO).

Cell culture

HEK-293 cells were transfected with the hDAT and characterized as previously described (Eshleman et al., 1995). Cells were maintained in Dulbecco's modified Eagle's medium supplemented with 10% fetal bovine serum and 0.05 U penicillin/streptomycin. Stock plates were grown on 150-mm-diameter tissue culture dishes in 10% CO_2 at 37°C. The SR-AI macrophage scavenger receptor (MSR) cDNA was originally derived from human placenta as previously described (Lysko et al. 1999). The macrophage scavenger receptor (MSR) cDNA was subcloned into pcDNA3.1 (with zeocin resistance) and approximately 1 μg of DNA was transfected into HEK-hDAT cells using lipofectamine. Expression of the MSR increased cell adherence, a necessity for the rigorous washing procedures and prolonged release experiments (Robbins and Horlick 1998; Saunders et al. 2000). The hVMAT2 cDNA was generously supplied by Dr. Robert Edwards (University of California at San Francisco) and subcloned into pcDNA3.1 (with G418 resistance). Approximately 1 μg of DNA was transfected into HEK-hDAT cells using lipofectamine.

Binding Assay

The binding of [^{125}I]3β-(4-iodophenyl)tropane-2β-carboxylic acid methyl ester ([^{125}I]RTI-55), or [^{3}H]DHTB to the hDAT or hVMAT2, respectively, in HEK-hDAT and HEK-hDAT-hVMAT2 cells was performed as previously described, with minor modifications (Eshleman et al. 1999). In short, cells were grown to confluence, and washed with 5 mL of PBS buffer. Cells were scraped from plates, resuspended and homogenized in 3-5 mL of 0.32 M sucrose with a Polytron homogenizer at setting 7 for 5-10 s. For RTI-55 binding assays, the homogenate was centrifuged at 400 x g for 5 min. at 4°C. The supernatant was decanted and centrifuged at 22,000 x g for 15 min. at 4°C.

The resulting pellet was then resuspended in 3 mL of buffer and homogenized with a Polytron homogenizer at setting 7 for 5-10 s. The assays contained approximately 75-150 μg of membrane protein for DHTB binding (less than 15% of the radioactivity added was bound), or 25-50 μg of membrane protein for RTI-55 binding (less than 25% of radioactivity added was bound), drug, and [^{125}I]RTI-55 (60 pM final concentration), or [^{3}H]DHTB (6 nM final concentration) in a final volume of 250 μl. Krebs-HEPES buffer (25 mM HEPES, 122 mM NaCl, 5 mM KCl, 1.2 mM $MgSO_4$, 2.5 mM $CaCl_2$, 1 μM pargyline, 100 μM tropolone (see [^{3}H]DA uptake assay, below), 2 mg glucose/ml, 0.2 mg ascorbic acid/ml, pH 7.4) was used for all assays, except as indicated. Specific binding was defined as the difference in binding observed in the absence and presence of 10 μM mazindol ([^{125}I]RTI-55 binding), or 2 μM DHTB ([^{3}H]DHTB binding). The membranes were incubated for 90 min (equilibrium) at room temperature in the dark. Assays were terminated by filtration through Wallac Filtermat A filters using a 96-well Tomtec cell harvester. Scintillation fluid (50 μl) was added to each filtered spot, and the radioactivity remaining on the filters was determined using a Wallac 1205 Betaplate scintillation counter. Saturation binding experiments were conducted with duplicate determinations at each ligand concentration, that included radiolabeled and non-radiolabeled ligand for final concentrations ranging from 6 nM to 200 nM for DHTB, or 60 pM to 20 nM for RTI-55. Protein concentrations for this and all other experiments requiring protein normalization were performed using a modified BCA protein assay.

Time course of [^{3}H]DA Uptake

Cells were plated on poly-l-lysine-coated 24-well plates and grown to confluence. Media was decanted and cells were prepared for [^{3}H]DA uptake. Cells were incubated in

the presence or absence of DHTB (1 μM), or mazindol (10 μM for nonspecific) for at least 10 minutes prior to addition of [^{3}H]DA. The uptake assay (final volume 0.5 ml) was initiated by the addition of 50 nM [^{3}H]DA and 2 μM DA in Krebs-HEPES buffer. Pargyline (monoamine oxidase (MAO) inhibitor) and tropolone (catechol-o-methyl transferase (COMT) inhibitor) were included in the buffer so that results could be compared with studies done using tissue from animals, which require the addition of MAO and COMT inhibitors. In previous studies, Vindis et al. (2000) found no evidence for MAO activity in HEK-293 cells, however, other studies suggest the presence of COMT activity in HEK-293 cells (Eshleman et al. 1997). Pifl et al. (1995) using African green monkey kidney (COS-7) cells, in the absence of MAO or COMT inhibitors, reported that 70-80% of the tritium released from hDAT cells and 80-90% of the tritium released from hDAT/rVMAT2 cells was [^{3}H]DA, suggesting that DA metabolites comprise only a small part of the recovered tritium. Therefore, recovered tritium will be referred to as [^{3}H]DA here. Assays were carried out at the temperatures indicated for time points ranging from 5 to 90 minutes. Experiments were terminated by aspiration and treatment with 250 μl of 0.1 M HCl. Radioactivity remaining in each well was determined using liquid scintillation spectrometry. Experiments were conducted with duplicate determinations.

[^{3}H]DA Saturation curve

Experiments were carried out as described for time course of [^{3}H]DA uptake experiments with the following exceptions. Experiments were conducted with concentrations of unlabelled DA ranging from 0-25 μM. Cells were preincubated with

drug(s) for 10 minutes. Assays were initiated by the addition of [^{3}H]DA (approximately 40 nM) and carried out at 22°C for 5 minutes.

Time Course of [^{3}H]DA Retention

Experiments were carried out as described for time course of [^{3}H]DA uptake experiments with the following exceptions. The uptake assay (final volume 0.5 ml) was initiated by the addition of 20 nM [^{3}H]DA in Krebs-HEPES buffer at 37°C. Mazindol was not present during [^{3}H]DA uptake in retention or release assays. [^{3}H]DA uptake continued for 60 minutes, the time required to reach steady-state, and was terminated by decanting the buffer.

After uptake, cells were washed once with 400 µl of buffer. The release assay was initiated by the addition of 400 µl of buffer with or without 1 µM DHTB. The buffer was aspirated at time points ranging from 0 to 90 minutes, 250 µl of 0.1 M HCl was added to the wells and radioactivity remaining in each well was determined by liquid scintillation spectrometry. All experiments were conducted with duplicate determinations, unless otherwise noted.

Drug-induced [^{3}H]DA Release

Cells were prepared as described for [^{3}H]DA release time course experiments, with the following exceptions. The release assay was initiated by addition of 400 µl of vehicle (Krebs-HEPES buffer with 0.75% DMSO for lobeline) with or without 1 µM DHTB and with or without drug (METH, lobeline, dopamine and p-tyramine, concentration ranges as indicated). This concentration of DMSO had no effect on [^{3}H]DA uptake or release (data not shown). For assays using cocaine to block drug effects on [^{3}H]DA release, cells were incubated for 10 minutes with cocaine prior to

initiation of release. The release assay was terminated after 30 minutes, the buffer was decanted, and 250 µl of 0.1 M HCl was added to each well.

Confocal Microscopy

Cells were grown on poly-l-lysine coated coverslips and fixed with 4% formaldehyde at 37°C for 20 minutes. Cells were rinsed two times with 2 mL of phosphate buffered saline (PBS: 0.1 M H_2PO_4, 150 mM NaCl pH 7.4) for and then blocked overnight with blocking solution (4% goat serum, 1% bovine serum albumin, 0.2% triton x-100) at 4°C. Cells were washed three times for 1 minute each with PBS at 22°C. Cells were incubated with primary antibody (DAT (anti-rat) 1:500 (Chemicon) and/or VMAT2 (anti-rabbit) 1:500 (Chemicon)) for 1 hour at 22°C. Cells were washed three times for 10 minutes each with PBS at 22°C. Cells were incubated with secondary antibodies (goat anti-rat 1:400 (alexa Fluor 488 (Invitrogen) and goat anti-rabbit 1:400 (alexa Fluor 594 (Invitrogen)). Cells were washed three times with PBS for 10 minutes at 22°C and then washed once with H_20 at 22°C. Slides were then mounted on coverslips and examined.

Data Analysis

Prism software (GraphPad Software, San Diego, CA) was used to analyze all kinetic, retention, and drug-induced release data, and Analysis of Variance (ANOVA) with Bonferroni post-tests. Data shown are mean ± SEM, except as indicated. T-tests (two-tailed, unpaired) were performed using Microsoft Excel (Microsoft Corp., Redmond, WA).

Results

HEK-hDAT cells were transfected with cDNA for the hVMAT2 and characterized for expression of hDAT and hVMAT2 using [^{125}I]RTI-55 or [^{3}H]DHTB respectively (Figure 2.1). Analysis of [^{125}I]RTI-55 binding to the hDAT indicated a B_{max} of 5.03 ± 0.44 pmol/mg of protein for the parent HEK-hDAT cell line, while HEK-hDAT-hVMAT2 cells had a B_{max} of 5.99 ± 1.52 pmol/mg of protein. No statistical difference between the parent and the cotransfected cell line, as measured by two-tailed Students t-test, was observed for the affinity or B_{max} of [^{125}I]RTI-55 binding (HEK-hDAT K_d = 2.96 ± 0.70 nM; HEK-hDAT-hVMAT2 K_d = 3.13 ± 1.07 nM). Cotransfected cells had a B_{max} of 2.80 ± 0.51 pmol/mg protein and a K_d of 8.91 ± 0.98 nM for [^{3}H]DHTB binding to the hVMAT2. HEK-hDAT cells also had specific [^{3}H]DHTB binding, with a K_d of 98.2 ± 22 nM and a B_{max} of 0.93 ± 0.32 pmol/mg protein. The binding to hDAT cells has a significantly lower ($p<0.05$) affinity and B_{max} ($p<0.05$) as compared to the cotransfected cells.

HEK-hDAT cells were further characterized to determine the presence or absence of functional hVMAT2 expression. [^{3}H]DA uptake time courses (2.02 μM DA total concentration; 20 nM [^{3}H]DA) at both 37°C and 22°C were carried out using HEK-hDAT and HEK-hDAT-hVMAT2 cells (Figure 2.2). This concentration of DA was chosen because it is close to the K_m for [^{3}H]DA uptake in attached cells (Saunders et al., 2000). At 37°C, but not at 22°C, HEK-hDAT-hVMAT2 cells exhibit increased [^{3}H]DA uptake as compared with DHTB treated cells. [^{3}H]DA uptake in HEK-hDAT cells was not affected by 1 μM DHTB. This concentration of DHTB was chosen to block the hVMAT2 because it is approximately 100 fold higher than the K_d for DHTB at the

Figure 2.1

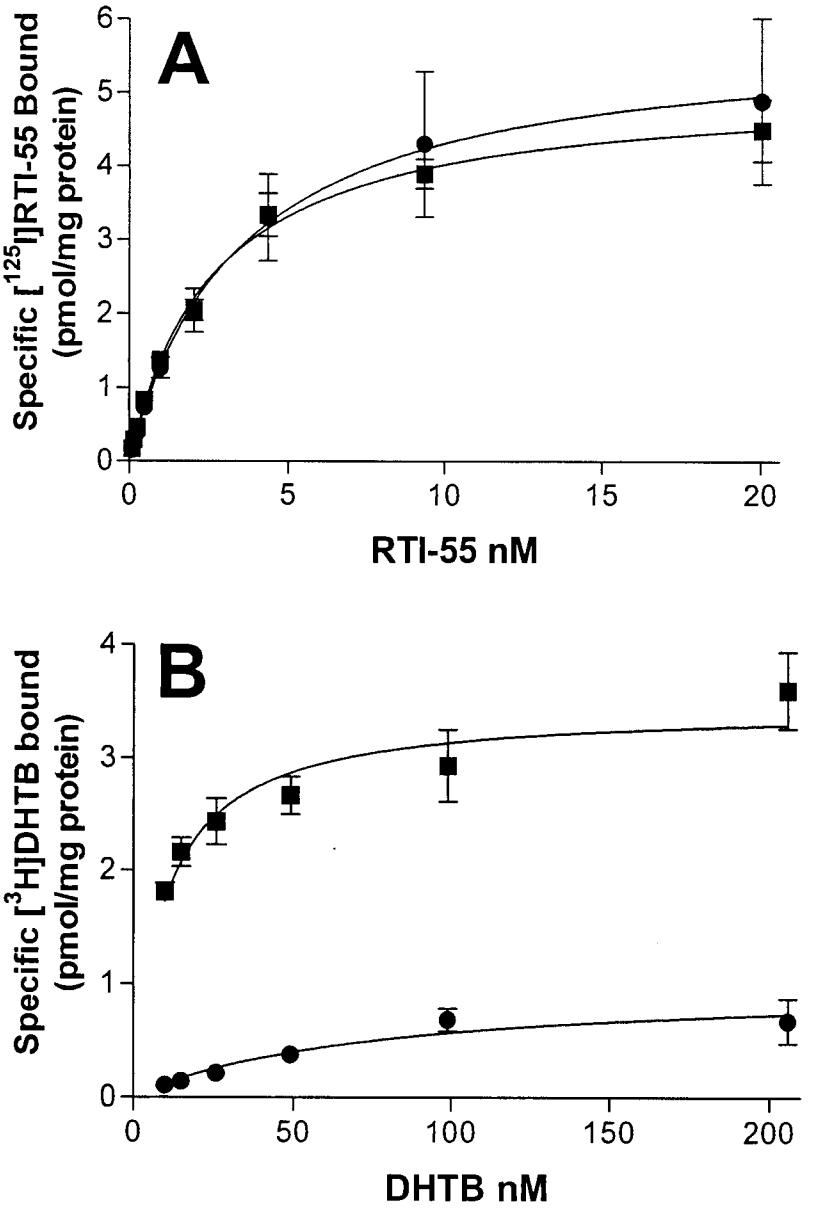

Figure 2.1: [^{125}I]RTI-55 and [^{3}H]DHTB binding to HEK-hDAT and HEK-hDAT-hVMAT2 cells. Experiments were carried out as described in the text. Solid squares (■) represent HEK-hDAT-hVMAT2 cells, solid circles (●) represent HEK-hDAT cells. A: [^{125}I]RTI-55 binding, B: [^{3}H]DHTB binding data shown are the average of at least three independent experiments conducted with duplicate determinations.

Figure 2.2

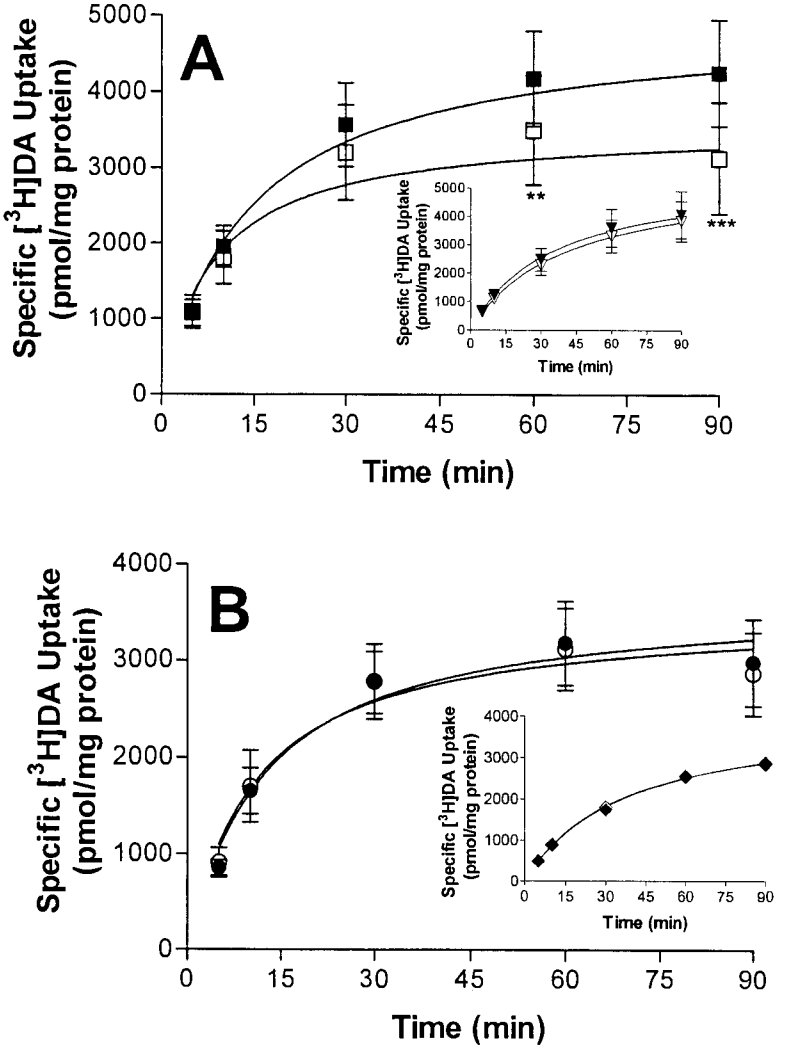

Figure 2.2: [^{3}H]DA uptake time course in HEK-hDAT and HEK-hDAT-hVMAT2 cells. A: Experiments were carried out at 37°C as described in the text. Solid squares (■) represent HEK-hDAT-hVMAT2 cells, open squares (□) represent HEK-hDAT-hVMAT2 cells treated with DHTB (1 μM). Inset: experiments were carried out at 22°C. Solid triangles (▼) represent HEK-hDAT-hVMAT2 cells, open triangles (▽) represent HEK-hDAT-hVMAT2 cells treated with DHTB (1 μM). Data shown are the mean of at least three independent experiments conducted with duplicate determinations. B: Assay was conducted at 37°C. Solid circles (●) represent HEK-hDAT cells, Open circles (○) represent HEK-hDAT cells treated with DHTB (1 μM). Inset: assay was conducted at 22°C. Solid diamonds (♦) represent HEK-hDAT cells, open diamonds (◊) represent HEK-hDAT cells treated with DHTB (1 μM).

hVMAT2 (see binding data above) and because hDAT function at this concentration was not affected.

No difference in the K_m values were found between HEK-hDAT cells or HEK-hDAT-hVMAT2-transfected cells under any of the conditions used to measure [^{3}H]DA uptake (Figure 2.3, Table 2.1). HEK-293 cells expressing only the hVMAT2 did not exhibit any specific uptake in saturation experiments (data not shown). Further, 1 μM DHTB did not affect the V_{max} for [^{3}H]DA uptake by HEK-hDAT cells. These data suggest that the low affinity [^{3}H]DHTB binding to HEK-hDAT cells is not a measure of hVMAT2 expression. Untreated HEK-hDAT-hVMAT2 cells had significantly increased [^{3}H]DA uptake at a DA concentration of 10 μM, when compared with DHTB treated cells (Figure 2.3).

Retention of [^{3}H]DA by HEK-hDAT-hVMAT2 cells and HEK-hDAT cells over time (Figure 2.4) was also assessed. HEK-hDAT-hVMAT2 cells had a significant decrease in [^{3}H]DA retention over time in the presence of DHTB (Figure 2.4). However, DHTB had no effect on [^{3}H]DA retention in HEK-hDAT cells (inset Figure 2.4).

The effects of hVMAT2 expression on [^{3}H]DA disposition were further investigated by inducing [^{3}H]DA release with METH under four conditions involving DHTB-induced blockade of the hVMAT2. As seen in Figure 2.2, when DHTB is present, there is a significant decrease in [^{3}H]DA uptake following a 60 minute incubation at 37°C. For release experiments, the 30 minute time point was chosen because it was the time at which there was a significant and reliable difference in [^{3}H]DA retention between untreated and DHTB treated HEK-hDAT-hVMAT2 cells (Figure 2.4).

Figure 2.3

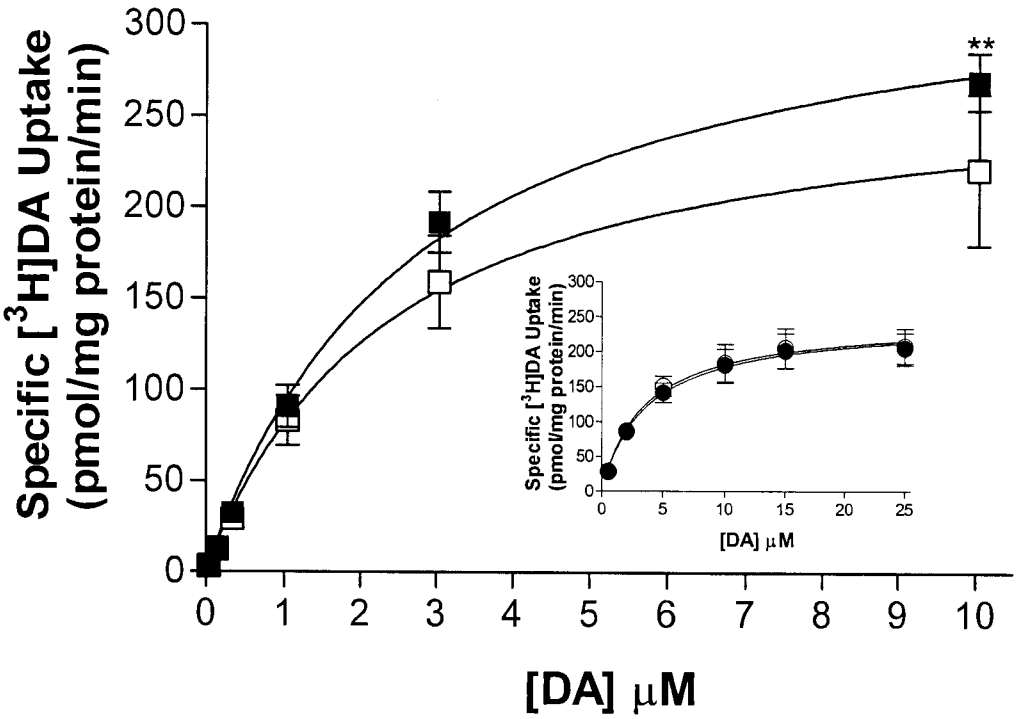

Figure 2.3: [^{3}H]DA uptake saturation curves in HEK-hDAT and HEK-hDAT-hVMAT2 cells. Experiments were carried out as described in the text. Solid squares (■) represent HEK-hDAT-hVMAT2 cells, Open squares (□) represent HEK-hDAT-hVMAT2 cells treated with DHTB (1 μM). Inset: Solid circles (●) represent HEK-hDAT cells, Open circles (○) represent HEK-hDAT cells treated with DHTB (1 μM). Data shown are the mean of at least three independent experiments conducted with duplicate determinations. Statistical analysis was carried out by two-way ANOVA followed by Bonferroni post-tests comparing uptake in the presence and absence of 1 μM DHTB. *$p<0.05$; **$p<0.01$

Figure 2.4

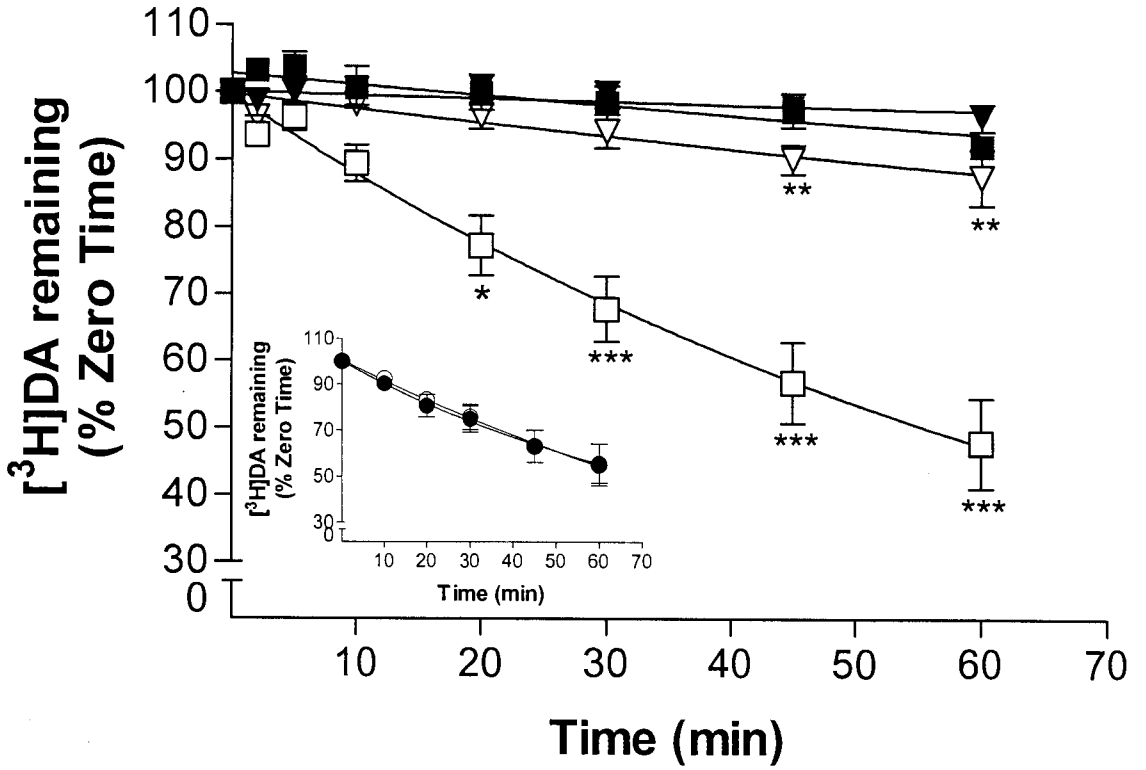

Figure 2.4: [^{3}H]DA efflux at 37°C and 22°C in the presence or absence of DHTB. [^{3}H]DA uptake was conducted for 60 minutes at 37°C in HEK-hDAT-hVMAT2 cells. Cells treated with 1 μM DHTB during [^{3}H]DA release at 22°C are shown in open triangles (▽), and cells treated with 1 μM DHTB during [^{3}H]DA release at 37°C are shown in open squares (□). Untreated cells kept at 22°C are shown in solid triangles (▼), and cells kept at 37°C are shown as solid squares (■). Lines were fit to a one-phase exponential decay. Inset: [^{3}H]DA efflux at 37°C in the presence or absence of DHTB from HEK-hDAT cells. Solid circles (●) represent HEK-hDAT cells, Open circles (○) represent HEK-hDAT-hVMAT2 cells treated with DHTB (1 μM). Each curve represents the average of at least three independent experiments conducted with duplicate determinations. Statistical analysis was carried out by two-way ANOVA followed by Bonferroni post-tests comparing release in the presence and absence of 1 μM DHTB at 37°C or at 22°C. *$p<0.05$; **$p<0.01$; ***$p<0.001$

There was no significant difference in METH-induced release between hDAT-hVMAT-transfected cells treated with DHTB during both uptake and release, as compared with cells treated with DHTB during uptake only. In both groups, 30 minutes of exposure to METH induced the release of only about 20% of the [^{3}H]DA (Figure 2.5, Table 2.2). In contrast, METH induced the release of 61% of the [^{3}H]DA in the cells that were treated with DHTB during the release phase of the experiment. This is a significant ($p<0.05$) increase in [^{3}H]DA release as compared to METH-induced [^{3}H]DA release from cells in the absence of DHTB. Significant differences in release between cells exposed to buffer during uptake and release, and cells treated with DHTB only during release, were observed at concentrations of METH above 2.5 μM (Figure 2.5, Table 2.2). The potency of METH shifted from 33.8 μM to 3.2 μM with the addition of DHTB during release. Thus, DHTB treatment only during release increases both the potency and the efficacy of METH-induced [^{3}H]DA release (see Figure 2.5, Table 2.1).

To determine if another drug that had previously been reported to interact with the VMAT2 had similar effects on efflux, the effects of lobeline were also examined (Figure 2.5, Table 2.2). At the highest concentration of lobeline tested (750 μM) and in the absence of DHTB, there was a 27% release of the [^{3}H]DA from the cells. The difference between untreated cells and cells treated with DHTB only during the release phase of the experiment reached statistical significance ($p<0.05$) at concentrations of lobeline above 250 μM. Under any conditions where DHTB was present, lobeline did not induce [^{3}H]DA release (Figure 2.5, Table 2.2).

An endogenous substrate and a trace amine were also tested for their effects on [^{3}H]DA retention in this system. DA and p-tyramine had similar maximal effects on

Figure 2.5

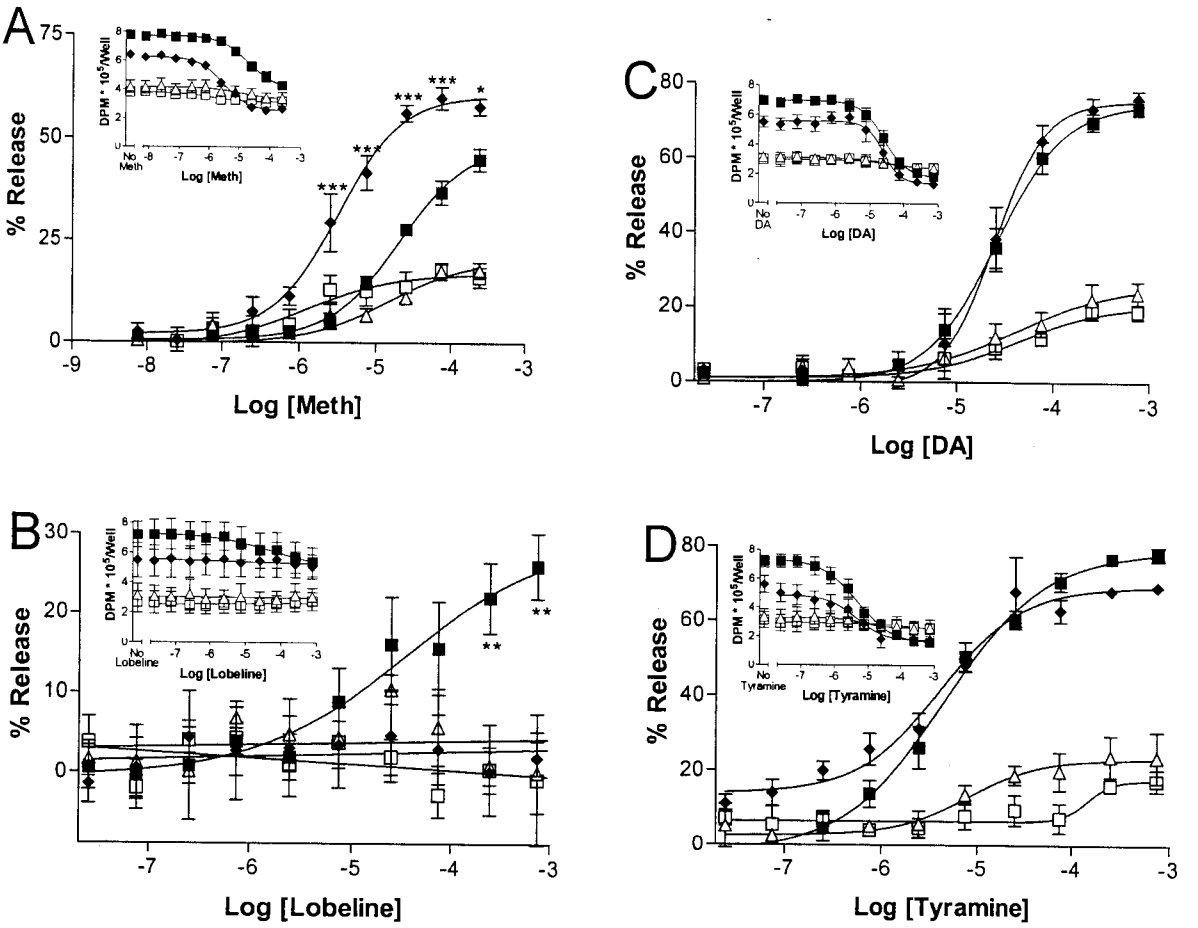

Figure 2.5: Drug-induced release in HEK-hDAT-hVMAT2 cells. [^{3}H]DA uptake was conducted for 60 minutes at 37°C in HEK-hDAT-hVMAT2 cells. There were four treatment groups in this experiment. Solid squares (■) denote untreated cells exposed to buffer (Krebs-HEPES) during uptake, and treated with drug at the indicated concentrations during release. Solid diamonds (♦) denote cells exposed to buffer only during uptake, and treated with various drug concentrations and 1 μM DHTB during release. Open triangles (Δ) denote cells treated with 1 μM DHTB during uptake, and with drug during release. Open squares (□) denote cells treated with 1 μM DHTB during uptake and with 1 μM DHTB and drug during release. Inset: represents the average DPM/well of each experiment. A: METH-induced release B: Lobeline-induced release C: DA-induced release D: P-tyramine-induced release. Data are expressed as a percentage of total [^{3}H]DA released in cells after 30 minutes of release in the absence of drug, and with the appropriate DHTB treatment. Sigmoidal dose-response curves were generated with Prism software. Curves represent the average of at least three independent experiments, each conducted with duplicate determinations. Statistical analysis was carried out by two-way ANOVA comparing release from cells exposed to buffer during both uptake and release (■) and release from cells exposed to buffer during uptake and DHTB during release (♦). *$p<0.05$; **$p<0.01$; ***$p<0.001$

[^{3}H]DA release, but differed in their potencies by roughly an order of magnitude, with p-tyramine being more potent than DA. Maximal effects for these drugs, in the absence of DHTB during uptake, were about 75% (Figure 2.5, Table 2.2). Unlike METH, DHTB treatment during release did not affect the potency or efficacy of DA or p-tyramine. Blockade of the hVMAT2 during [^{3}H]DA uptake resulted in a significantly decreased maximal effect of both DA and p-tyramine on [^{3}H]DA release, down to about 20-25%, as compared with cells that were not pretreated with DHTB (Figure 2.5, Table 2.2).

To further explore the effects of METH, lobeline, DA and p-tyramine on [^{3}H]DA disposition, HEK-hDAT cells were also examined for drug-induced [^{3}H]DA release. When 60 minutes of [^{3}H]DA uptake (steady-state) were followed by 30 minutes of drug-induced release, higher concentrations of lobeline blocked [^{3}H]DA efflux from HEK-hDAT cells (Figure 2.6). Similarly, METH, DA and p-tyramine caused only slight increases in [^{3}H]DA release (Figure 2.6). All of these affect in HEK-hDAT cells were minimal (approximately 5%).

In order to determine the physiological nature of the putative VMAT2-expressing vesicles, drug-induced [^{3}H]DA release was evaluated in the presence or absence of Ca^{2+} (figure 2.7). The absence of Ca^{2+} in the buffer had virtually no effect on drug-induced release. A relatively small increase in lobeline-induced [^{3}H]DA release was observed in the absence of Ca^{2+}.

Cocaine, a reuptake blocker, was examined for its ability to block drug-induced [^{3}H]DA release from HEK-hDAT-hVMAT2 cells. The concentration of cocaine chosen for these studies was approximately 30 times its IC_{50} for blocking uptake (Eshleman et al. 1995). Two concentrations of each releasing drug were chosen, one near the EC_{50} and

Figure 2.6

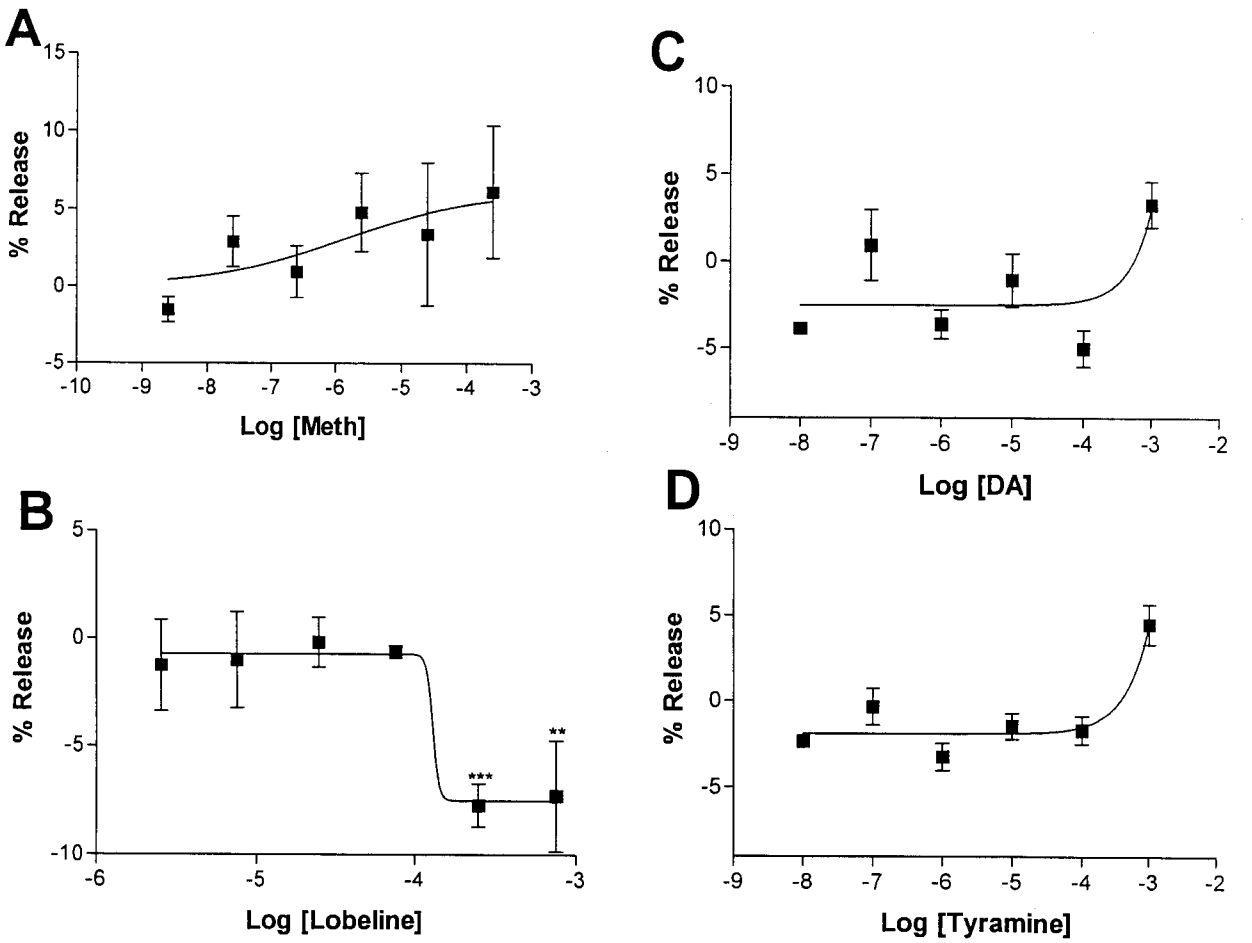

Figure 2.6: Drug effects on [^{3}H]DA release from HEK-hDAT cells. [^{3}H]DA uptake was conducted in buffer for 60 minutes at 37°C in HEK-hDAT cells. Release was carried out in buffer with concentration of drug added as indicated at 37°C. Curves are a representative graph of two independent experiments conducted with similar results (lobeline), or an average of at least three independent experiments (METH, P-tyramine and DA) conducted with triplicate determinations. Statistical analysis was carried out by two-way ANOVA comparing release from cells exposed to buffer during release. *p<0.05; **p<0.01; ***p<0.001

Figure 2.7

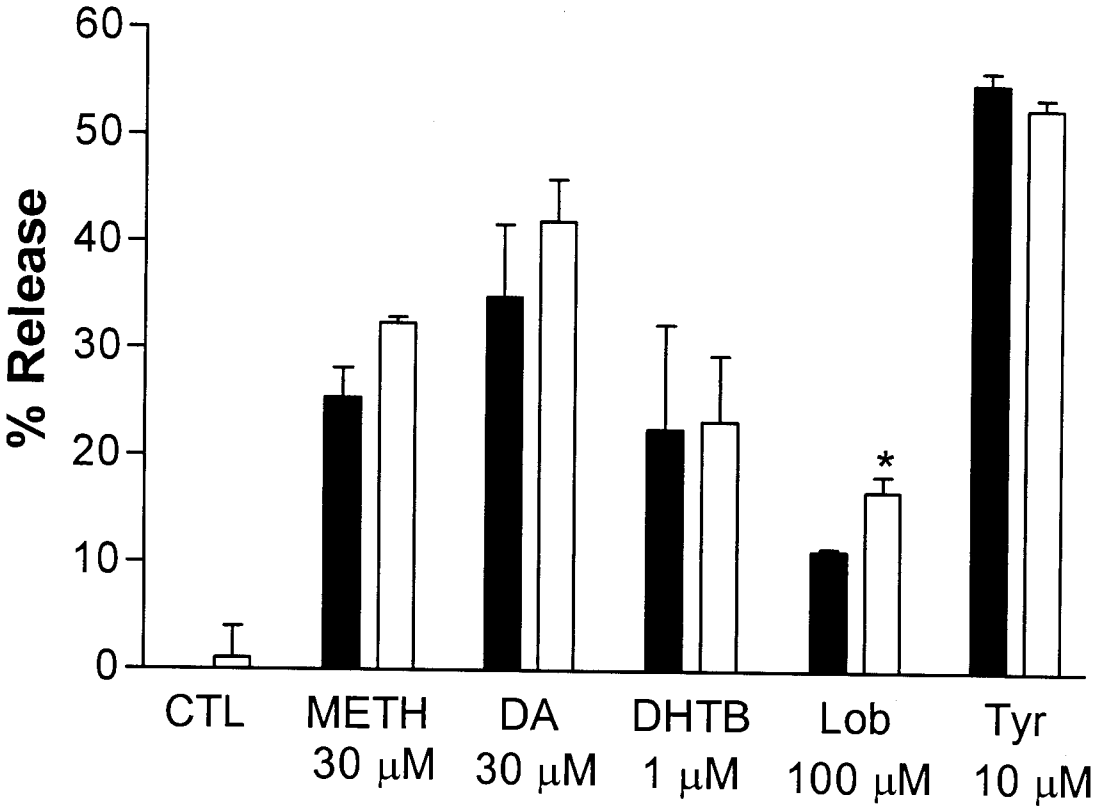

Figure 2.7: Effects of Ca^{2+} on drug-induced release from HEK-hDAT-hVMAT2 cells. [^{3}H]DA uptake was conducted for 60 minutes at 37°C. Closed bars represent cells exposed to Krebs-HEPES buffer containing 2.5 mM Ca^{2+} during drug-induced release. Open bars represent cells exposed to Krebs-HEPES buffer lacking 2.5 mM Ca^{2+} during drug-induced release. Drug-induced release was conducted for 30 minutes at 37°C. Data are an average of at least three independent experiments conducted with duplicate determinations. Statistical analysis was carried out using a two-tailed, unpaired student's T-test comparing treatments with or without Ca^{2+} present. *$p<0.05$

one near the maximal effect on release (Figure 2.8). Treatment with 10 μM cocaine resulted in a small but statistically significant loss of [^{3}H]DA (about 10%). Cocaine also significantly reduced tyramine-and DA-induced release. At this concentration of cocaine, there was no effect on methamphetamine- or lobeline-induced [^{3}H]DA release. A dose-response curve for cocaine's effects on METH-induced release was also constructed. Cocaine (750 μM) by itself induced release of approximately 15% of the available [^{3}H]DA. A high concentration of METH (100 μM) was used in order to elicit a maximal effect on release. A significant inhibition of METH-induced release was observed at concentrations of 25 μM cocaine and above (figure 2.9).

Confocal microscopy experiments examining immunolabelling by DAT and VMAT2 were performed on DAT and DAT-VMAT2 cells (Figure 2.10). DAT labeline was primarily localized to the cell surface. A small amount of background VMAT2 labeling was present in DAT cells. DAT-VMAT2 cells exhibited ubiquitous VMAT2 labeling.

Discussion

HEK-293 or HEK-hDAT cells do not express a functional hVMAT2, as demonstrated by a lack of high-affinity [^{3}H]DHTB binding sites, and the failure of DHTB to affect [^{3}H]DA uptake in HEK-hDAT cells. There is a significant DHTB-induced decrease in [^{3}H]DA uptake in HEK-hDAT-hVMAT2 cells in both the [^{3}H]DA uptake time course and [^{3}H]DA saturation experiments. This is not a result of functional cell surface expression of the hVMAT2; no specific uptake is seen in cells expressing only the hVMAT2 (data not shown). Therefore, the results suggest this difference is due to sequestration of intracellular [^{3}H]DA by the hVMAT2, which decreases the "effective"

Figure 2.8

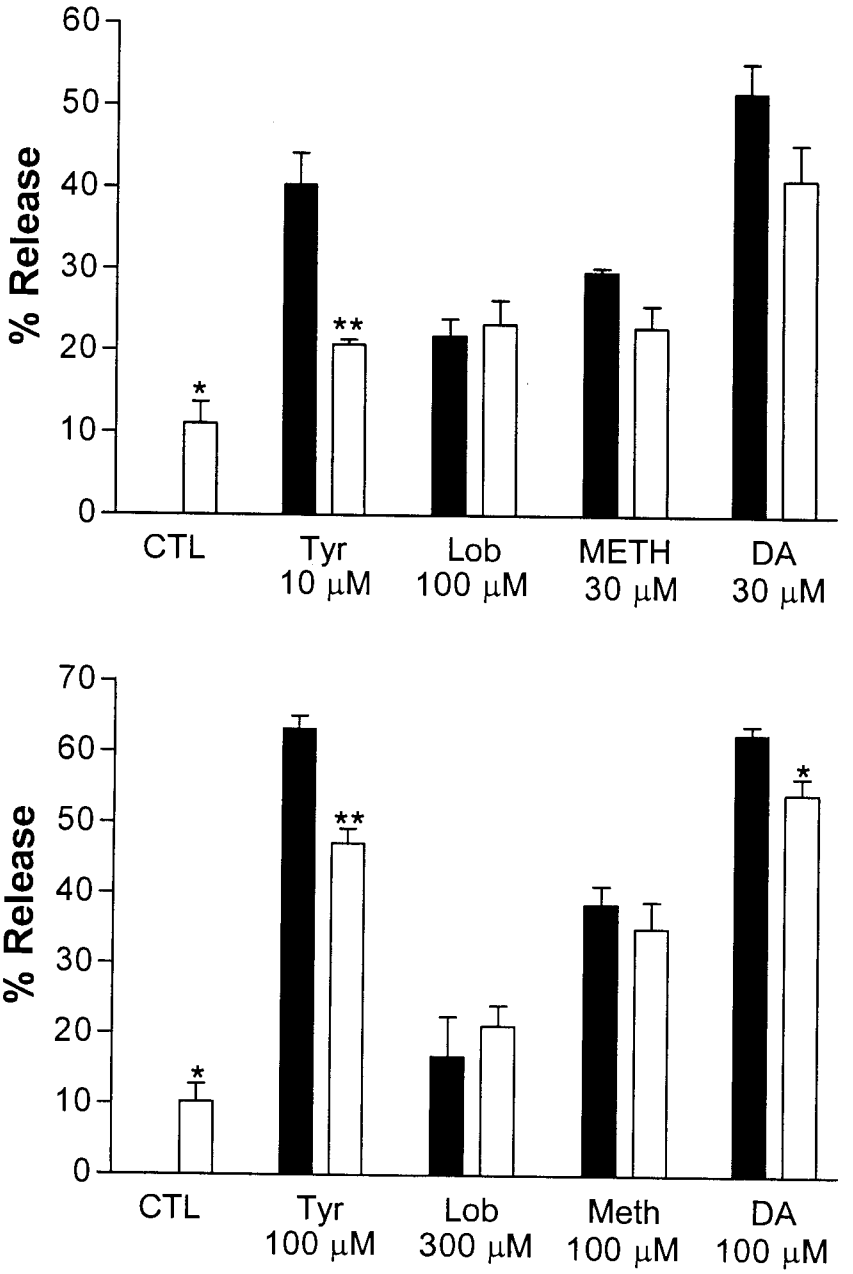

Figure 2.8: Cocaine antagonism of drug-induced release from HEK-hDAT-hVMAT2 cells. [^{3}H]DA uptake was conducted for 60 minutes at 37°C. Closed bars represent cells exposed to buffer for 10 minutes at 22°C prior to drug-induced release (with drug concentrations indicated). Open bars represent cells exposed to cocaine for 10 minutes at 22°C prior to and throughout drug-induced release (with drug concentrations indicated). Drug-induced release was conducted for 30 minutes at 37°C. Curves are an average of at least three independent experiments conducted with duplicate determinations. Statistical analysis was carried out using a two-tailed, unpaired student's T-test comparing each treatment in the absence or presence of 10 μM Cocaine. *$p<0.05$; **$p<0.01$

Figure 2.9

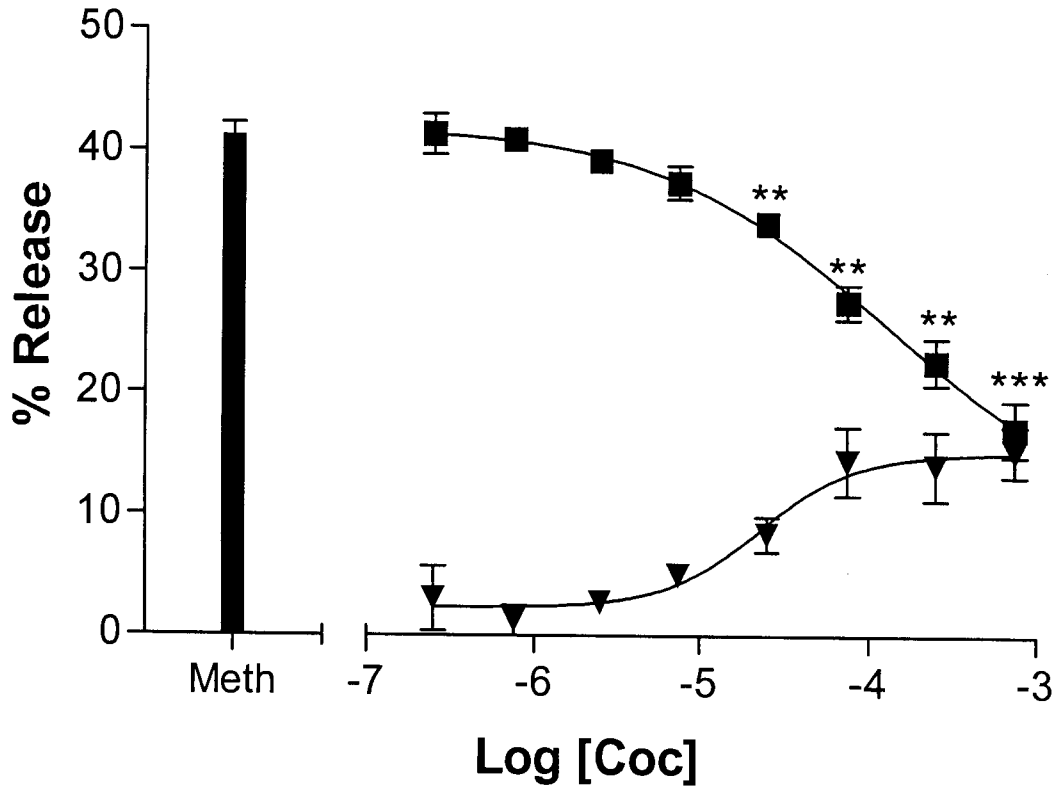

Figure 2.9: Cocaine antagonism of METH-induced release from HEK-hDAT-hVMAT2 cells. [^{3}H]DA uptake was conducted for 60 minutes at 37°C. Cells were incubated with cocaine (as indicated) for 10 minutes prior to treatment with METH. The solid bar represents the effect of 100 μM METH. Solid triangles (▼) represent cells exposed to cocaine only. Solid squares (■) represent the combined effect of 100 μM METH and cocaine (concentration indicated). Drug-induced release was conducted for 30 minutes at 37°C. Curves are an average of at least three independent experiments conducted with duplicate determinations. Statistical analysis was carried out using Student's t-test and comparing METH treatment to cotreatment with METH and cocaine. *$p<0.05$; **$p<0.01$; ***$p<0.001$

Figure 2.10

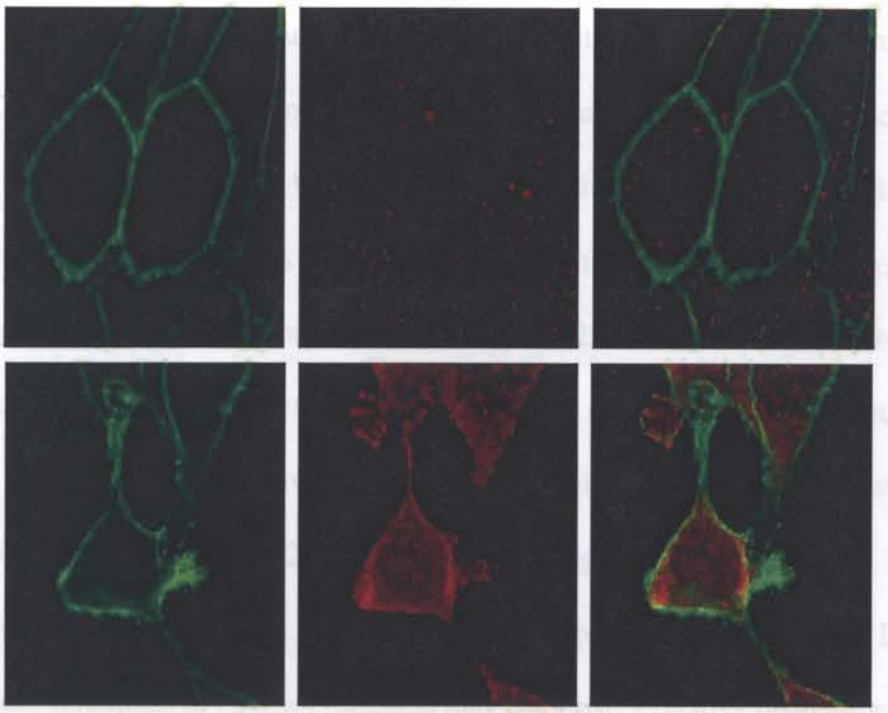

Figure 2.10 Confocal microscopy images of immunofluorescence labeling of DAT and VMAT2 in HEK-hDAT and HEK-hDAT-hVMAT2 cells. Top panels are HEK-hDAT cells, bottom panels are HEK-hDAT-hVMAT2 cells. Green labeling denotes DAT and red labeling denotes VMAT2. Left-most panels are labeling of DAT. Middle panels denote labeling by VMAT2. Right-most panels are an overlay of labeling by DAT and VMAT2.

cytoplasmic DA concentration, and results in an increase in the ability of the hDAT to accumulate more DA.

Previously, we characterized the ability of other cell expression systems to retain [^{3}H]DA. Monkey kidney Cos-7 cells and rat glioma C6 cells that expressed the hDAT were unable to retain [^{3}H]DA. In C6-hDAT cells, the efflux was so rapid that the cells could not be used in [^{3}H]DA release assays (Eshleman et al. 1994, Johnson et al. 1998). Coexpression of the hDAT and hVMAT2 in HEK-293 cells reveals both time- and temperature-dependent effects on [^{3}H]DA retention (Figure 2.4). Compared to untreated cells, DHTB-treated cells have significantly less [^{3}H]DA after 20 minutes at 37°C ($p<0.05$), and 45 minutes at 22°C ($p<0.01$). Although the effect is small at 22°C, it is augmented by an increase in temperature. The temperature dependence of DHTB-mediated inhibition of [^{3}H]DA retention may be due to a relative decrease in DAT and VMAT2 activity at temperatures that are significantly below physiological conditions (Vizi 1998). Therefore, transporter-mediated efflux will be reduced by a decrease in temperature. Blockade of the hVMAT2 with DHTB inhibits hVMAT2-mediated sequestration, allowing more rapid release of [^{3}H]DA. Furthermore, [^{3}H]DA retention by HEK-hDAT cells resembles that of DHTB-treated HEK-hDAT-hVMAT2 cells. The efflux profiles of HEK-hDAT-hVMAT2 cells suggests that activity of the hVMAT2 results in sequestration of [^{3}H]DA and the formation of a second pool of [^{3}H]DA.

With DHTB present during [^{3}H]DA uptake, METH released only 20% of the available [^{3}H]DA. In cells not treated with DHTB, or treated with DHTB during [^{3}H]DA release only, METH induced release of 51%, or 61% of available [^{3}H]DA, respectively. There was also an apparent increase in the potency of METH-induced efflux when

DHTB was present during the release portion of the experiment. During [^{3}H]DA uptake when the hVMAT2 was blocked, [^{3}H]DA could diffuse throughout the cell and become unavailable for release. In contrast, when the hVMAT2 was functioning, [^{3}H]DA could be concentrated and stored. The pool of [^{3}H]DA associated with hVMAT2 function may be more readily accessible to METH and other releasing drugs.

In the present study, the EC_{50} value of METH-induced [^{3}H]DA release was high (34 μM), compared to about 20 nM reported by Rothman et al. (2000) and Partilla et al. (2000) who used synaptosomal preparations. Unlike the present study, the synaptosomal preparations did not include a COMT inhibitor. Therefore, DA metabolism may play a role in the results obtained using synaptosomes. Further, reserpine, which alters DA disposition, was included in the synaptosomal studies. Other differences include the assay temperature (25°C versus 37°C here) and the use of attached cells here, versus the homogenized, centrifuged and resuspended preparations in synaptosomal studies. Lastly, there are receptors, trace amines and neuropeptides that may interact with METH or the preloaded [^{3}H]DA in the synaptosomal preparation. The model system described here allows measurement of direct effects of drugs on the transporters of interest.

Lobeline released 27% of the available [^{3}H]DA. The presence of DHTB completely blocked lobeline's effects. Therefore, the mechanism of lobeline-induced [^{3}H]DA release probably involves a direct interaction of the drug with the hVMAT2 and not with the hDAT. This hypothesis is supported by studies from Teng et al. (1998) who reported that lobeline displaces [^{3}H]DHTB from rat striatal synaptic vesicles, and Miller et al. (2001) who reported that lobeline enhances tritium overflow from rat striatal slices preloaded with [^{3}H]DA. Lobeline is a potential pharmacotherapeutic and has been used

to treat nicotine addiction. Some nicotinic acetylcholine receptors are located on norepinephrine neurons (Rao et al., 2003). Thus, lobeline might aid individuals addicted to nicotine by reducing the amount of norepinephrine available for release from vesicles. Therefore, when nicotine stimulates nicotinic acetylcholine receptors, in the presence of lobeline, less norepinephrine will be released. Our results support this hypothesis, and demonstrate a significant effect of lobeline on vesicular neurotransmitter storage.

The endogenous substrate DA and the trace amine p-tyramine had significant effects on [^{3}H]DA release. Interestingly, these drugs exhibit higher maximal effects on release than METH. Unlike METH, however, their effects on release are not additive with the effects of DHTB; DHTB treatment during release did not increase the potency or efficacy of either DA or p-tyramine on [^{3}H]DA release. METH might act as a weak base within vesicular structures to dissipate the proton gradient, thereby, decreasing vesicular content (Cubells et al. 1994). The finding that neither DA, nor p-tyramine, which like METH, are substrates for both the hDAT and hVMAT2, do not have additive effects when co-administered with DHTB during release, suggests that METH may be acting through an additional mechanism.

Drug-induced release of [^{3}H]DA was also carried out using HEK-hDAT cells. Lobeline did not enhance [^{3}H]DA release in these cells. At higher concentrations it weakly blocked [^{3}H]DA efflux. This finding confirmed the results from the HEK-hDAT-hVMAT2 studies, which suggested that lobeline interacts primarily with the hVMAT2. Likewise, METH, DA and p-tyramine induced only a small amount of [^{3}H]DA efflux (<10%) from HEK-hDAT cells, emphasizing the importance of the hVMAT2 in mediating the effects of METH. These data suggest that while efflux of [^{3}H]DA by

HEK-hDAT cells is robust, under these conditions, only a relatively small proportion of the [^{3}H]DA taken up is available for drug-induced release via the hDAT.

Our results are comparable to those of Pifl et al. (1995) who found that transient coexpression of hDAT and rVMAT2 caused an apparent shift in METH-induced release, as compared with cells expressing only the hDAT. Those authors also reported a similar rate of efflux between cells coexpressing both hDAT and rVMAT2, and cells expressing only hDAT. However, we found differences in [^{3}H]DA retention between stably expressing HEK-hDAT and HEK-hDAT-hVMAT2 cells, as well as differences between control and DHTB-treated (hVMAT2-blocked) HEK-hDAT-hVMAT2 cells. This may be due to differences in methods, or differences in relative transporter expression between the studies. The use of a transient expression system (Pifl et al. 1995) may prevent consistent levels of hDAT and hVMAT2 protein expression across experiments.

To further determine the physiological significance of hVMAT2 expression in this cell line, drug-induced release, as well as non-stimulated efflux, was compared in the presence and absence of Ca^{2+}. In this model system, no component of drug-induced, or tonic [^{3}H]DA efflux was Ca^{2+}-dependent, in contrast to neurons, where vesicles fuse with the plasma membrane in a Ca^{2+}-dependent process.

Drug-induced neurotransmitter release may be a distinct physiological process independent of the uptake mechanism. Despite cocaine's ability to effectively block DA uptake, it may not be effective as an inhibitor of release (Eshleman et al. 1994). Cocaine was most effective at blocking release induced by the trace amine p-tyramine. There was also a slight inhibition of DA-mediated [^{3}H]DA release by cocaine. Cocaine (10 μM) had no effect on METH-induced [^{3}H]DA release. However, higher concentrations of

cocaine blocked the METH effect. The mechanism through which cocaine antagonizes METH-induced release is not clear. It is possible that cocaine blocks METH-induced [^{3}H]DA efflux through the DAT. Another possibility however, is that cocaine simply blocks the ability of METH to interact with the hDAT, thereby limiting METH's ability to interact with the hVMAT2.

Our data indicate that stable coexpression of hDAT and hVMAT2 resulted in formation of a sequestered [^{3}H]DA pool that was sensitive to METH, lobeline, DA and p-tyramine. In this simple model system, the overwhelming majority of METH-, DA- and p-tyramine-induced [^{3}H]DA release appears to come from the sequestered pool of [^{3}H]DA. In release experiments where DHTB is applied during the uptake portion of the experiment, [^{3}H]DA is not retained well by cotransfected cells, and the magnitude of the drug-induced release is either completely blocked (lobeline), or reduced (METH, DA and p-tyramine), suggesting that sequestration of [^{3}H]DA is the result of functional expression of hVMAT2 and is important for the releasing effects of these drugs. METH is a substrate for both the hDAT and hVMAT2. Our data suggest that the ability of the hVMAT2, in this model system, to sequester [^{3}H]DA at high concentrations makes it an essential part of the mechanism of METH effects on DA disposition. This compares favorably with studies by Jones et al. (1998), who found that both the hVMAT2 and hDAT were important for amphetamine-induced release from striatal mouse slices, but that the rate-limiting step was the interaction of amphetamine with the hVMAT2. Thus, blocking METH interactions with the hVMAT2 may be a more relevant target for developing pharmacotherapies that effectively treat symptoms of METH intoxication, abuse, and withdrawal.

Table 2.1 [^{3}H]DA uptake

Treatment	HEK-hDAT-hVMAT2		HEK-DAT	
Uptake	K_m(μM)	V_{max}(pmol/mg/min)	K_m (μM)	V_{max}(pmol/mg/min)
Buffer	2.41 ± 0.54	430 ± 70	2.9 ± 0.80	240 ± 60
DHTB	2.09 ± 0.52	340 ± 50	2.1 ± 0.20	230 ± 70

Assays were conducted and analyses performed as described in the text. Buffer indicates that cells were preincubated in buffer prior to and during [^{3}H]DA uptake; DHTB indicates that cells were preincubated in DHTB (1μM) prior to and during [^{3}H]DA uptake. Values are the means from at least three independent experiments, each conducted with triplicate determinations.

Table 2.2 Potency and efficacy of drug-induced release in HEK-hDAT-hVMAT2 cells.

Treatment	Buffer-Buffer		Buffer-DHTB		DHTB-Buffer		DHTB-DHTB	
	EC_{50} (μM)	Max Effect (% Release)	EC_{50} (μM)	Max Effect (% Release)	EC50(μM)	Max Effect (% Release)	EC50(μM)	Max Effect (% Release)
METH	33.8 ± 1.6	51 ± 1%	3.2 ± 1.0	61 ± 2%	14.7 ± 5.5	20 ± 2%	9.71 ± 7.8	17 ± 2%
Lobeline	77 ± 65	27 ± 2%	ND	ND	ND	ND	ND	ND
DA	26.1 ± 4.8	74 ± 2%	25.1 ± 6.4	75 ± 2%	45.7 ± 9.7	28 ± 7%	40.4 ± 8.7	21 ± 2%
P-tyramine	1.5 ± 0.4	79 ± 2%	1.5 ± 0.2	73 ± 2%	3.1 ± 1.9	25 ± 6%	19.7 ± 8.9	16 ± 1%

Assays were conducted and analyses performed as described in the text. Buffer/Buffer indicates that cells were incubated in buffer during [^{3}H]DA uptake and during [^{3}H]DA release; Buffer/DHTB indicates that cells were incubated in buffer during [^{3}H]DA uptake and with DHTB (1μM) during [^{3}H]DA release, etc. The Maximal Effect is the amount of [^{3}H]DA efflux in the presence of METH or lobeline as compared to cells not treated with METH or lobeline. Values are the means from at least three independent experiments, each conducted with duplicate determinations. Values identified as "ND" indicate that the EC_{50} value or maximal effect were not determined due to the lack of drug effect.

III. Hydrogen ion concentration differentiates effects of methamphetamine and dopamine on transporter-mediated efflux

As published in the Journal of Neurochemistry

February 2006

ABSTRACT

Methamphetamine (METH) causes release of stored intracellular dopamine (DA). We explored the interactions of METH with the recombinant human vesicular monoamine (hVMAT2) and/or human DA transporters (hDAT) in transfected mammalian (HEK-293) cells and compared the findings with those for DA. In "static" release assays at 37°C, less than 20% of preloaded [^{3}H]DA was lost after 60 minutes, while nearly 80% of preloaded [^{3}H]METH was lost at 37°C under non-stimulated conditions. Results obtained by measuring substrate release using a superfusion apparatus revealed an even greater difference in substrate efflux. At pH 7.4, nearly all of the preloaded [^{3}H]METH was lost after just six minutes, compared with the loss of 70-80% of preloaded [^{3}H]DA (depending on cell type) after superfusion for 32 minutes. Increasing the extracellular pH from 7.4 to 8.6 had opposite effects on [^{3}H]DA and [^{3}H]METH retention. At pH 8.6, [^{3}H]METH was retained more effectively by both hDAT and hDAT-hVMAT2 cells, compared with results obtained at extracellular pH 7.4. [^{3}H]DA, however, was more effectively retained at pH 7.4 than at pH 8.6. These data suggest that DA and METH interact differently with the DAT and VMAT2, and require different H^+ concentrations to exert their effects.

Introduction

Primary targets of amphetamines (methamphetamine (METH), amphetamine, methylenedioxymethamphetamine (MDMA, ecstasy), etc.) are the cell surface monoamine neurotransmitter transporters for dopamine, norepinephrine and serotonin (DAT, NET, and SERT respectively)(Eshleman et al., 1999). The amphetamines act rapidly at these sites through an apparent reversal of transporter function and competitive inhibition of neurotransmitter interactions, but also affect long-term homeostasis by regulating the function and expression of these proteins (Eshleman et al., 1994, Johnson et al., 1998, Saunders et al., 1999). Electrophysiological and intracellular accumulation studies demonstrate that the amphetamines are substrates for these transporters, unlike other transporter antagonists such as cocaine and mazindol (Pifl, et al., 1999, Schuldiner et al., 1993, Sonders et al., 1997, Xie et al., 2000). Once inside the cell, amphetamines interact with the vesicular monoamine transporter (VMAT2). This protein, via a proton-dependent process, packages neurotransmitters into vesicles in preparation for stimulated release (Erickson et al., 1992). Vesicles provide a concentrated pool of neurotransmitter that can be effectively released into the intracellular milieu by amphetamines through pharmacological reversal, blockade of the VMAT2, or by decreasing the pH gradient (Pifl, et al., 1995, Wilhelm et al., 2004, Sulzer et al. 1990). Measuring inhibition of [^{3}H]reserpine binding, Schuldiner et al. (1993) found that the amphetamine derivatives fenfluramine and MDMA interact competitively for binding to the VMAT2. Unlike these drugs, however, p-chloroamphetamine (PCA) did not interact directly with the VMAT2. In addition, Peter et al. (1994) found that METH displaced [^{3}H]reserpine and blocked

serotonin uptake by the VMAT2. However, it is unclear from these studies whether METH and DA are transported and packaged by the VMAT2 in the same manner.

Previous reports indicate that both the DAT and VMAT2 are important for mediating the effects of the amphetamines on DA disposition (Pifl, et al., 1995, Wilhelm et al., 2004). Neurons isolated from VMAT2 null mutant mice have only a fraction of the amphetamine-induced DA release of neurons isolated from wild-type littermates (Fon et al., 1997). Therefore, to fully understand the actions of amphetamines on DA homeostasis, it is essential to study drug effects in a system expressing both the DAT and VMAT2. In the present study, we sought to characterize the differences between [^{3}H]DA and [^{3}H]METH disposition. Few studies have examined directly the uptake of METH or its analogs. Early studies found conflicting results, with some studies suggesting that the uptake of METH is not mediated by the DAT (Schmidt & Gibbs 1985). More recent studies, however, have clearly identified METH as a substrate. Zaczek et al. (1991a, 1991b) found uptake of [^{3}H]amphetamine into rat brain synaptosomes to be a high affinity, time- and temperature-dependent process. Uptake of [^{3}H]amphetamine was blocked by DA (257 nM), cocaine (172 nM), methylphenidate (53 nM), and GBR12909 (5 nM); both the rank order of potency and the high affinity blockade by GBR12909 (a DAT-specific antagonist) suggest that this transport is mediated by the DAT (Zaczek et al. 1991a & b). Likewise, Sitte et al. (1998) reported that intracellular accumulation of amphetamine is sensitive to oubain (a Na^+/K^+ ATPase inhibitor) and dependent on the extracellular sodium concentration. [^{3}H]METH uptake is blocked by cocaine at concentrations of METH below 100 μM (Xie et al., 2000). Using electrophysiological techniques, Sonders et al. (1997) found that amphetamine elicits a transport current similar to that of DA. These studies

underscore the similarity between DA and METH. To our knowledge, no studies have analyzed the retention of [^{3}H]METH in a simple model system expressing either the hDAT, or hDAT and hVMAT2.

Using both "static" and superfusion release methods, we found that [^{3}H]METH release was almost instantaneous and complete, but less than 10% of preloaded [^{3}H]DA was lost in "static" release assays (at 37°C), and as little as 70% of preloaded [^{3}H]DA was lost after 32 minutes of superfusion. We also examined whether a change in the extracellular pH could, by itself, affect the retention of [^{3}H]DA or [^{3}H]METH. Surprisingly, increasing the extracellular pH had opposite effects on METH and DA retention; at pH 8.6, [^{3}H]METH was better retained, while [^{3}H]DA efflux occurred more rapidly. Our findings suggest that these two substrates, though transported into the cells in a similar manner, are stored very differently.

MATERIALS AND METHODS

Materials

[^{3}H]DA (3,4-[7-^{3}H]dihydroxyphenylethylamine, 5.8–9.7 Ci/mmol) was purchased from Amersham Biosciences (Piscataway, NJ). [^{3}H]METH (Specific Activity 22.3 Ci/mmol) was generously supplied by the National Institute on Drug Abuse. Eco-Lume scintillation fluid was purchased from ICN biochemicals, Inc. (Aurora, OH). Dihydrotetrabenazene (DHTB) was purchased from American Radiolabeled Chemicals, Inc. (St. Louis, MO). 5-and 6-carboxyseminapthorhodofluor-1 acetoxymethyl ester (carboxy-SNARF-1 AM) was purchased from Molecular Probes (Eugene, OR). All water used in these experiments was purified by a Milli-Q system (Millipore Corp., Bedford, MA, U.S.A.). METH, pargyline, tropolone and most other chemicals were purchased from

Sigma-Aldrich (St. Louis, MO) or other commercial sources. The VMAT2 cDNA was generously provided by Dr. Robert Edwards, University of California at San Francisco.

Cell Culture

HEK-293 cells expressing the hDAT, or coexpressing the hDAT and hVMAT2 were transfected, selected and grown as previously described (Eshleman et al. 1995, Wilhelm et al., 2004). Cells were maintained in Dulbecco's modified Eagle's medium supplemented with 10% fetal bovine serum and 0.05 U penicillin/streptomycin. Cell stocks were grown on 15 cm diameter tissue culture dishes in 10% CO_2 at 37°C.

[^{3}H]DA Uptake

Cells were grown until confluent. The media was removed and cells were washed with 5 mL of calcium- and magnesium-free phosphate buffered saline (138 mM NaCl, 4.1 mM KCl, 5.1 mM Na_2HPO_4, 1.5 mM KH_2PO_4, 0.2% w/v glucose pH 7.3). Cells were removed from the plate by triturating and resuspended in 5-10 mL of Krebs-HEPES buffer (25 mM HEPES, 122 mM NaCl, 5 mM KCl, 1.2 mM $MgSO_4$, 2.5 mM $CaCl_2$, 1 μM pargyline, 100 μM tropolone, 2 mg glucose/ml, 0.2 mg ascorbic acid/ml, pH 7.4). The cells were centrifuged at 140 x g at 4°C for 10 min, and the supernatant was decanted. The cells were resuspended in Krebs-HEPES buffer, divided into multiple treatment groups and preincubated with drug (as indicated) for 10 minutes at 22°C. Uptake was initiated by the addition of 40 nM [^{3}H]DA at 37°C in a final volume of 2-3 ml, and was terminated after 60 minutes when the cells were centrifuged at 140 x g at 4°C for 10 min. The supernatant was discarded and the cells were resuspended in 2-3 ml of Krebs-HEPES buffer. Remaining radioactivity in the cell fraction was determined by liquid scintillation spectroscopy

(Beckman LS 3801). Experiments were performed with triplicate determinations unless otherwise indicated.

[^{3}H]METH Uptake Assay

Uptake assays were performed as described for [^{3}H]DA uptake assays with the following modifications. Assays were performed with 100-200 μg of protein per well. Uptake was initiated by the addition of 3 μM [^{3}H]METH (Specific activity 0.2 Ci/mmol) at 22°C. The cells were incubated for 60 min at room temperature. Assays were terminated by filtration through Wallac Filtermat A filters using a 96-well Tomtec cell harvester. Scintillation fluid (50 μl) was added to each filtered spot, and the radioactivity remaining on the filters was determined using a Wallac 1205 Betaplate scintillation counter. 10 μM mazindol was used to assess nonspecific uptake. Experiments were conducted with duplicate determinations.

[^{3}H]DA Release Assay

Cells were plated on poly-l-lysine coated 24-well plates and grown for at least 36 hours. Media was decanted and 400 μl of buffer was added to each well. Uptake was initiated by the addition of 20 nM [^{3}H]DA at 37°C in a final volume of 500 μl. Uptake continued for 60 minutes (steady-state), the buffer was decanted and cells were washed once with 400 μl of buffer. An additional 400 μl of buffer was added to initiate the release assay, which continued for times ranging from 0 to 60 minutes. For assays examining the effect of pH, cells were loaded for 30 minutes at 22°C and release of substrate was measured at 8 minutes. The assay was terminated by removal of buffer, followed by addition of 250 μl of 0.1 N HCl. The remaining radioactivity within each well was

determined by liquid scintillation spectroscopy. Experiments were performed with triplicate determinations unless otherwise indicated.

[^{3}H]METH Release Assay

Cells were grown as described above. Release assays were performed as described for [^{3}H]DA, above, except that [^{3}H]METH (20 nM) was used.

Superfusion Assay

Cells for superfusion assays were prepared as described for [^{3}H]DA uptake with the following exceptions: Uptake was initiated by the addition of 20 nM [^{3}H]DA plus 980 nM DA, or [^{3}H]METH plus unlabelled METH totaling 1 μM, at 22°C in a final volume of 1-2 mls Krebs-HEPES buffer at pH 7.4. Following centrifugation, cells were resuspended in 1-2 mls of Krebs-HEPES buffer (pH 7.4 or pH 8.6) with or without drug (30 nM GBR 12935 or 10 μM cocaine) and 280 μl were loaded into superfusion chambers containing polyethylene filter discs (Brandel) on the top and bottom of the chamber. Chambers were then placed into the Brandel 20-chamber superfusion apparatus. Sixteen two-minute samples of Krebs-HEPES buffer with or without drug (30 nM GBR 12935 or 10 μM cocaine) at pH 7.4 or pH 8.6 were collected. Samples contained about 1.1 ml of buffer (the liquid flow rate was 0.55 ml/min). Four additional fractions were collected following exposure of cells to 1% SDS. These latter fractions were collected in 2.5-minute intervals. The radioactivity within each fraction was determined by liquid scintillation spectroscopy. Experiments were performed with duplicate determinations unless otherwise indicated.

Fluorescent Measurement of Cytosolic pH

Measurement of cytosolic pH was conducted by a modification of the method of Holman et al. (2002). Briefly, hDAT or hDAT-hVMAT2 cells were grown to confluence on poly-l-lysine coated 12-well plates. Media was removed and cells were loaded with carboxy-SNARF-1 AM (5 μM) for 30 minutes at 37°C in Krebs-HEPES buffer at pH 7.4. Buffer was removed and cells were washed once with Krebs-HEPES buffer. Cells were exposed to high (8.6), or normal (7.4) pH Krebs-HEPES buffer for 32 minutes at 22°C. The pH-sensitive probe was excited at 488 nM with an argon laser and scanned using a Typhoon 9410 variable mode scanner. Fluorescence emissions were collected in series and emissions at 580-610 nm and 610-640 nm were collected using band-pass filters. The experiments were performed with triplicate determinations and the average emission ratio 580-610/610-640 was compared with a calibration curve. The calibration curve was acquired by measuring the signal ratios of carboxy-SNARF-1-AM-loaded hDAT and hDAT-hVMAT2 cells in high K^+ buffer (25 mM HEPES, 145 mM KCl, 0.8 mM $MgCl_2$, 1.8 mM $CaCl_2$, 5.5 mM glucose, pH 7.1, 7.4, 7.7, 8.0, 8.3 or 8.6) at different pHs following a 32-minute incubation at 22°C in the presence of 1 μM nigericin.

Data Analysis

The percent release of tritium outflow per minute (fractional release) was calculated by dividing the amount of radioactivity in a 2-min superfusate fraction by the sum total of the radioactivity recovered from all superfusion fractions in that experiment. Prism software (GraphPad Software, San Diego, CA) was used to analyze all kinetic and retention data, and analysis of variance (ANOVA) with Bonferroni post-tests. Data shown are mean

± SEM, except as indicated. T-tests (two-tailed, unpaired) were performed using Microsoft Excel (Microsoft Corp., Redmond, WA).

Results

HEK-293 cells expressing the hDAT, hVMAT2, or both transporters were characterized as previously described (Wilhelm et al., 2004, Eshleman et al., 1995, 2002). Significant differences in [^{3}H]DA uptake and retention were found between cells expressing only the hDAT and cells expressing the hDAT and hVMAT2 (Wilhelm et al. 2004). [^{3}H]DA uptake was sensitive to the hVMAT2-specific antagonist dihydrotetrabenazine (DHTB) in hDAT-hVMAT2 transfected cells, but not in hDAT transfected cells. No specific uptake of [^{3}H]DA was observed in attached cells expressing only the hVMAT2 (data not shown).

To characterize the integrity of the cell membranes when cells are in suspension (as used in subsequent superfusion experiments), [^{3}H]DA uptake experiments were conducted with hDAT and/or hVMAT2 transporter antagonists. Specifically, mazindol (10 μM; approximately 1000 times the IC_{50} for inhibition of [^{3}H]DA uptake (Eshleman et al. 1999)) was used to determine nonspecific uptake and DHTB (1 μM; approximately 100 times the K_d for DHTB binding to the hVMAT2 (Wilhelm et al., 2004)) was used to block specific interactions with the hVMAT2.

Figure 3.1 illustrates [^{3}H]DA uptake (40 nM) in cells expressing the hDAT, hVMAT2, or both transporters. Cells expressing only the hVMAT2 did not specifically accumulate [^{3}H]DA; [^{3}H]DA uptake was unchanged in the presence and absence of the VMAT2 blocker DHTB. Cells expressing the hDAT accumulated significantly higher levels of [^{3}H]DA in the absence of mazindol (4.3 ± 0.6 pmol/mg protein) compared to

Figure 3.1

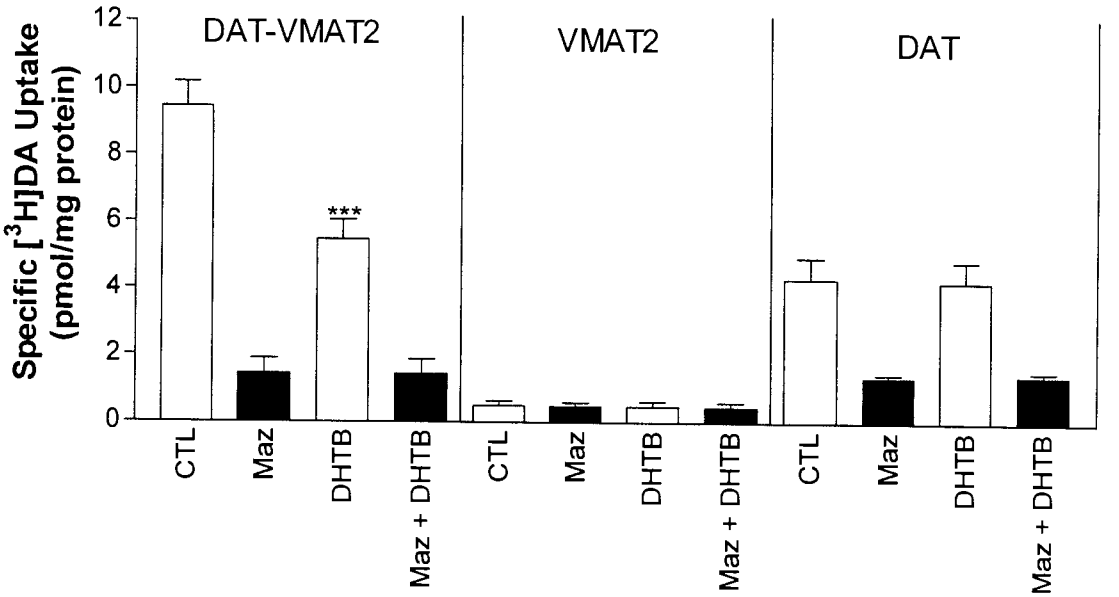

Figure 3.1. Uptake of [^{3}H]DA by multiple cell lines. Experiments were carried out as described in the text. CTL: cells exposed only to Krebs-HEPES buffer. Maz: cells treated with 10 μM mazindol. DHTB: cells treated with 1 μM DHTB. Maz + DHTB: cells treated with both mazindol (10 μM) and DHTB (1 μM). Data shown are the average ± SEM of at least three independent experiments conducted with triplicate determinations. ***$p<0.001$ denotes t-test two-tailed unpaired comparison of CTL versus DHTB conditions.

[^{3}H]DA accumulated in the presence of mazindol (1.3 ± 0.1 pmol/mg protein). DHTB did not affect [^{3}H]DA uptake by hDAT-expressing cells (4.3 ± 0.6 pmol/mg protein untreated versus 4.2 ± 0.6 pmol/mg protein with DHTB present), confirming that DHTB is VMAT2-specific and that there is no endogenous expression of hVMAT2 in these cells. In cells expressing the hDAT and hVMAT2, mazindol blocked specific uptake of [^{3}H]DA. No further decrease in uptake was measured in the presence of both mazindol and DHTB (1.4 ± 0.4 pmol/mg protein with mazindol only, versus 1.4 ± 0.4 pmol/mg protein with mazindol and DHTB present). This agrees with our previous study, as well as those of others who have coexpressed the hDAT and hVMAT2 in immortalized cells, and indicates that the hVMAT2 does not contribute directly to uptake of [^{3}H]DA, but rather sequesters intracellular [^{3}H]DA (Pifl et al., 1995, Wilhelm et al., 2004). Our previous report showed that the parent hDAT cell line, and the hDAT-hVMAT2 cell line express the hDAT at similar levels. Therefore, the significant differences in uptake between hDAT-hVMAT2 cells and hDAT cells (9.5 ± 0.7 pmol/mg protein versus 4.3 ± 0.6 pmol/mg protein respectively; $p<0.01$ Student's t-test two-tailed, unpaired), or hDAT-hVMAT2 cells treated with DHTB (9.5 ± 0.7 pmol/mg protein for untreated versus 5.5 ± 0.6 pmol/mg protein with 1 μM DHTB; $p<0.05$ Student's t-test, two-tailed, unpaired) can be attributed to the expression of a functional hVMAT2. Specific [^{3}H]DA uptake in hDAT-hVMAT2 transfected cells was 8.1 pmol/mg protein, more than twice the specific [^{3}H]DA uptake observed in hDAT cells (3 pmol/mg protein). Treatment of hDAT-hVMAT2 cells with DHTB decreased [^{3}H]DA uptake (5.5 ± 0.6 pmol/mg protein) to a level not significantly different than [^{3}H]DA uptake in hDAT cells (4.3 ± 0.6 pmol/mg protein). The above data

confirm that the integrity of the cells is maintained following the cell preparation protocol for superfusion, as described in the research methods.

Both hDAT and hDAT-hVMAT2 cells took up [^{3}H]METH in a mazindol-sensitive fashion (Figure 3.2). For both cell types, non-specific uptake in the presence of mazindol (10 μM) accounted for 36-41% of the total [^{3}H]METH taken up. At pH 7.4, specific uptake of [^{3}H]METH was 55.6 ± 18 pmol/mg protein and 61.0 ± 6.7 pmol/mg protein for hDAT and hDAT-hVMAT2 cells respectively. At pH 8.6, specific [^{3}H]METH uptake was unchanged in hDAT cells (61.8 ± 11.2 pmol/mg protein), while hDAT-hVMAT2 cells exhibited a significant increase in [^{3}H]METH uptake (103.6 ± 11.86 pmol/mg protein ($p<0.05$)).

We compared the retention of [^{3}H]DA and [^{3}H]METH in hDAT and hDAT-hVMAT2 cells (Figure 3.3A & B). Using attached cells grown in 24-well plates, less than 15% of preloaded [^{3}H]DA is lost from hDAT or hDAT-hVMAT2 cells after 10 minutes at either 22°C, or 37°C. In contrast, greater than 50% of [^{3}H]METH is lost after 10 minutes. Loss of preloaded [^{3}H]METH plateaus at 80-85% in both DAT and DAT-VMAT2 expressing cells after 20 minutes at 37°C in these "static" release assays (Figure 3.3B). The data for [^{3}H]METH retention at 37°C is best fit to a one-phase exponential decay model. At 22°C, the curves are better fit by a two-phase exponential decay model that includes a rapid loss of [^{3}H]METH within the first 10 minutes (50-60% of preloaded [^{3}H]METH is lost), followed by a slower, more linear efflux of substrate that continues through 60 min. At 22°C, hDAT cells lost only 20% of the preloaded [^{3}H]DA after 60 minutes, and lost about 40% of preloaded [^{3}H]DA at 37°C. Regardless of temperature, hDAT-hVMAT2 cells lost less than 10% of preloaded [^{3}H]DA over the full assay time

Figure 3.2

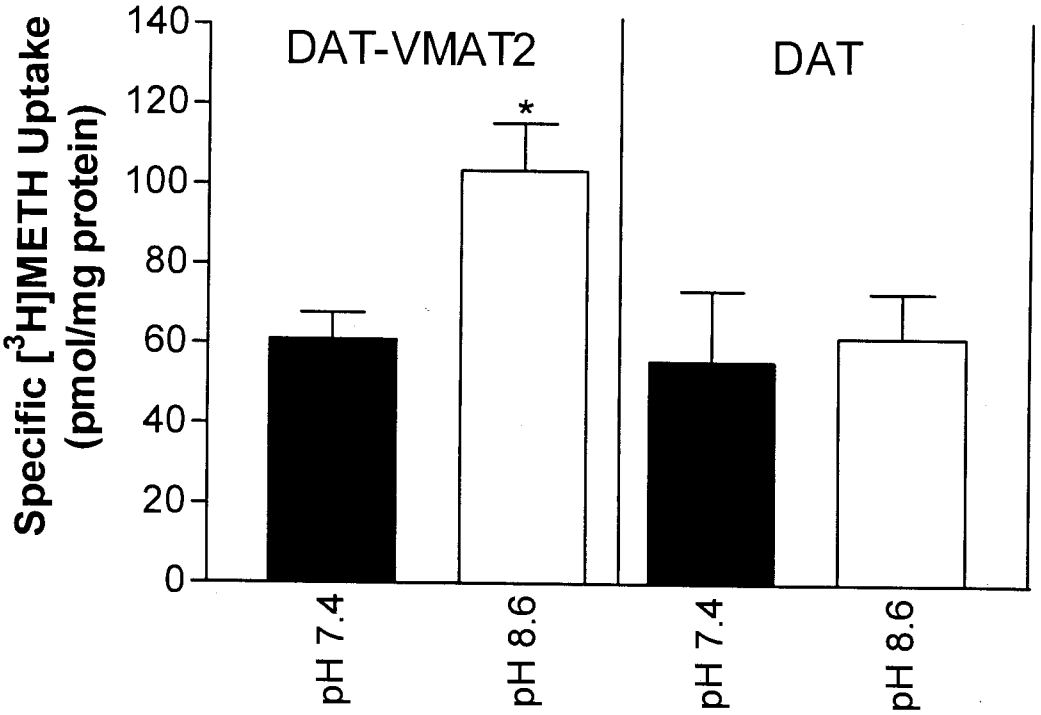

Figure 3.2. Effect of pH on uptake of [^{3}H]METH in hDAT or hDAT-hVMAT2 cells. Experiments were carried out as described in the text. Data shown are the average ± SEM of at least three independent experiments conducted with triplicate determinations. *$p<0.05$ denotes t-test two-tailed unpaired comparison of uptake at pH 7.4 versus uptake at pH 8.6.

Figure 3.3

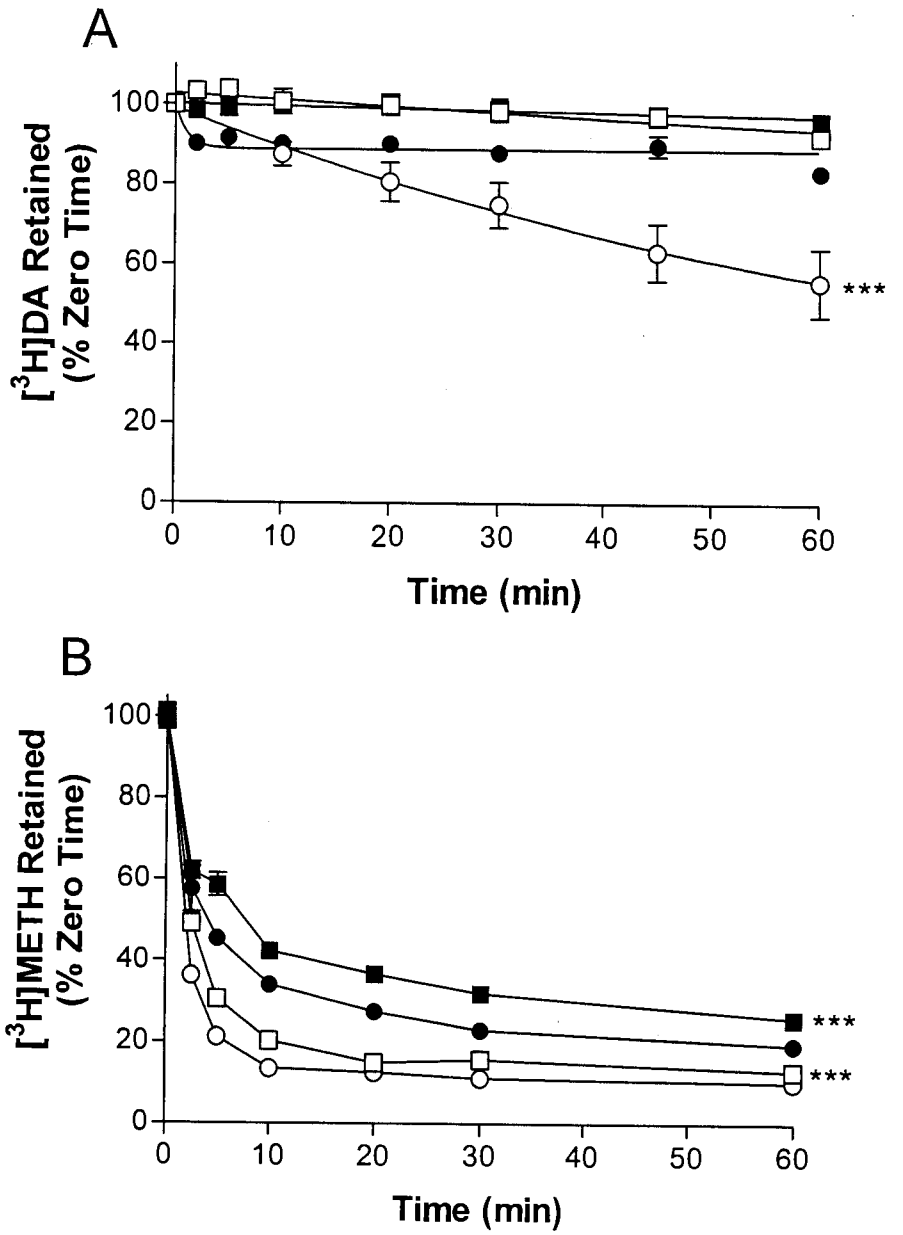

Figure 3.3 Retention of [^{3}H]Substrates in HEK-hDAT or HEK-hDAT-hVMAT2 cells at 22°C or 37°C in attached cells. Experiments were carried out as described in the text. Open squares (□) represent HEK-hDAT-hVMAT2 cells at 37°C. Closed squares (■) represent HEK-hDAT-hVMAT2 cells at 22°C. Open circles (○) represent HEK-hDAT cells at 37°C. Closed circles (●) represent HEK-hDAT cells at 22°C. A: [^{3}H]DA release B: [^{3}H]METH release. For [^{3}H]METH, data shown is a representative figure of an experiment that was repeated with similar results. For [^{3}H]DA, data shown is the average ± SEM of at least three independent experiments. ***$p<0.001$ denotes significant differences when comparing retention of [^{3}H]DA or [^{3}H]METH within cell types at 37°C versus 22°C. A portion of panel A was republished with permission from the American Society for Pharmacology and Experimental Therapeutics (Wilhelm et al., 2004).

course. The data suggest that there are major differences in the disposition of the [^{3}H]DA and [^{3}H]METH within hDAT and hDAT-hVMAT2 expressing cells.

The weak base action of METH results in the efflux of [^{3}H]DA from intracellular stores (Sulzer et al. 1995). Therefore, we hypothesized that altering the extracellular pH may similarly affect the retention of both [^{3}H]DA and [^{3}H]METH. Figure 3.4 illustrates the effect of pH on the retention of transporter substrates at 22°C. We chose this temperature because, as shown in figure 3.3, METH leaked more slowly and with lower efficacy at 22°C, than at 37°C. We chose the 8-minute time point because this is within the linear range of the [^{3}H]METH release time curve (figure 3.3B). In attached cell release assays, changes in extracellular pH did not affect retention of [^{3}H]DA, but significantly affected [^{3}H]METH retention. DAT expressing cells retained 27.8 ± 1.0% of the preloaded [^{3}H]METH at pH 7.4, compared with retention of 46.5 ± 1.1% at pH 8.6. The higher pH increased [^{3}H]METH retention by nearly 70% ($p<0.001$, t-test). At pH 7.4, hDAT-hVMAT2 cells retained 23.1 ± 1.5% of the preloaded [^{3}H]METH, compared with retention of 42.1 ± 1.2% of [^{3}H]METH at pH 8.6; a pH-induced increase of nearly 100% ($p<0.001$, t-test).

To determine if the observed differences in [^{3}H]DA and [^{3}H]METH retention were due to efflux, instead of a combination of efflux and reuptake, a superfusion technique was used. Figures 3.5-6 illustrate the retention of [^{3}H]DA or [^{3}H]METH by hDAT or hDAT-hVMAT2 cells. Superfusion assays can be divided into two distinct phases, the initial phase, which is a period of rapid loss of substrate and generally includes the first 2-3 fractions (4-6 minutes), and an equilibrium phase (26 minutes long), during which the recovered radioactivity has reached a plateau and generally shows little variation from

Figure 3.4

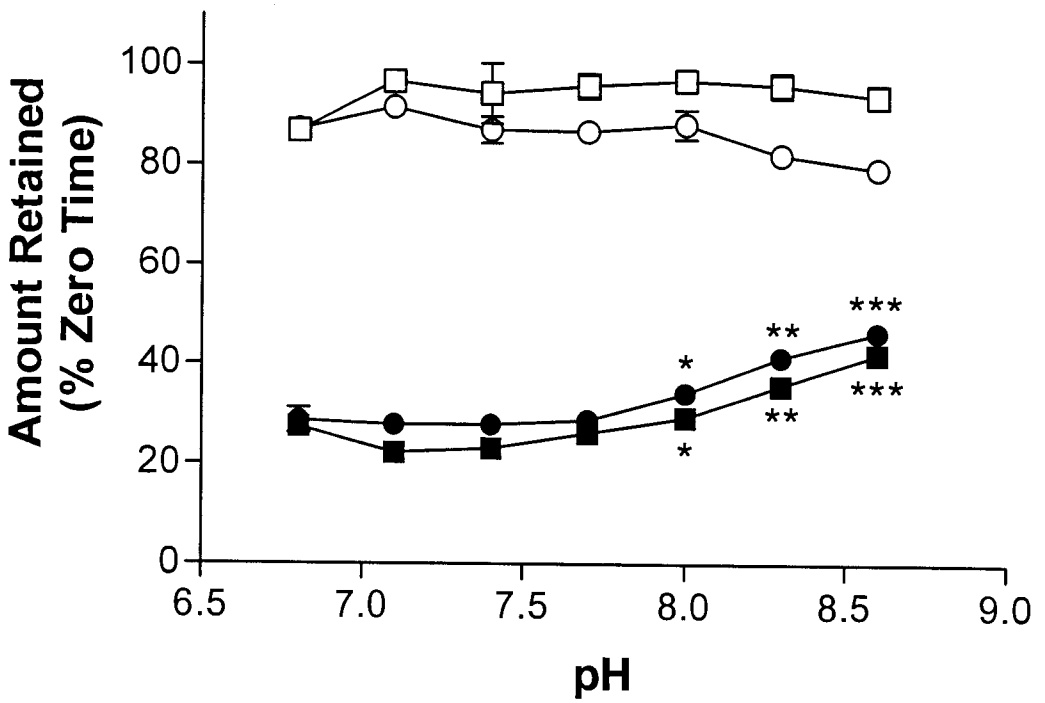

Figure 3.4. Effect of pH on retention of [^{3}H]substrates in attached cell assays at 22°C in HEK-hDAT or HEK-hDAT-hVMAT2 cells. Experiments were carried out as described in the text. Following [^{3}H]radioligand uptake, cells were exposed to the pH indicated on the x-axis for 8 min at 22°C. _Open squares (□) represent HEK-hDAT-hVMAT2 and open circles (○) represent HEK-hDAT cells loaded with [^{3}H]DA. Closed squares (■) represent HEK-hDAT-hVMAT2 cells and closed circles (●) represent HEK-hDAT cells loaded with [^{3}H]METH. Data shown is a representative figure of an experiment repeated with similar results. Comparisons are of the percentage of radioligand retained after eight minutes at the pH indicated, versus the percentage of radioligand retained after eight minutes at pH 7.4. * $p<0.05$, ** $p<0.01$, *** $p<0.001$ t-tests, two-tailed, unpaired.

Figure 3.5

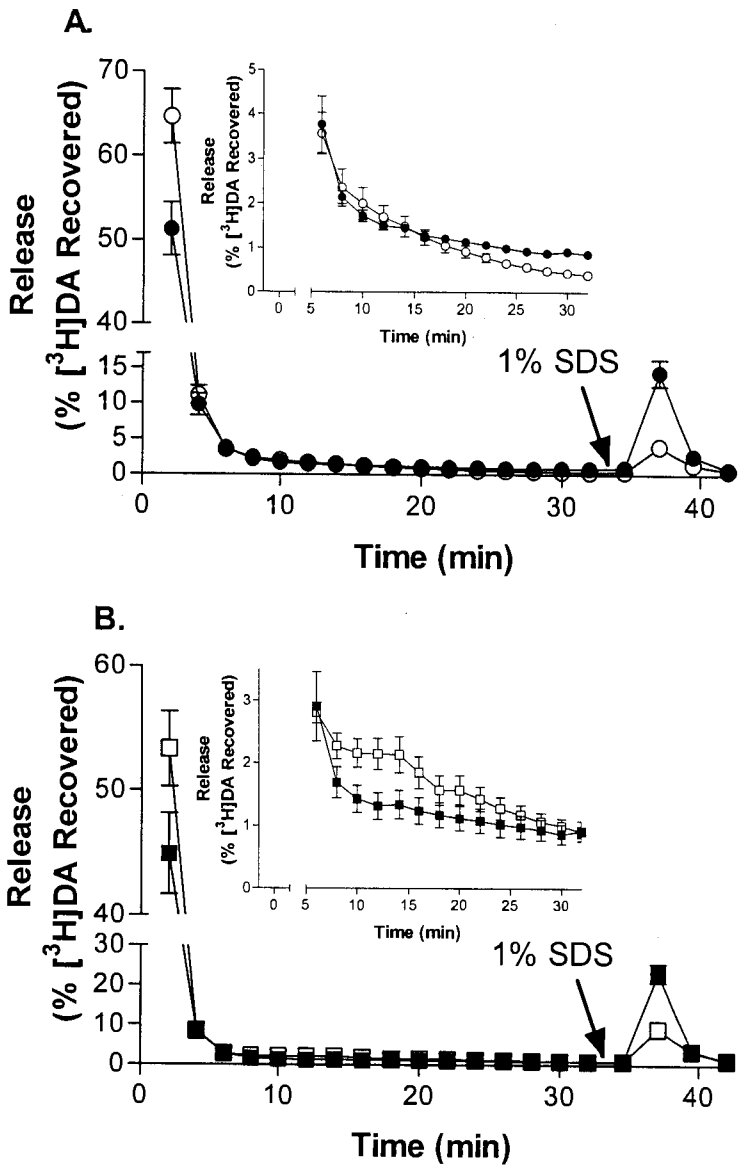

Figure 3.5: Analysis of pH effects on [^{3}H]DA retention in HEK-hDAT and HEK-hDAT-hVMAT2 cells. Experiments were carried out as described in the text. Open circles (○) represent HEK-hDAT cells superfused with buffer at pH 8.6. Closed circles (●) represent HEK-hDAT cells superfused with buffer at pH 7.4. Open squares (□) represent HEK-hDAT-hVMAT2 superfused with buffer at pH 8.6. Closed squares (■) represent HEK-hDAT-hVMAT2 cells superfused with buffer at pH 7.4. A: HEK-hDAT cells B: HEK-hDAT-hVMAT2 cells. *Insets* are the release time course from 6-32 min, which does not include SDS fractions (32-42 min). Data shown is the average ± SEM of at least three independent experiments conducted with duplicate determinations. The average [^{3}H]DA recovered from HEK-hDAT superfusion experiments was 89,900 DPM at pH 7.4 and 90,200 DPM pH 8.6. The average [^{3}H]DA recovered from HEK-hDAT-hVMAT2 superfusion experiments was 109,000 DPM at pH 7.4 and 110,000 DPM at pH 8.6.

Figure 3.6

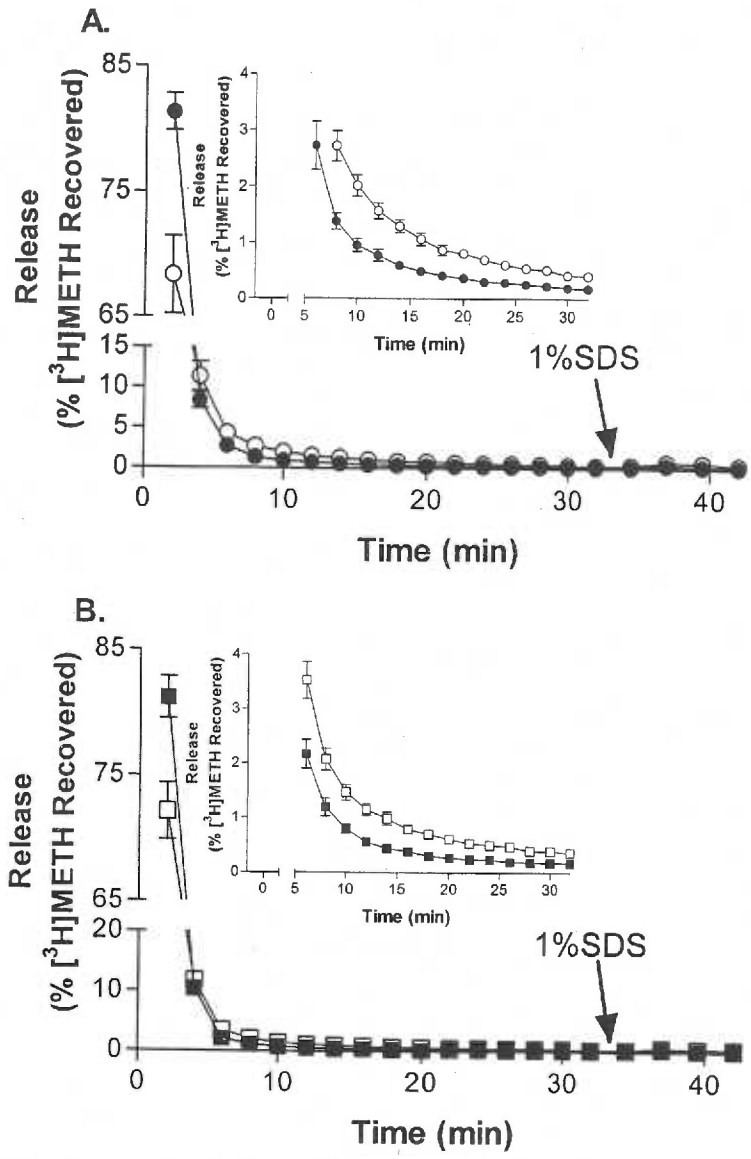

Figure 3.6: Analysis of pH effects on [^{3}H]METH retention in HEK-hDAT and HEK-hDAT-hVMAT2 cells. Experiments were carried out as described in the text. Open circles (○) represent HEK-hDAT cells superfused with buffer at pH 8.6. Closed circles (●) represent HEK-hDAT cells superfused with buffer at pH 7.4. Open squares (□) represent HEK-hDAT-hVMAT2 superfused with buffer at pH 8.6. Closed squares (■) represent HEK-hDAT-hVMAT2 cells superfused with buffer at pH 7.4. A: HEK-hDAT cells B: HEK-hDAT-hVMAT2 cells. *Insets* are the release time course from 6-32 min, which does not include SDS fractions (32-42 min). Data shown is the average ± SEM of at least three independent experiments conducted with duplicate determinations. The average [^{3}H]METH recovered from HEK-hDAT superfusion experiments was 49,000 DPM at pH 7.4 and 45,000 DPM pH 8.6. The average [^{3}H]METH recovered from HEK-hDAT-hVMAT2 superfusion experiments was 42,000 DPM at pH 7.4 and 43,000 DPM at pH 8.6.

fraction to fraction. Assays were terminated by exposure of cells to 1% SDS, which solubilizes the membranes, and allows for the recovery of any radioactivity remaining within the cells (10 minutes long, 4 fractions). Increasing the pH from 7.4 to 8.6 resulted in a greater loss of preloaded [^{3}H]DA from hDAT cells (Fig 3.5A). The largest difference is observed in the first fraction. At pH 7.4 the first fraction contains 51.3 ± 3.2%, compared with 64.6 ± 3.2% recovered in the first fraction at pH 8.6. The amount of [^{3}H]DA recovered following termination of the superfusion experiment and exposure to 1% SDS from hDAT cells exposed to pH 8.6 was 6.5 ± 0.6% compared with 19.0 ± 1.9% from hDAT cells exposed to pH 7.4 (Figure 3.7). hDAT-hVMAT2 cells had a similar increased loss of [^{3}H]DA in the first fraction at pH 8.6, but also exhibited subsequent loss of [^{3}H]DA between the 6 and 16 minute time points of the superfusion assay (Figure 3.5B).

There were also other differences in [^{3}H]DA retention between hDAT and hDAT-hVMAT2 cells. A higher percentage of the total [^{3}H]DA is recovered in the first fraction from hDAT cells than from hDAT-hVMAT2 cells independent of pH (51.3 ± 3.2% and 64.6 ± 3.2% at pH 7.4 and 8.6 respectively in hDAT cells, versus 44.9 ± 3.2% and 53.0 ± 3.0% for pH 7.4 and 8.6 respectively, in hDAT-hVMAT2 cells). In contrast, more [^{3}H]DA is recovered in the SDS fractions from hDAT-hVMAT2 cells than hDAT cells (at pH 7.4, 19.0 ± 1.9% recovered (hDAT), versus 28.8 ± 2.3% (hDAT-hVMAT2) $p<0.01$, at pH 8.6, 6.5 ± 0.6% recovered (hDAT) versus 14.7 ± 1.6% (hDAT-hVMAT2) $p<0.001$) indicating that the hVMAT2 increases the ability of cells to retain [^{3}H]DA. At pH 7.4, the equilibrium fractions recovered from hDAT cells gradually decreased from a high of 4% at 6 min (fraction 3), down to a low of about 1% at 32 min (fraction 16). This is in contrast to hDAT-hVMAT2 cells at pH 7.4, which exhibit nearly a constant efflux of 1-1.5% of the

total [^{3}H]DA recovered from 10 min (fraction 5) through 32 min (fraction 16). In hDAT-hVMAT2 cells, the curve generated at pH 7.4 had a rapid loss of [^{3}H]DA, followed by a prolonged and relatively small (about 1%) leakage of substrate, while at pH 8.6 the initial rapid loss of [^{3}H]DA is followed by a prolonged efflux of about 2% (8-16 minute fractions). This finding demonstrates that increased pH has a time-dependent component that is found only in hDAT-hVMAT2 cells, and a rapid component that is present in hDAT and hDAT-hVMAT2 cells.

Figure 3.6 (A & B) illustrates the differences in [^{3}H]METH retention as measured in superfusion assays at pH 7.4 or pH 8.6. In [^{3}H]METH superfusion experiments, there is no large SDS fraction peak at the end of the assay. In contrast to [^{3}H]DA, essentially all of the preloaded [^{3}H]METH is lost during the course of the initial and equilibrium phases of the experiment. In hDAT and hDAT-hVMAT2 cells, more [^{3}H]METH is lost from the first fraction at pH 7.4, than at pH 8.6 (81.4 ± 1.5% at pH 7.4 versus 68.4 ± 3.1% at pH 8.6 in hDAT cells, $p<0.05$; 81.2 ± 1.5% at pH 7.4 versus 72.2 ± 2.3% at pH 8.6 in hDAT-hVMAT2 cells, $p<0.05$). In subsequent fractions, more [^{3}H]METH is recovered at pH 8.6, than at pH 7.4 in both cell types. Therefore, [^{3}H]METH is retained for a longer amount of time at pH 8.6, than at pH 7.4 largely due to the decreased [^{3}H]METH recovered in the first fraction at pH 8.6 compared with pH 7.4. To summarize, the increased retention of [^{3}H]METH at pH 8.6 versus pH 7.4 is seen as a decrease in the amount of [^{3}H]METH recovered in the first fraction and subsequent increases in the amount of [^{3}H]METH recovered in the following fractions (Figure 3.6 A & B). There are essentially no differences between the [^{3}H]METH superfusion curves for hDAT and hDAT-hVMAT2 cells. This is in contrast to the superfusion curves for [^{3}H]DA, which illustrated clear

differences between the cell types. Also, as mentioned above, increasing the pH from 7.4 to 8.6 results in better retention of [^{3}H]METH, an effect that is opposite to the effect of pH on [^{3}H]DA efflux.

To determine if substrate efflux was transporter mediated, cells were incubated with DAT antagonists. Figure 3.7 includes the effect of GBR 12935 (30 nM) or cocaine (10 μM) treatment on [^{3}H]DA or [^{3}H]METH retention. Both GBR 12935 and cocaine significantly increased [^{3}H]DA recovered in SDS fractions from hDAT cells at pH 8.6. For both drugs, the effect is due to a decrease in the amount of [^{3}H]DA recovered in the first fraction (data not shown). No effect on [^{3}H]DA retention was observed in hDAT-hVMAT2 cells. Cocaine caused a significant reduction in [^{3}H]METH recovered at pH 8.6 in hDAT-hVMAT2 cells.

We used the pH-sensitive fluorescent probe, SNARF, to detect changes in intracellular pH in response to changes in extracellular pH. Cells were exposed to Krebs-HEPES buffer at either pH 7.4, or pH 8.6 for 32 minutes. hDAT-hVMAT2 cells exhibit a higher intracellular pH than DAT cells when exposed to pH 7.4 (7.75 ± 0.03 versus 7.52 ± 0.06 respectively; $p<0.05$). Following exposure to Krebs-HEPES buffer at pH 8.6, there was not a significant difference between cell types, however, the intracellular pH of both hDAT and hDAT-hVMAT2 cells was significantly increased (Table 3.1).

DISCUSSION

The focus of these experiments was to determine the differences in disposition between [^{3}H]DA and [^{3}H]METH in a simple model system expressing either the hDAT, or both the hDAT and hVMAT2. DA and METH are substrates for the hDAT and are structurally similar, hence the initial hypothesis that disposition of these two molecules

Figure 3.7

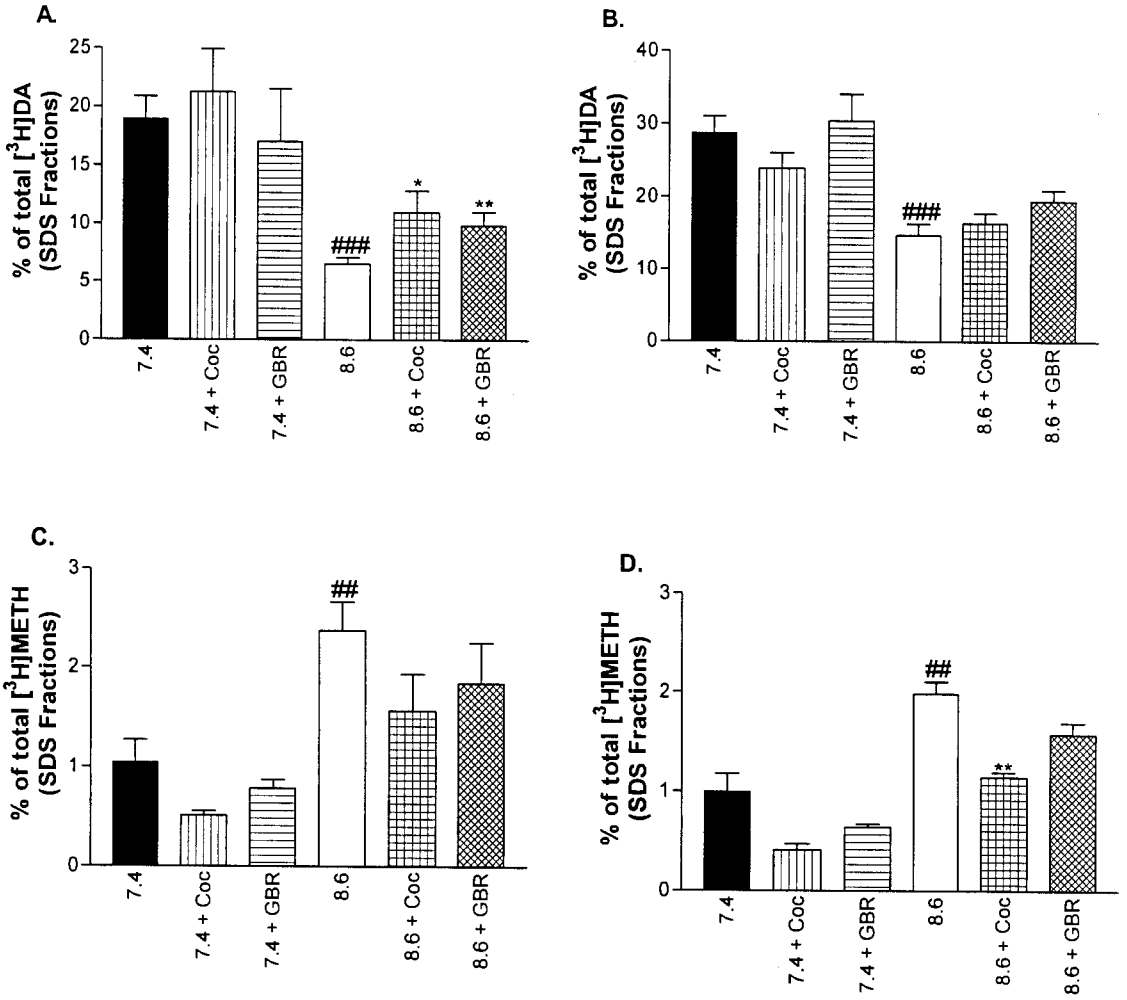

Figure 3.7. [^{3}H]Substrate recovered from SDS fractions of HEK-hDAT and HEK-hDAT-hVMAT2 cells during superfusion. Coc indicates that cocaine (10 μM) was present following resuspension and loading of cells and throughout the superfusion assay. GBR indicates that GBR 12935 (30 nM) was present following resuspension and loading of cells and throughout the superfusion assay. A. The percentage of the total [^{3}H]DA recovered from SDS fractions from HEK-hDAT cells under each condition described. A: The percentage of the total [^{3}H]DA recovered from SDS fractions from HEK-hDAT cells under each condition described. B: The percentage of the total [^{3}H]DA recovered from SDS fractions from HEK-hDAT-hVMAT2 cells under each condition described. C: The percentage of the total [^{3}H]METH recovered from SDS fractions from HEK-hDAT cells under each condition described D: The percentage of the total [^{3}H]METH recovered from SDS fractions from HEK-hDAT-hVMAT2 cells under each condition described Data shown are the mean ± SEM of at least three independent experiments repeated with similar results. * $p<0.05$; **$p<0.01$ t-test two-tailed unpaired, comparison of % tritium recovered with drug versus % tritium recovered without drug at the same pH. ## $p<0.01$; ###$p<0.001$ t-test two-tailed unpaired, comparison of % tritium recovered at pH 7.4 versus pH 8.6.

would be similar (Pifl et al., 1999, Sonders et al., 1997). The results described above suggest otherwise.

The first set of experiments confirmed that cells retain membrane integrity following the procedure required for superfusion. The data demonstrated that hVMAT2 cells do not specifically take up [^{3}H]DA, indicating that hVMAT2 expression does not affect the surface transport of [^{3}H]DA into HEK-293 cells. hDAT and hDAT-hVMAT2 cells exhibited specific [^{3}H]DA transport that was sensitive to mazindol. Treatment with the VMAT2 antagonist, DHTB, had no effect on hDAT cells, but reduced [^{3}H]DA uptake in hDAT- hVMAT2 cells to the same level observed in hDAT-transfected cells. Thus, the cells remained intact and viable following removal from culture plates and preparation for superfusion. The data also demonstrated that function of the hVMAT2 is required to alter [^{3}H]DA homeostasis in hDAT-hVMAT2 cells.

We also determined the effect of external pH changes on the uptake of [^{3}H]METH. Changes in extracellular pH did not affect [^{3}H]METH uptake in hDAT cells. hDAT-hVMAT2 cells showed a significant increase in [^{3}H]METH uptake at pH 8.6 compared with pH 7.4. This suggests that increasing the extracellular pH and subsequently the intracellular pH (Table 3.1) results in greater association of [^{3}H]METH with the hVMAT2. The hVMAT2 associates with acidic intracellular compartments (Eshleman et al., 2002). Concentration of [^{3}H]METH inside these compartments could enhance the ion trapping phenomenon (see below for further discussion) and lead to increased compartmentalization of [^{3}H]METH, thereby allowing more [^{3}H]METH to be accumulated within the cell.

Differences in substrate retention by hDAT or hDAT-hVMAT2 cells were examined. The data indicated that unlike [^{3}H]DA, [^{3}H]METH is not effectively retained by

cells expressing the hDAT or hDAT-VMAT2. In attached cells, about 80% of the preloaded [^{3}H]METH was released after only 20 minutes. In contrast, most of the preloaded [^{3}H]DA was retained after 20 minutes.

Studies by Sulzer and Rayport (1990) indicated that amphetamine and similar psychostimulants reduce the pH gradient required for substrate transport into vesicles by the VMAT2. This and similar findings were the foundation of the weak base hypothesis, which proposes that METH may disrupt the proton gradient required for VMAT2 function, resulting in decreased concentrations of vesicle-sequestered DA, and an increased concentration of cytosolic DA (Sulzer et al. 1995). Alteration of the intracellular pH will exert effects on the hVMAT2 because its function is directly coupled to a proton gradient. However, the effects of pH on the cell surface DAT are unclear. Uptake of DA was not affected between pH 7.0 and pH 8.2 (Berfield et al., 1999). Lowering the pH (pH<7.0), resulted in a decrease in the K_m, a decreased uptake velocity at 56 nM [^{3}H]DA, but no change in the V_{max}. Thus, an ionizable amino acid residue within the transporter was likely responsible for the observed [^{3}H]DA uptake pH profile. This suggests that the DAT may have a pH sensor(s). Cao et al. (1997; 1998) explored a pH-sensitive transport current that is associated with the rat, but not human forms of the serotonin transporter (SERT). At acidic pH, transport-associated currents were potentiated. A threonine residue at position 490 on the rat SERT was necessary for pH sensitivity, and a glutamic acid residue at 493 was responsible for the potentiation of the transport-associated current. The threonine residue at position 490, which conferred pH sensitivity, is present in the hDAT, but the glutamic acid residue at position 493, which mediates the pH-induced potentiation of transport-associated current is lacking in the hDAT.

As described in the results above, there are two distinct effects of pH on [^{3}H]DA disposition. The most robust of these is on the hVMAT2, which requires a proton gradient to transport substrates. The effect is seen as an elevation in the [^{3}H]DA recovered in equilibrium fractions (8-16 minutes) at pH 8.6 compared to pH 7.0 (Figure 3.5). The different superfusion profiles (over time and/or pH) between hDAT cells and hDAT-hVMAT2 cells suggest that increased extracellular pH may result in reversal of DAT function. In hDAT cells, the effect of increasing pH occurs very rapidly and disappears completely after 6 minutes. In contrast,hDAT-hVMAT2 cells exhibit both a difference in the first fraction, as well as differences in later fractions (8-16 minutes). While [^{3}H]DA taken up by hDAT-hVMAT2 cells may be sequestered by the hVMAT2 into "vesicle-like" compartments, this phenomenon does not occur in hDAT cells, leaving the [^{3}H]DA available for immediate release. Thus, an amino acid pH sensor (Cao et al., 1998) in the DAT may respond to alterations in pH homeostasis by enhancing reversal of transport. Further evidence is provided by the ability of GBR 12935 (30 nM) and cocaine (10 μM) to block pH-induced [^{3}H]DA efflux from hDAT cells (Figure 3.7), thereby providing pharmacological evidence that this phenomenon of DAT-mediated, pH-induced efflux could be a protective mechanism in DA neurons. Under conditions where there is an excess of cytosolic DA due to METH exposure or other interference with intracellular DA homeostasis, DA would accumulate in the cytosol and could increase the intracellular pH (DA pK_{a1} = 8.86, pK_{a2} = 10.5 (Berfield et al. 1999)). The change in pH could alter hDAT function by enhancing outward transport, thereby decreasing the intracellular concentration of DA and the resulting DA-induced oxidative stress.

No previous studies have examined the effect of pH on release. "Static" release experiments demonstrated a pH-induced increase in the amount of [^{3}H]METH retained over time that was not mirrored by an increase in [^{3}H]DA retention. Superfusion experiments identified an effect of pH on [^{3}H]DA retention that was not apparent in the "static" release assays. In "static" release assays, the cells were attached to 24 well plates, and released [^{3}H]DA remained in the extracellular milieu and was still available for reuptake. In contrast, the constant flow of buffer by the superfusion apparatus washed away released substrate. At pH 8.6, [^{3}H]DA is not retained within cells as effectively as it is at pH 7.4. The data suggests the possibility that a pH-induced change in the conformation of the transporter may be responsible for the enhanced [^{3}H]DA release at pH 8.6.

In superfusion experiments, cells expressing both the hVMAT2 and hDAT lost a smaller amount of [^{3}H]DA relative to cells expressing the hDAT alone. These results compare favorably with those of Pifl et al., (1995) who found that [^{3}H]DA is better retained within HEK-293 cells transfected with both the hDAT and a rat isoform of the VMAT2, than in cells transfected with the hDAT alone. This indicates that the hVMAT2 is packaging [^{3}H]DA intracellularly, thereby enhancing retention.

Retention of [^{3}H]METH was nearly identical in both hDAT and hDAT-hVMAT2 cells indicating that although METH exerts effects on the hVMAT2, it is not sequestered in a fashion similar to that of DA. Peter et al. (1994) reported that METH displaced [^{3}H]reserpine binding to the VMAT2, suggesting that METH interacts directly with the VMAT2. Knoth et al. (1984) found that transport of tyramine by chromaffin granule cells that express the VMAT1, a transporter that is highly homologous to the VMAT2, was

significantly decreased compared with transport of DA. They concluded that two aromatic hydroxyl groups on phenethylamines, though not required for transport, are required for effective storage and accumulation. This compares favorably with the data for METH, a molecule that is similar to DA, but lacks both of the aromatic hydroxyl groups. The observed differences in the storage of METH and DA may be explained by the ability of METH to alleviate the pH gradient required by the VMAT2 for transport of substrates. Another possibility is that METH may not be a substrate for the VMAT2, or, as proposed for tyramine by Knoth et al. (1984), METH may be transported by the VMAT2, but it may not be effectively stored due to its lack of aromatic hydroxyl groups.

In superfusion experiments, [^{3}H]METH remained within cells for a greater period of time at pH 8.6, compared to pH 7.4. This rules out the possibility that cell death or decreased membrane integrity at pH 8.6 is responsible for the loss of [^{3}H]DA. In superfusion experiments at pH 7.4, nearly all of the loaded [^{3}H]METH is washed out after only 6 minutes, in contrast to a loss of 70-80% of total [^{3}H]DA over the entire 32 minute superfusion assay (depending on whether or not the VMAT2 is coexpressed). [^{3}H]METH recovered from cells following solubilization by SDS represented 0.4-2.4% of the total [^{3}H]METH recovered.

The pH effect on [^{3}H]METH retention may be due to ion trapping, a phenomenon whereby a basic molecule such as METH (pK_a = 9.9) prefers more acidic environments. Increasing the extracellular pH would make the intracellular pH acidic relative to the outside of the cell, leading to increased [^{3}H]METH retention. Following exposure of cells to pH 8.6 for 32 minutes, intracellular pH increased in both hDAT and hDAT-hVMAT2 cells by nearly 0.5 pH units (0.48 and 0.54 pH units respectively). This translates into a

greater than 3-fold decrease in the intracellular hydrogen ion concentration. Therefore, the driving force for protons through the hVMAT2 and into the cytosol will be increased and may result in the transport of protons without the counter-transport of substrate. This could lead to a decrease in the ability of the hVMAT2 to store substrates and result in the net accumulation of substrate in the cytosol. Another possibility is that an increase in the intracellular pH may result in a conformational change in the hVMAT2 due to the presence of ionizable amino acid residues, resulting in a hVMAT2 protein that has a lower affinity and/or lower efficacy for the transport of substrates. Also, the substrates themselves are sensitive to pH (see below). According to the Henderson-Hasselbach equation ($pH = pK_a +$ log ($METH/METH^+$)), the relative abundances of METH in the neutral and cation forms are 0.3% and 99.7% respectively at pH 7.4. Increasing the pH to 8.6 leads to an increase to 4.8% in the neutral form of METH and to a decrease in the cationic form to 95.2%. The increase in the neutral form of METH at pH 8.6 would increase the probability of diffusion across the membrane, resulting in increased loss of [^{3}H]METH. The results, however, demonstrate that [^{3}H]METH remains in cells longer at pH 8.6, than at pH 7.4, likely due to the ion trapping phenomenon described above. Neither cocaine, nor GBR 12935 blocked [^{3}H]METH efflux at pH 7.4 or pH 8.6 or [^{3}H]DA efflux at pH 7.4. Leakage of [^{3}H]DA in hDAT and hDAT-hVMAT2 cells at pH 7.4 may be due to nonspecific mechanisms, which could explain the inability of cocaine and GBR 12935 to block this phenomenon. Surprisingly, cocaine (30 μM) decreased the amount of [^{3}H]METH recovered from the SDS fractions (i.e., increased release into previous fractions) of hDAT-hVMAT2 cells. Despite the use of a superfusion apparatus, substrate reuptake is still possible, though much less so than in "static" release systems. The difference in [^{3}H]METH recovered at pH 8.6

with or without cocaine is about 1% and may be explained by the ability of cocaine to block reuptake of [^{3}H]METH. The inability of GBR 12935 or cocaine to block the efflux of [^{3}H]METH suggests that this efflux may not be DAT-mediated. Thus, diffusion may play a larger role in efflux of [^{3}H]METH.

An increase in the neutral form of [^{3}H]DA may contribute to the increased loss of [^{3}H]DA observed at pH 8.6. The ability of GBR 12935 and cocaine to block pH-induced [^{3}H]DA efflux, however, argues against diffusion being the major source of [^{3}H]DA loss. Ion-trapping, similar to that with METH, may occur with DA as well. DA has multiple ionic forms: cation, zwitterion, neutral and anion. At a given pH, the prevalence of each ionic form can be calculated using the following equations (Berfield et al., 1999, Mack and Bönisch, 1979 and Armstrong and Barlow 1976):

$$\% \text{ neutral} = 100/(1 + \text{antilog}(pK_{a1} - pH) + \text{antilog}(pH - pK_{a2})$$

% neutral is composed of the neutral and zwitterions forms, with a ratio of 1:7.83 respectively (Armstrong and Barlow 1976)

$$\% \text{ positive} = 100/(1 + \text{antilog}(pH - pK_{a1}) + \text{antilog}(2pH - pK_{a1} - pK_{a2}))$$

$$\% \text{ negative} = 100 - \% \text{ neutral} - \% \text{positive}$$

From these calculations, the relative abundances of DA at pH 7.4 are: 96.6% cation, 0.4% neutral, 2.9% zwitterion, and 0.1% anion. At pH 8.6, the relative abundances are: 64.2% cation, 4.5% neutral, 30.8% zwitterion, and 0.5% anion. Since [^{3}H]DA is stored more effectively than [^{3}H]METH, the effect of ion trapping of DA may be outweighed by a pH-induced release of [^{3}H]DA.

These data provide new insight into the retention of [^{3}H]METH and demonstrate that the disposition of [^{3}H]METH within this simple model system is strikingly different from the

disposition of [^{3}H]DA. Furthermore, the results described here suggest that pH plays an essential role in the maintenance of DA homeostasis and that there may be very significant differences in the disposition of endogenous DA and the psychoactive drug METH.

Table 3.1. Extracellular pH Effects Intracellular pH

Extracellular pH	hDAT	hDAT-hVMAT2
7.4	7.52 ± 0.06	7.75 ± 0.07#
8.6	8.00 ± 0.12*	8.29 ± 0.13**

The data depicts the effect of extracellular pH (7.4, or 8.6) on the intracellular pH of hDAT or hDAT-hVMAT2 cells. Numbers are the average ± SEM of at least three independent experiments conducted with triplicate determinations. * $p<0.05$, ** $p<0.01$ comparing the intracellular pH of either hDAT or hDAT-hVMAT2 cells at pH 7.4 and pH 8.6. # denotes $p<0.05$ comparing the intracellular pH of hDAT cells at pH 7.4 and hDAT-hVMAT2 cells at pH 7.4.

IV. Mechanisms of methamphetamine interactions: diffusion versus transporter-mediated uptake

In Preparation

ABSTRACT

Methamphetamine (METH) interacts with both the dopamine- (DA) and vesicular monoamine transporters (DAT and VMAT2 respectively) to cause efflux of DA. We examined uptake of [^{3}H]METH in DAT and DAT-VMAT2 expressing human embryonic kidney (HEK-293) cells. [^{3}H]METH uptake was sensitive to pharmacological inhibition with the following rank order of potency RTI-55 > nomifensine > DA > lobeline > reserpine. The same compounds were used to block METH-induced [^{3}H]DA release from DAT-VMAT2 cells. DA and reserpine both increased [^{3}H]DA release above the effect of 100 μM METH alone. Lobeline, which was the most efficacious compound for inhibiting [^{3}H]METH uptake (IC_{50} = 1.8 - 4 μM; 29-37% of control [^{3}H]METH accumulation), decreased METH-induced [^{3}H]DA release to 77% of control with an IC_{50} of 135 μM. Nomifensine reduced METH-induced [^{3}H]DA release to 38% of control with an IC_{50} of 9.5 ± 2.5 μM. Though nomifensine was the second most potent compound at blocking [^{3}H]METH uptake, it was marginally efficacious, and decreased [^{3}H]METH accumulation to 68-76% of control. RTI-55 reduced METH-induced [^{3}H]DA release to 38 ± 5% of control with an IC_{50} of 364 ± 110 nM, but was both more potent and efficacious than nomifensine at blocking [^{3}H]METH accumulation (IC_{50} = 6 - 7 nM; 49 - 56% of control [^{3}H]METH accumulation). Inhibition of METH-induced [^{3}H]DA release required concentrations significantly higher than the concentrations required to inhibit transporter-mediated [^{3}H]METH uptake, suggesting that DAT-mediated uptake is not necessary for METH to induce DA release.

INTRODUCTION

The dopamine (DA) transporter (DAT) is a putative twelve-transmembrane domain protein that is expressed on the cell surface of dopaminergic neurons and whose primary function is to recover extracellular DA (Uhl 2003). The DAT cotransports Na^+ and Cl^- down their concentration gradients to provide energy for the reuptake of DA. The psychostimulant methamphetamine (METH) is a substrate of the DAT and competes for reuptake with the endogenous substrate DA (Sonders et al. 1997, Eshleman et al. 1999). This competition for uptake sites prolongs the half-life of DA within the synapse and leads to increased activation or excitiation of postsynaptic receptors. METH also reverses DA transport by the DAT (Falkenburger et al. 2001, Sulzer et al. 1995, Kahlig et al. 2005). This results in the loss of cytosolic DA, thereby further increasing both the extracellular concentration of DA and the excitation or activation of postsynaptic neurons. Interactions with the DAT are a primary mechanism of METH action (Eshleman et al. 1994).

The vesicular monoamine transporter (VMAT2) is a twelve-transmembrane domain transport protein that is responsible for concentrating neurotransmitter into vesicles (Feany et al. 1992, Peter et al. 1994). The VMAT2 couples the counter-transport of H^+ with the uptake of neurotransmitter into vesicles (Erickson et al. 1992). These vesicles can then fuse to the plasma membrane and release neurotransmitter into the synapse. Whether through a direct interaction with the VMAT2 (antagonism, or competition with neurotransmitter for uptake), or through a mechanism such as the weak base hypothesis as proposed by Sulzer and Rayport (1990), METH redistributes DA out of the vesicles and into the cytosol. An increase in cytosolic DA decreases the efficiency of the DAT, and provides a source of DA for reversal of transport induced by METH. Efficient retention of

DA is dependent upon the expression and function of the VMAT2 (Pifl et al. 1999, Wilhelm et al. 2004). METH is structurally similar to DA, and may be concentrated into vesicles in a similar fashion as DA. The VMAT2 confers resistance to 1-methyl-4-phenylpyridinium, a neurotoxic compound that is a substrate for the DAT, and may scavenge other harmful molecules from within the cell (Morriyama et al. 1993). Our previous work, however, suggests that following uptake, METH is rapidly lost from both DAT and DAT-VMAT2 expressing cells, indicating that direct interactions of METH with the VMAT2 are transitory (Wilhelm et al. 2006).

Few studies have examined the direct interactions of METH or its analogs with the DAT or VMAT2. Zaczek et al. (1991a & b) demonstrated that [^{3}H]amphetamine sequestration in rat brain synaptosomes was a saturable process that was inhibited by serotonin transporter- or DAT-specific antagonists (dependent upon which brain region(s) were studied). A simple model system is ideal for studying the direct interactions of METH with the DAT and VMAT2. We have previously developed a HEK-293 model system that expresses either the DAT alone, or the DAT and VMAT2 (Eshleman et al. 1995, Wilhelm et al. 2004). These are the key proteins involved in DA transport within dopaminergic neurons. Electrophysiological studies by Sonders et al. (1997) elegantly identify METH as a substrate of the DAT. This means that METH is taken up by the DAT in the same manner as the endogenous substrate DA. It has not been established whether METH is a substrate of the VMAT2. Regardless, it is the direct or indirect actions of METH with the DAT and VMAT2 that mediate its effects on dopaminergic neurons. METH is a lipophillic molecule, and thus is more likely to diffuse across cell membranes

(Sulzer et al. 2005). This may decrease the importance of the DAT in relation to METH effects.

METH acts through a number of distinct mechanisms to alter DA homeostasis. A clear relationship between METH uptake and METH-induced DA release has not been established. In this manuscript, we examine the uptake of [^{3}H]METH by DAT or DAT-VMAT2 expressing cells to determine the importance of the VMAT2 to METH uptake. We also explore the ability of DAT antagonists (RTI-55, lobeline and nomifensine), the DAT and VMAT2 substrate (DA), and VMAT2 antagonists (lobeline and reserpine) to block uptake of METH, as well as to inhibit METH-induced DA release. The results demonstrate that inhibition of [^{3}H]METH uptake does not coincide with blockade of METH-induced [^{3}H]DA release.

MATERIALS AND METHODS

Materials

[^{3}H]DA (3,4-[7-^{3}H]dihydroxyphenylethylamine, 5.8–9.7 Ci/mmol) was purchased from Amersham Biosciences (Piscataway, NJ). [^{3}H]METH (Specific Activity 22.3 Ci/mmol) was generously supplied by the National Institute on Drug Abuse. Eco-Lume scintillation fluid was purchased from ICN biochemicals, inc. (Aurora, OH). All water used in these experiments was purified by a Milli-Q system (Millipore Corp., Bedford, MA, U.S.A.). RTI-55 was a generous gift from the Research Triangle Institute (Research Triangle Park, NC). METH, lobeline, nomifensine, pargyline, reserpine, tropolone and most other chemicals were purchased from Sigma-Aldrich (St. Louis, MO) or another commercially available source.

Cell Culture

HEK-293 cells expressing the hDAT, or coexpressing the hDAT and hVMAT2 were transfected, selected and grown as previously described (Eshleman et al. 1995, Wilhelm et al., 2004). Cells were maintained in Dulbecco's modified Eagle's medium supplemented with 10% fetal bovine serum and 0.05 U penicillin/streptomycin. Cell stocks were grown on 15 cm diameter tissue culture dishes in 10% CO_2 at 37°C.

[^{3}H]METH uptake

DAT or DAT-VMAT2 cells were plated on poly-l-lysine coated 24-well plates and grown until 80-100% confluent. The media was removed and nonspecific wells were exposed to mazindol (10 μM) for 10 minutes. Uptake was initiated by the addition of 10 nM [^{3}H]METH in Krebs-HEPES (25 mM HEPES, 122 mM NaCl, 5 mM KCl, 1.2 mM $MgSO_4$, 2.5 mM $CaCl_2$, 1 μM pargyline, 100 μM tropolone, 2 mg glucose/ml, 0.2 mg ascorbic acid/ml, pH 7.4) buffer. Uptake continued at either 22°C or 37°C for times ranging from 1 to 40 minutes. The assay was terminated by aspiration followed by a wash with 400 μl of Kreb-HEPES buffer. Cells were solubilized with 250 μl of 0.1 M HCl, and the contents of each well were transferred to scinitillation vials containing 4 mL of Ecolume scintillation fluid. The radioactivity was determined using liquid scintillation spectrometry. Experiments were conducted with duplicate determinations. Two wells from each plate were used to determine the protein concentration using the bicinchoninic acid (BCA) method.

Inhibition of METH-induced [^{3}H]DA release

DAT-VMAT2 cells were plated on poly-l-lysine-coated 24-well plates and grown until 80-100% confluent. The media was removed and [^{3}H]DA uptake (final volume 0.5 ml) was

initiated by the addition of 20 nM [^{3}H]DA in Krebs-HEPES buffer at 37°C. [^{3}H]DA uptake continued for 60 minutes, the time required to reach steady-state, and was terminated by decanting the buffer. After uptake, cells were washed once with 400 µl of buffer. Unlabelled dopamine, lobeline, RTI-55, nomifensine or reserpine were added to the cells and allowed to incubate at 22°C for 10 min. The release assay was initiated by the addition of 100 µM METH at 22°C and continued for 30 min. The assay was terminated by decanting the buffer and addition of 250 µl of 0.1 M HCl to each well. The radioactivity remaining in each well was determined by liquid scintillation spectrometry. All experiments were conducted with duplicate determinations, unless otherwise noted.

Blockade of [^{3}H]METH uptake

hDAT, or hDAT-hVMAT2 cells were plated on poly-l-lysine-coated 24-well plates and grown until 80-100% confluent. The media was removed and the cells were incubated with inhibitors (DA, lobeline, nomifensine, reserpine and RTI-55 at the concentrations indicated) for 40 min in Krebs-HEPES buffer at 22°C. Uptake was initiated by the addition of 50 nM [^{3}H]METH and continued for 2 min at 22°C. The assay was terminated by decanting the buffer, followed by a wash with 300 µl of Krebs-HEPES buffer. 250 µl of 0.1M HCl was added to each well. The remaining radioactivity was determined by liquid scintillation spectrometry. All experiments were conducted with triplicate determinations, unless otherwise noted.

Data Analysis

Prism Software (GraphPad Software, San Diego, CA) was used to analyze all sigmoidal dose-response curves and to generate IC_{50} and maximal effect values, and to perform

Analysis of Variance (ANOVA). Data shown are mean ± standard error of the mean (SEM) unless otherwise noted.

Results

[^{3}H]METH uptake is temperature dependent (Figure 4.1). At 37°C, the $T_{1/2}$ was significantly shorter than the corresponding $T_{1/2}$ at 22°C in both DAT and DAT-VMAT2 cells ($T_{1/2}$ for DAT cells: 1.13 ± 0.22 min at 37°C, 4.57 ± 1.83 min at 22°C, $p<0.05$; $T_{1/2}$ for DAT-VMAT2 cells: 0.90 ± 0.18 min at 37°C, 6.37 ± 1.05 min at 22°C, $p<0.001$). In contrast, more [^{3}H]METH accumulation was observed at 22°C than at 37°C in DAT-VMAT2 cells ([^{3}H]METH uptake plateau of 2.73 ± 0.38 pmol/mg protein at 22°C and 1.10 ± 0.10 pmol/mg protein at 37°C, $p<0.01$). Likewise, DAT cells had higher (though not statistically significant) uptake at 22°C than at 37°C ([^{3}H]METH uptake plateau of 0.86 ± 0.19 pmol/mg protein at 22°C and 0.50 ± 0.07 pmol/mg protein at 37°C). No differences were observed in nonspecific, mazindol-insensitive [^{3}H]METH accumulation. Cells expressing both the hDAT and hVMAT2 took up significantly more [^{3}H]METH than hDAT cells (22°C ($p<0.01$) and 37°C ($p<0.001$)).

METH interacts directly with both the hDAT and hVMAT2. To further explore the interactions of METH with each transporter, hDAT and hVMAT2 substrates and antagonists (DA, lobeline, nomifensine, reserpine and RTI-55) were used to block the accumulation of [^{3}H]METH into HEK-293 cells expressing hDAT, or hDAT and hVMAT2 (Figure 4.2, Table 4.1).

DA decreased [^{3}H]METH accumulation to 68 ± 4% (DAT cells) and 41 ± 2% (DAT-VMAT2 cells) of control levels, exhibiting greater efficacy for blockade of

Figure 4.1

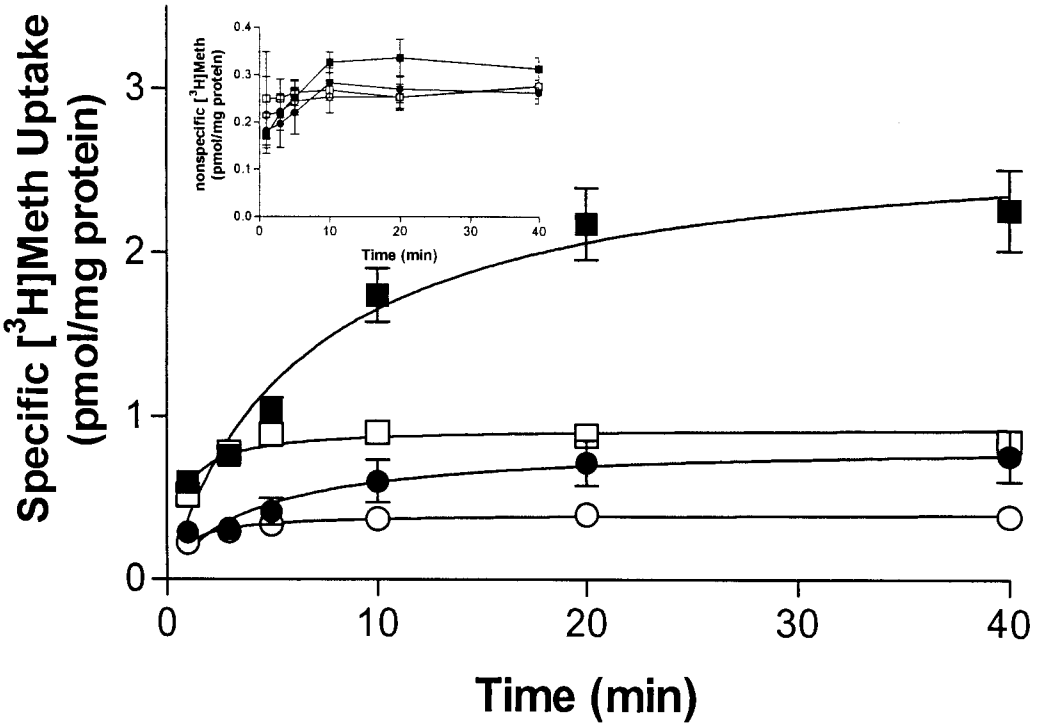

Figure 4.1. [^{3}H]METH uptake time course in DAT and DAT-VMAT2 cells. Solid circles (●) represent DAT cells at 22°C, open circles (○) represent DAT cells at 37°C. Solid squares (■) represent DAT-VMAT2 cells at 22°C, open squares (□) represent DAT-VMAT2 cells at 37°C. *Inset* represents the [^{3}H]METH accumulated in the presence of 10 μM mazindol. Data shown are the average ± SEM of at least three independent experiments. Experiments were carried out as described in text.

Figure 4.2

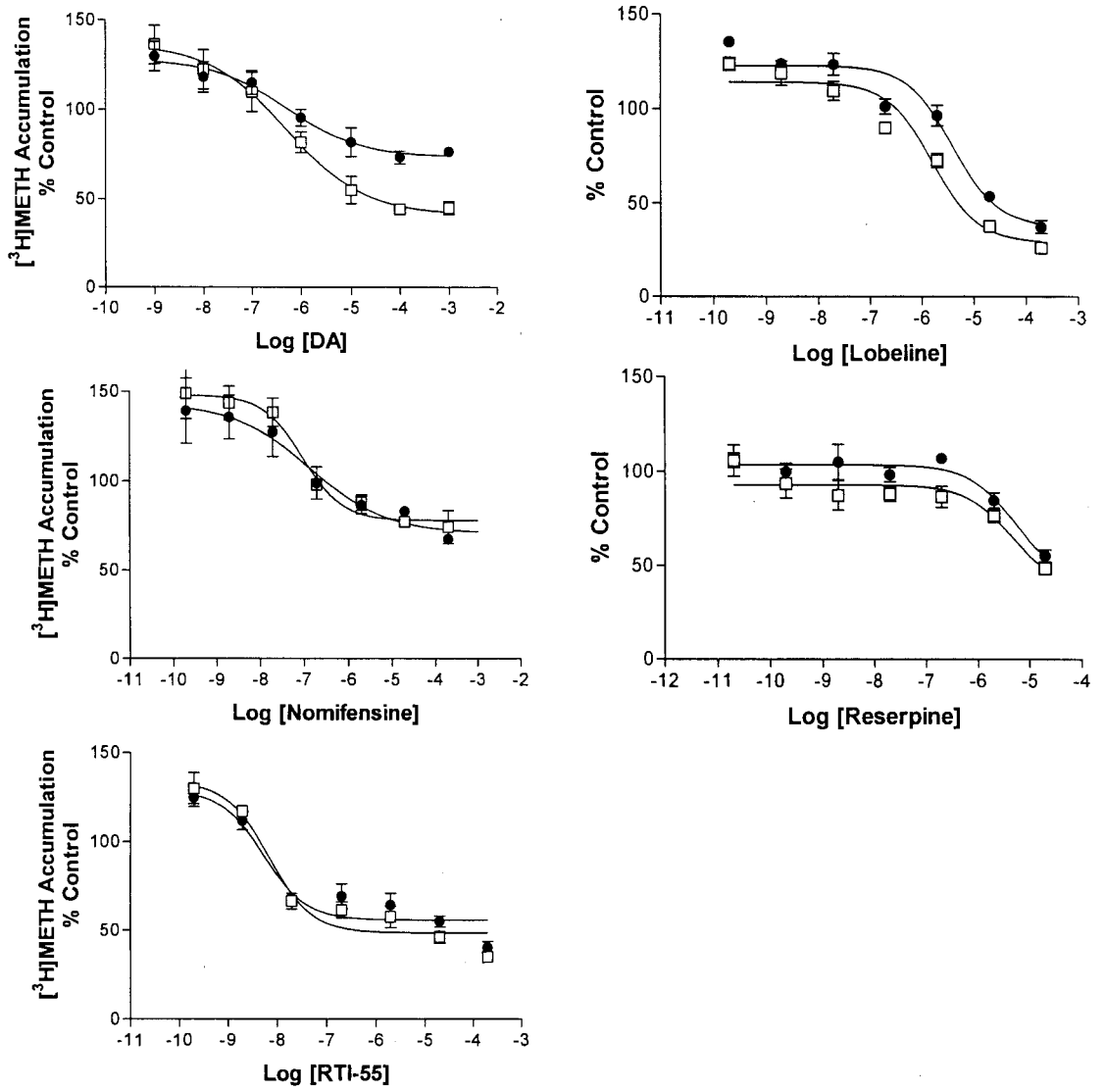

Figure 4.2. Inhibition of [^{3}H]METH accumulation in DAT and DAT-VMAT2 cells. Solid circles (●) represent the effect of drug at the concentration denoted by the x-axis in DAT cells. Open squares (□) represent the effect of drug at the concentration indicated by the x-axis on DAT-VMAT2 cells. Data shown are the average ± SEM of at least three independent experiments. Experiments were carried out as described in text.

[^{3}H]METH accumulation in DAT-VMAT2 cells than DAT cells ($p<0.01$). No difference between cell types was observed in the IC_{50} values for DA inhibition of [^{3}H]METH accumulation. Lobeline attenuated [^{3}H]METH accumulation in both hDAT and hDAT-hVMAT2 cells with no difference in affinity. The hDAT antagonist nomifensine had the second highest affinity for blocking [^{3}H]METH accumulation but had a relatively small effect. The VMAT2 inhibitor reserpine blocked [^{3}H]METH accumulation with an IC_{50} greater than 20 μM in both hDAT or hDAT-hVMAT2 cells, consistent with its affinity for inhibiting uptake mediated by the hDAT (unpublished observation). The cocaine analog and hDAT antagonist RTI-55 blocked [^{3}H]METH accumulation with an IC_{50} of 6 ± 2 nM and 7 ± 1 nM in hDAT and hDAT-hVMAT2 cells, consistent with its affinity for inhibiting [^{3}H]DA uptake via the DAT (Eshleman et al. 1999). The rank order of potency for inhibition of [^{3}H]METH accumulation was RTI-55 > Nomifensine > DA > Lobeline > reserpine and was not dependent on cell type (hDAT or hDAT-hVMAT2). Lobeline was the most effective compound, limiting [^{3}H]METH accumulation to just 37 ± 2% and 29 ± 4% of control in hDAT and hDAT-hVMAT2 cells, and was followed by reserpine, DA (hDAT-hVMAT2 cells), RTI-55, and nomifensine/DA (hDAT cells).

Next, we examined the ability of these drugs (DA, lobeline, nomifensine, reserpine and RTI-55) to inhibit METH-induced [^{3}H]DA release from hDAT-hVMAT2 cells (Figure 4.3). Previous experiments indicated that METH was not an effective releaser of [^{3}H]DA from hDAT cells when [^{3}H]DA uptake is at equilibrium, therefore, experiments were performed on hDAT-hVMAT2 cells (Wilhelm et al. 2004). 100 μM METH was used because it is approximately the EC_{70} for METH-induced [^{3}H]DA release from hDAT-hVMAT2 cells. A less than maximal concentration of METH was chosen so we could

Figure 4.3

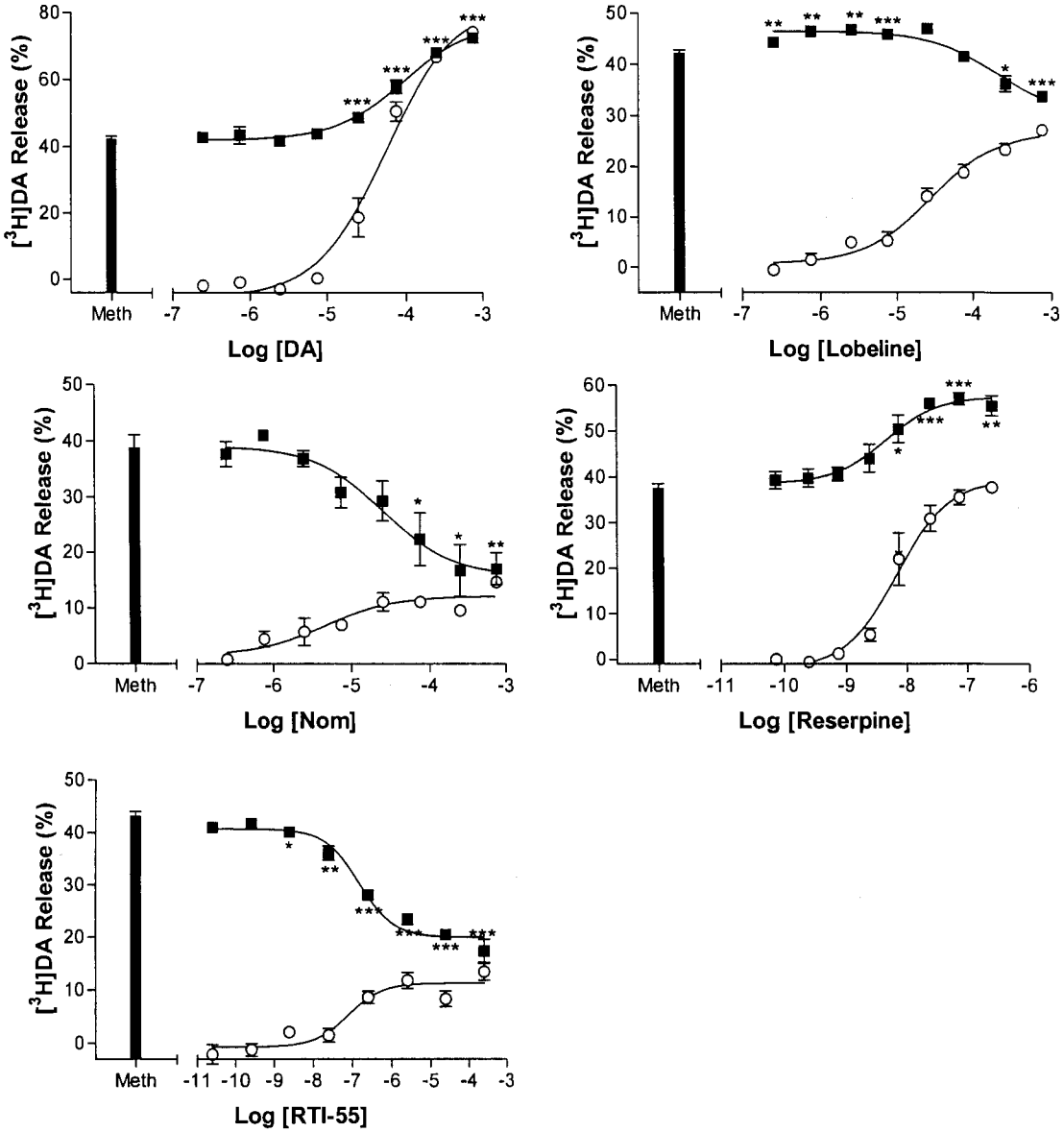

Figure 4.3. Inhibition of METH-induced [^{3}H]DA release from hDAT-hVMAT2 cells. Bars represent [^{3}H]DA efflux in the presence of 100 μM METH. Solid squares (■) represent the combined effect of 100 μM METH and the concentration of drug as indicated on the x-axis. Open circles (○) represent the [^{3}H]DA efflux in the presence of drug as indicated on the x-axis. Data shown are the average ± SEM of at least three independent experiments. Experiments were carried out as described in text.

monitor compounds that increased or decreased release of [^{3}H]DA. The effects of METH and DA together were additive. DA caused release of [^{3}H]DA by itself and also combined with METH to increase [^{3}H]DA release. Lobeline attenuated the effect of METH alone. The hDAT antagonist nomifensine was very effective at blocking METH-induced [^{3}H]DA release. In the presence of the VMAT2 inhibitor reserpine, METH-induced [^{3}H]DA release was increased. Like nomifensine, RTI-55 reduced METH-induced [^{3}H]DA release significantly. Excluding drugs that enhanced METH-induced [^{3}H]DA release, the rank order of potency was RTI-55 > nomifensine > lobeline. DA and reserpine both enhanced METH-induced [^{3}H]DA release.

Discussion

Expression of the hVMAT2 led to an increase in [^{3}H]METH accumulation over time, but did not significantly impact the affinity of any of the drugs tested. The interaction of METH with the VMAT2 is unclear. In VMAT2 transfected cells, d-amphetamine displaces [^{3}H]DHTB with relatively low potency (K_i 301 μM) providing evidence that the effects of METH are not dependent on a direct interaction with the VMAT2 (Gonzalez et al. 1994). In contrast, Peter et al. (1994) found METH blocked [^{3}H]reserpine binding to the VMAT2 with an IC_{50} of 2.7 μM. The uptake data suggest that [^{3}H]METH was sequestered by the VMAT2, as evidenced by the increased uptake of [^{3}H]METH in hDAT-hVMAT2 cells compared with DAT cells. In contrast, the VMAT2 inhibitor reserpine did not block [^{3}H]METH accumulation at concentrations in the nanomolar range (the affinity of reserpine at the VMAT2)(Peter et al. 1994). Reserpine blocks [^{3}H]Serotonin uptake into permeabilized African monkey kidney cells expressing the VMAT2 with an IC_{50} of 12 nM,

confirming that reserpine blocks substrate accumulation by the VMAT2 with high affinity (Erickson et al. 1996). Additionally, purified vesicle preparations from VMAT2-transfected HEK-293 cells and from mouse striatum do not specifically accumulate [^{3}H]METH (unpublished observation). Our previous study demonstrated that METH is not effectively stored or concentrated within vesicular structures, and suggests that despite the structural similarity METH shares with DA and norepinephrine, METH may not be a VMAT2 substrate (Wilhelm et al. 2006). Clearly, the relationship between METH and the VMAT2 is highly complex. DA exhibited a significantly greater ability to block [^{3}H]METH accumulation in DAT-VMAT2 cells, than in DAT cells (for DA, 68 ± 4% in DAT cells, versus 41 ± 2% in DAT-VMAT2 cells. DA inhibits [^{3}H]serotonin accumulation into vesicles purified from transfected cells with a K_i of 1.56 μM, a concentration similar to the IC_{50} of DA blockade of [^{3}H]METH accumulation (Peter et al. 1994). This concentration is also near the K_m for [^{3}H]DA uptake by the DAT, however, thereby confounding a correlation with binding or uptake to the DAT or VMAT2 (Wilhelm et al. 2004). The data suggest that DA is a more effective inhibitor of [^{3}H]METH uptake in the presence of the VMAT2. One possible explanation for this phenomenon is that [^{3}H]METH is associated with the VMAT2, thereby allowing DA to more effectively target and inhibit [^{3}H]METH accumulation.

Lobeline interacts with nicotinic acetylcholine receptors, the DAT, and the VMAT2 (Miller et al. 2004). Perhaps due to this lack of specificity, lobeline was the most effective compound for blocking [^{3}H]METH accumulation in both hDAT and hDAT-hVMAT2 cells. Teng et al. (1997) found lobeline had an IC_{50} of 80 μM for inhibition of [^{3}H]DA uptake in striatal synaptosomes, which represent uptake predominantly by the DAT. In

contrast, lobeline blocked [^{3}H]DA uptake into vesicles with an IC_{50} of 880 nM (Teng et al., 1997). Thus, lobeline blocked vesicular uptake with about 100-fold more potency than it blocked cell surface uptake by the DAT (880 nM at the VMAT versus 80 μM at the DAT). Lobeline inhibits [^{3}H]METH accumulation with an IC_{50} of 3-7 μM, which does not correlate well with either the affinity of lobeline at the VMAT2 or at the DAT. Miller et al. (2004) reported that lobeline displaced [^{125}I]RTI-55 with an IC_{50} of 5.4 μM. This closely resembles the IC_{50} of lobeline for blockade of [^{3}H]METH accumulation and suggests that inhibition of RTI-55 binding may be an accurate indication of a drug's affinity for blocking [^{3}H]METH accumulation. The data also suggest that an interaction with the RTI-55 binding site may be a key-component of DAT-mediated [^{3}H]METH uptake.

Despite the ability of DA to inhibit [^{3}H]METH accumulation by DAT and DAT-VMAT2 cells, DA did not inhibit METH-induced [^{3}H]DA release in DAT-VMAT2 cells. This is not surprising, however, since DA is known to cause [^{3}H]DA release (Wilhelm et al. 2004). At very high concentrations (> 20 μM), reserpine was able to inhibit [^{3}H]METH accumulation. Coadministration of 100 μM METH with reserpine, however, led to increased [^{3}H]DA release. The concentration of reserpine required to enhance METH-induced [^{3}H]DA release was in the low nanomolar range. This agrees with previous studies that suggest that VMAT2-inhibitors such as reserpine and DHTB can increase METH-induced [^{3}H]DA release (Pifl et al. 1996, Wilhelm et al. 2004). Studies using DAT knockout mice demonstrate that the VMAT2 is an important target of action for METH (Jones et al. 1998).

The rank order of potency for inhibition of [^{3}H]METH uptake and inhibition of [^{3}H]METH-induced [^{3}H]DA release are the same (excluding DA and reserpine, compounds

that were additive with METH) RTI-55 > nomifensine > lobeline. Affinity and maximal effect, did not, however, correlate. Lobeline was the most effective compound for inhibiting [^{3}H]METH accumulation, followed by RTI-55 and nomifensine. Interestingly, nomifensine only blocked 25-30% of [^{3}H]METH accumulation, yet was able to decrease METH-induced [^{3}H]DA release to less than half of METH alone. Therefore, [^{3}H]METH accumulation does not necessarily correlate with METH-induced [^{3}H]DA release. METH is a more lipophillic molecule than DA and thus, may diffuse across membranes, instead of being actively taken up like DA.

Lobeline, nomifensine, and RTI-55 each blocked METH-induced [^{3}H]DA release. Lobeline was the most efficacious compound for blocking [^{3}H]METH accumulation, but inhibited the smallest percentage of METH-induced [^{3}H]DA release (lobeline decreased METH-induced [^{3}H]DA release to 77.2 ± 2% of METH alone). Lobeline alone caused [^{3}H]DA release and thus, made it less effective as an inhibitor of METH-induced [^{3}H]DA release. These assays were performed in a static release system, which allows for the reuptake of released [^{3}H]DA. In this assay, a small amount of [^{3}H]DA release is observed in both RTI-55 and nomifensine (~10%). This small amount of apparent drug-induced release is likely inhibition of reuptake. Lobeline was an approximately 20-fold less potent inhibitor of METH-induced [^{3}H]DA release than an inhibitor of [^{3}H]METH accumulation. Nomifensine decreased METH-induced [^{3}H]DA release to 38% of control and was a 35-fold less potent inhibitor of METH-induced [^{3}H]DA release than an inhibitor of [^{3}H]METH accumulation. RTI-55 also dramatically decreased METH-induced [^{3}H]DA release (38% of METH alone), but was a 50-fold less potent inhibitor of METH-induced [^{3}H]DA release than inhibitor of [^{3}H]METH accumulation. The IC_{50} for RTI-55 blockade of METH-

induced [^{3}H]DA release was 364 ± 110 nM. Based on this data, it is possible that RTI-55 and nomifensine decreased METH-induced [^{3}H]DA release by blocking [^{3}H]DA efflux through the DAT. RTI-55, nomifensine and lobeline required significantly higher concentrations to inhibit METH-induced [^{3}H]DA release, suggesting that DAT-mediated uptake of METH is not required for METH to elicit release of [^{3}H]DA.

Our findings provide new insight into the search for a pharmacotherapeutic to treat METH addiction. The specific VMAT2 antagonists reserpine and DHTB increase the efficacy of METH for inducing [^{3}H]DA release (Wilhelm et al. 2004). Likewise, the endogenous substrate DA, though able to decrease [^{3}H]METH uptake, increased [^{3}H]DA release in the presence of METH. Lobeline, which inhibits both the DAT and the VMAT2, blocked [^{3}H]METH uptake effectively, but did not excel at blocking METH-induced [^{3}H]DA release. The specific DAT-antagonist nomifensine blocked both [^{3}H]METH accumulation and METH-induced [^{3}H]DA release. Finally, the lack of a correlation between the affinities of RTI-55, nomifensine and lobeline for inhibiting [^{3}H]METH uptake and inhibiting METH-induced [^{3}H]DA release suggest that DAT-mediated uptake of METH is not required for the DA releasing effects of METH.

Table 4.1. Inhibition of [^{3}H]Methamphetamine uptake

Drug	**IC_{50} (nM)**		**Maximal Effect (% CTL)**	
	DAT	DAT-VMAT2	DAT	DAT-VMAT2
Dopamine	691 ± 160	476 ± 244	68 ± 4	41 ± 2**
Lobeline	4000 ± 560	1800 ± 790	37 ± 2	29 ± 4
Nomifensine	140 ± 53	120 ± 20	68 ± 8	76 ± 6
Reserpine	>20000	>20000	43 ± 6	40 ± 4
RTI-55	6 ± 2	7 ± 1	56 ± 5	49 ± 4

Data shown are the average ± SEM of at least three independent experiments. Experiments were carried out as described in text. The maximal effect is the amount of [^{3}H]METH accumulated in the presence of the most efficacious concentration of drug (as calculated by Prism software) measured as a percentage of the amount of [^{3}H]METH in the absence of drug. Comparisons are of the IC_{50} or maximal effect of each drug in DAT versus DAT-VMAT2 cells. Due to solubility concerns and potential effects of the solvent DMSO, concentrations of reserpine greater than 20 μM were not tested. ** $p<0.01$, comparing the maximal effect of drug in DAT cells versus DAT-VMAT2 cells.

Table 4.2. Inhibition of METH-induced [^{3}H]DA release in DAT-VMAT2 cells

Drug	IC_{50} (μM)	% Release (METH + Drug)	% Release METH + Drug / % Release METH
Dopamine	96 ± 25	76 ± 3	179 ± 8
Lobeline	135 ± 30	33 ± 1	77 ± 2
Nomifensine	9.5 ± 2.5	15 ± 3	38 ± 7
Reserpine	0.006 ± 0.003	57 ± 2	150 ± 5
RTI-55	0.364 ± 0.110	16 ± 2	38 ± 5

Data shown are the average ± SEM of at least three independent experiments. Experiments were carried out as described in text. EC_{50} is the concentration required for 50% of the maximal drug effect observed in the presence of 100 μM METH. % Release (METH + Drug) is the amount of stimulated [^{3}H]DA efflux in presence of the most efficacious concentration of drug (as calculated by Prism software). % Release METH + Drug/% Release METH is the ratio of the % Release (METH + Drug) as described above to the % Release in the presence of 100 μM METH.

V. Release of [^{3}H]DA by VMAT2 inhibitors

ABSTRACT

The purpose of this study was to determine if blockade of the vesicular monoamine transporter (VMAT2) is sufficient to cause release of stored intracellular dopamine (DA). The effects of the VMAT2 inhibitors reserpine and dihydrotetrabenazine (DHTB) were explored in human embryonic kidney cells (HEK-293 cells) expressing the human isoforms of the VMAT2 and DA transporter (DAT). Both compounds, DHTB and reserpine, caused a dose-dependent release of preloaded [^{3}H]DA from these cells. The results suggest that blockade of the VMAT2 is sufficient to cause release of intracellular DA.

Introduction

Dopamine (DA) is synthesized from the amino acid tyrosine. DA is then concentrated into vesicles by the vesicular monoamine transporter (VMAT2) in preparation for stimulated release. Once released, DA is recovered from the extracellular space by the cell surface DA transporter (DAT) and transported back into the cytosol where it is either enzymatically degraded, or repackaged by the VMAT2 into vesicles. The DAT and VMAT2 are key proteins involved in mediating dopaminergic signaling in the brain.

Some drugs of abuse such as amphetamine (AMPH) and AMPH-like compounds interact with both the cell surface DAT and the intracellular VMAT2 to disrupt DA homeostasis (Pifl et al. 1995, Wilhelm et al. 2004). Other drugs of abuse such as cocaine block the reuptake of DA through a direct inhibition of the DAT. It is not clear however, if compounds that interact specifically with the VMAT2 can induce the release of DA. Studies by Teng et al. (1998) demonstrate that lobeline inhibits dihydrotetrabenazine (DHTB) binding to the VMAT2 with relatively high affinity, and can cause the release of preloaded DA in brain slices. Unfortunately, lobeline also exerts effects on the DAT, so it is not clear if the lobeline-induced DA release is solely due to an interaction with the VMAT2, or with both the VMAT2 and the DAT.

To determine whether inhibition of the VMAT2 alone is sufficient to induce DA release, we examined the effects of the VMAT2 inhibitors reserpine and DHTB on mammalian cells expressing the human (h) isoforms of the DAT and VMAT2 (Wilhelm et al. 2004). Both reserpine and DHTB were able to induce [^{3}H]DA release from hDAT-hVMAT2 cells using a superfusion apparatus.

Material and Methods

Materials

[^{3}H]DA (3,4-[7-^{3}H]dihydroxyphenylethylamine, 5.8–9.7 Ci/mmol) was purchased from Amersham Biosciences (Piscataway, NJ). Eco-Lume scintillation fluid was purchased from ICN biochemicals, inc. (Aurora, OH). DHTB was purchased from American Radiolabeled Chemicals, Inc. (St. Louis, MO). All water used in these experiments was purified by a Milli-Q system (Millipore Corp., Bedford, MA, U.S.A.). Methamphetamine, lobeline, pargyline, tropolone and most other chemicals were purchased from Sigma-Aldrich (St. Louis, MO).

Cell Culture

HEK-293 cells expressing the hDAT, or coexpressing the hDAT and hVMAT2 were characterized as previously described (Eshleman et al. 1995, Wilhelm et al., 2004). Cells were maintained in Dulbecco's modified Eagle's medium supplemented with 10% fetal bovine serum and 0.05 U penicillin/streptomycin. Stock plates were grown on 150-mm-diameter tissue culture dishes in 10% CO_2 at 37°C.

[^{3}H]DA Uptake

Cells were grown until confluent on 15 cm tissue culture plates. The media was removed and cells were washed with 5 mL of calcium and magnesium free phosphate buffered saline (138 mM NaCl, 4.1 mM KCl, 5.1 mM Na_2HPO_4, 1.5 mM KH_2PO_4, 0.2% w/v glucose pH 7.3). Cells were removed from the plate by triturating and resuspended in 7 mL of Krebs-HEPES buffer (25 mM HEPES, 122 mM NaCl, 5 mM KCl, 1.2 mM $MgSO_4$, 2.5 mM $CaCl_2$, 1 μM pargyline, 100 μM tropolone, 2 mg glucose/ml, 0.2 mg ascorbic acid/ml, pH 7.4). Cells were centrifuged at about 40x g at 4°C for 5 min and the

supernatant was decanted. Uptake was initiated by the addition of 200 nM [^{3}H]DA at 37°C in a final volume of 3 ml. After 60 minutes, the cells were centrifuged at 40x g at 4°C for 5 min. Cells were resuspended in 5-7 mls of Krebs-HEPES buffer and 280 µl was loaded into superfusion chambers containing polyethelyene filter discs (Brandel). One disc was placed on the bottom of the chamber, and a second disc was place on top of the chamber after the cells were loaded. Chambers were then placed into the superfusion apparatus and the assay was initiated. Fractions were collected every 2 min following a 20 min washout period that was discarded. Three fractions were collected as a baseline, with cells exposed to Krebs-HEPES buffer only. Thirteen additional fractions were collected following exposure to drug or vehicle (as indicated). The radioactivity within each 2 min fraction was determined using liquid scintillation counting. Experiments were performed with triplicate determinations unless otherwise indicated. The liquid flow rate was 0.55 ml/min.

Data Analysis

The % release of tritium outflow per minute (fractional release) was calculated by dividing the amount of radioactivity in a 2-min superfusate fraction by the radioactivity remaining within the cells (the sum of the tritium recovered in the remaining fractions including the current fraction). Prism software (GraphPad Software, San Diego, CA) was used to analyze all kinetic, retention, and drug-induced release data.

Results

Both reserpine and DHTB induce dose-dependent [^{3}H]DA release from cells expressing both the hDAT and hVMAT2 (Figures 5.1 & 5.2). DHTB had an EC_{50} of 346 ± 205 nM and released an additional 31 ± 6% of preloaded [^{3}H]DA beyond baseline conditions (Figs 5.1 & 5.3). Reserpine had an EC_{50} of 531 ± 229 nM and released an

Figure 5.1

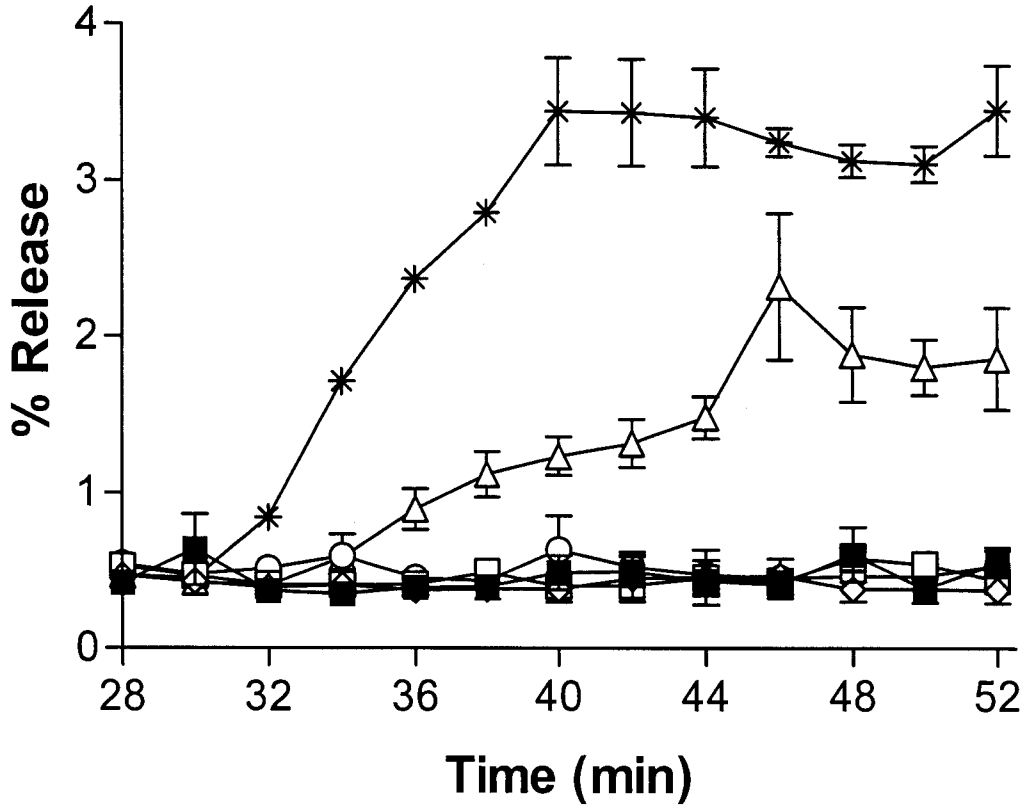

Figure 5.1: Dihydrotetrabenazine-induced [^{3}H]DA release in HEK-hDAT-hVMAT2 cells. Experiments were carried out as described in the text. Graph is a composite of at least three independent experiments carried out with duplicate determinations. [^{3}H]DA recovered for the previous two-minute period is plotted versus the total time cells have present in the superfusion chamber. Cells exposed to 0.01% DMSO are shown as closed squares (■). Cells exposed to 100 pM dihydrotetrabenazine (DHTB) are shown as open diamonds (◊). Cells exposed to 1 nM DHTB are shown as open squares (□). Cells exposed to 10 nM DHTB are shown as open circles (○). Cells exposed to 100 nM DHTB are shown as open triangles (Δ). Cells exposed to 1 μM DHTB are shown as asterisks (*).

Figure 5.2

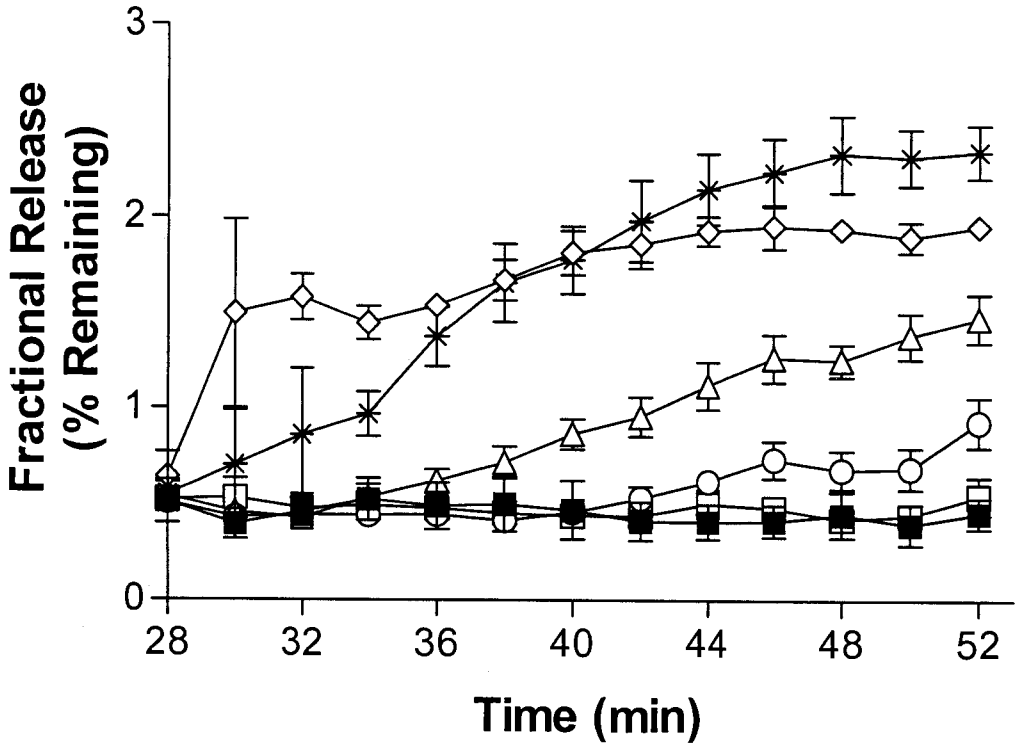

Figure 5.2: Reserpine-induced [^{3}H]DA release in HEK-hDAT-hVMAT2 cells. Experiments were carried out as described in the text. Graph is a composite of at least three independent experiments carried out with duplicate determinations. . [^{3}H]DA recovered for the previous two-minute period is plotted versus the total time cells have present in the superfusion chamber. Cells exposed to 0.1% DMSO are shown as closed squares (■). Cells exposed to 1 nM Reserpine are shown as open squares (□). Cells exposed to 10 nM Reserpine are shown as open circles (○). Cells exposed to 100 nM Reserpine are shown as open triangles (Δ). Cells exposed to 1 μM Reserpine are shown as asterisks (*). Cells exposed to 10 μM Reserpine are shown as open diamonds (◊).

additional 44.6 ± 8% of preloaded [^{3}H]DA beyond baseline conditions (Figs 5.2 & 5.3). Reserpine did not affect release in cells expressing only the hDAT (data not shown).

Discussion

In general, the cell surface DAT is responsible for taking up extracellular DA, and keeping cytoplasmic DA from being released. In this study, however, we demonstrate that disruption of dopaminergic storage by the VMAT2 is sufficient to cause the release of [^{3}H]DA. Both DHTB and reserpine (specific, high affinity VMAT2 inhibitors) were capable of inducing the release of [^{3}H]DA in superfusion experiments. A superfusion based assay is ideal for this study because it minimizes the reuptake of released [^{3}H]DA by providing a constant flow of buffer over the cells. Thus, increases in the fractional release of [^{3}H]DA can be attributed to an increase in the amount of [^{3}H]DA released, as opposed to blockade of reuptake, which is likely to occur in 'static' release systems.

Studies by Chantry et al. (1982) suggest that reserpine treatment alone is capable of releasing intracellular NE from the adrenal medulla. In contrast, studies by Kittner et al. (1987) using PC12 cells (endogenously express the highly homologous VMAT1) suggest that reserpine treatment results in the accumulation of DA in the cytosol, but not extracellularly. The results of previous studies may be confounded by the use of different model systems, different cell types, different concentrations of resperine and also catecholamine metabolism. In this study, dose-effect curves were generated for both DHTB- and reserpine-induced [^{3}H]DA release from HEK-293 cells expressing the human isoforms of the DAT and VMAT2.

Specific VMAT2 inhibitors may be useful as therapeutics for individuals with hyperactive brain monoaminergic activity (obsessive-compulsive disorder), and drug abuse

Figure 5.3

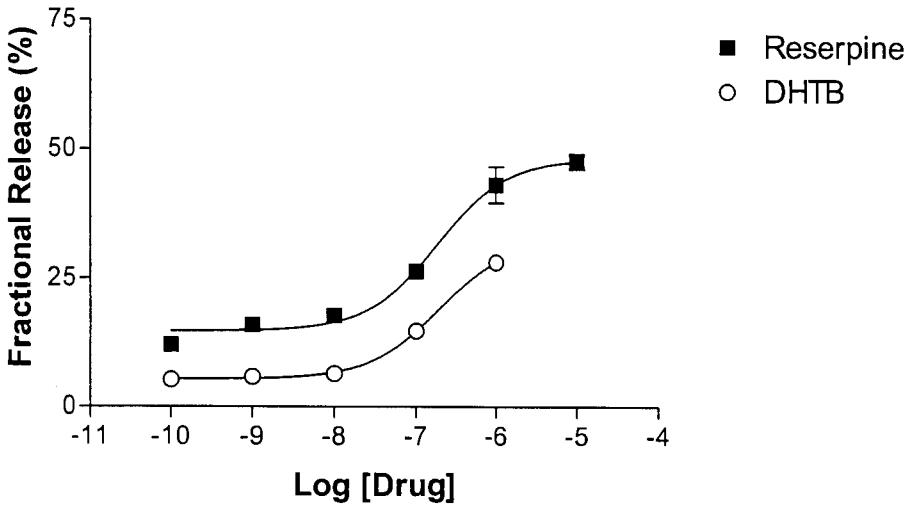

Figure 5.3. Dose-effect curve of drug-induced [^{3}H]DA release. Experiments were carried out as described in the text. The percentage of total [^{3}H]DA recovered during time 28-52 minutes of superfusion is graphed. Data shown is the average of at least three independent experiments.

treatment. Some studies suggest that reserpine can induce depression, hence, it's usefulness as a therapeutic may be questionable (Sigg et al. 1964). In contrast, tetrabenazine is used clinically to treat movement disorders (Ondo et al. 1999). Tetrabenazine is metabolized to dihydrotetrabenazine via first-pass metabolism (Ondo et al. 1999). Kuribara (1997) demonstrated that pretreatment with tetrabenazine could decrease methamphetamine- (METH) induced hyperactivity in mice. Mechanistically, treatment of METH abuse with tetrabenazine would be somewhat difficult. DHTB will decrease vesicular stores of monamines, however, coadministration of DHTB with methamphetamine leads to an increase in the potency of METH (Wilhelm et al. 2004, Kuribara 1997). Thus, in order for tetrabenazine to be an effective therapeutic with the intended results, it would be essential for tetrabenazine administration to occur long before an individual could be exposed to METH.

VI. [^{3}H]METH is not accumulated in vesicle preparations from transfected cells or mouse striatum

ABSTRACT

The time course of [^{3}H]Serotonin (5-HT), or [^{3}H]methamphetamine (METH) uptake was determined in heterologously expressed vesicular monoamine transporter-(VMAT2) transfected mammalian cells and in mouse striatum. The purpose of this study was to examine the uptake of [^{3}H]METH by the VMAT2. Nonspecific radioligand uptake was determined in the presence of 1 μM reserpine. Specific [^{3}H]5-HT uptake was present at each time point tested in both mammalian cells and mouse striatum vesicle preparations. In contrast, no specific uptake of [^{3}H]METH was observed in either mammalian cell, or mouse striatal preparations. The results suggest that METH is not a substrate of the VMAT2.

Introduction

The vesicular monoamine transporter (VMAT2) is a putative twelve-transmembrane domain spanning protein that is expressed on synaptic vesicles. The primary role of the VMAT2 is to concentrate neurotransmitters (dopamine (DA), serotonin (5-HT), norepinephrine (NE) and histamine) into vesicles in preparation for stimulated release. In order to accomplish this task, transport of neurotransmitters is coupled to counter transport of protons within the acidic lumen of the vesicle. Proton pumps, using ATP for energy, concentrate protons into vesicles, thereby providing the driving force for neurotransmitter uptake by the VMAT2.

The role of the VMAT2 in mediating the effects of methamphetamine (METH) and other amphetamine- (AMPH) like psychostimulants is unclear. Recent work suggests that AMPH, methylenedioxymethamphetamine (MDMA or ecstasy), parachloroamphetamine and fenfluramine inhibit [^{3}H]DA uptake by the VMAT2 in striatal vesicular preparations from rats (Schwartz et al. 2005). Schwartz et al. (2005) also found that these same compounds did not inhibit [^{3}H]tetrabenazine binding to the VMAT2. Both reserpine and tetrabenazine bind to the VMAT2 with high affinity (Peter et al. 1996, Peter et al. 1994). The binding sites of reserpine and tetrabenazine to the VMAT2 appear to be different (Scherman and Henry 1984). The K_i of reserpine for inhibition of NE uptake in bovine chromaffin granule cells (VMAT1) was similar to the K_d for binding of [^{3}H]reserpine (Scherman and Henry 1984). Therefore, reserpine probably binds at or near a site on the VMAT involved in NE uptake. The VMAT1 and VMAT2 do not differ in their affinities for reserpine binding, but do exhibit differences in tetrabenazine binding. METH displaces reserpine binding to both the VMAT1 and VMAT2 (Peter et al. 1994). Furthermore,

AMPH inhibits uptake of [^{3}H]DA by rat brain synaptic vesicles with a similar affinity to METH inhibition of reserpine binding. Structurally, METH and the endogenous substrate DA, are homologous. Compared with DA, METH contains two additional methyl groups, but lacks the aromatic hydroxyl groups present on DA. Based on this evidence, METH is likely a substrate of the VMAT2.

In this study, we examine the ability of vesicular preparations from HEK-293 cells stably transfected with the VMAT2 and from striatal synatic vesicles from mice to take up [^{3}H]serotonin or [^{3}H]METH. [^{3}H]serotonin was taken up in a time-dependent fashion, whereas [^{3}H]METH did not exhibit specific (reserpine-senstive) uptake at any time point tested. The results suggest that despite the structural similarities between METH and DA, METH is not likely a substrate of the VMAT2.

Materials and Methods

Materials. Serum was purchased from Hyclone (Logan, UT). Other reagents including culture media, METH and glucose were purchased from Sigma Chemical Co. (St. Louis, MO). [^{3}H]METH (22.3 Ci/mMol) was generously supplied by the National Institute on Drug Abuse. [^{3}H]5-HT (30 Ci/mMol) was purchased from Perkin Elmer (Boston, MA). C57/B6 mice were purchased from the Jackson Laboratory (Bar Harbor, ME).

Cell Culture

Human embryonic kidney (HEK-293) cells expressing the hVMAT2 were maintained in Dulbecco's modified Eagle's medium supplemented with 10% fetal bovine serum and 0.05 U penicillin/streptomycin. Cell stocks were grown on 15 cm diameter tissue culture dishes in 10% CO_2 at 37°C.

Vesicular uptake in HEK-hVMAT2 cells

One 15 cm plate of hVMAT2 cells was grown until confluent. The media was removed and the cells were rinsed with 5 ml of calcium and magnesium free phosphate buffered saline (138 mM NaCl, 4.1 mM KCl, 5.1 mM Na_2HPO_4, 1.5 mM KH_2PO_4, 0.2% w/v glucose pH 7.3). The cells were brought up in 4 ml of sucrose (0.32 M). Cells were homogenized 12 strokes with a glass/Teflon homogenizer and centrifuged at 1500x g for 10 minutes at 4°C. The supernatant was removed and saved on ice. The pellet was resuspended in 4 ml of sucrose, homogenized with 6 strokes in a glass/Teflon homogenizer and centrifuged for an additional 10 minutes at 1500x g at 4°C. The supernatants were combined and centrifuged at 20,000x g for 20 minutes at 4°C. The resulting pellet was resuspended by vortexing in 0.75 ml of sucrose. Adding 2.625 ml of ice cold H20 osmotically shocked the tissue. The tissue was homogenized with 12 strokes in a glass/Teflon homogenizer. Osmolarity was reestablished by adding 338 µl of 0.25 M Tris-HCl, 338 µl of 1 M potassium tartrate, and 4 µl of 0.9 M $MgSO_4$. The tissue was then centrifuged at 60,000x g for 20 minutes. The resulting pellet was resuspended in ~5 ml of VMAT2 buffer (100 mM potassium tartrate, 25 mM Tris, 4 mM KCl, 2 mM $MgSO_4$, 1.7 mM ascorbic acid, 0.5 mM EDTA, 100 µM tropolone, 10 µM pargyline, and 2 mM Mg-ATP). Radiolabelled substrate uptake assays were carried out in a final volume of 250 µl. 50 µl of membrane preparation was added to each well containing 175 µl of buffer with or without 1 µM reserpine. The plate was incubated for 10 minutes at 37°C. Uptake was initiated by the addition of 25 µl of [^{3}H]5-HT (final concentration 40 nM), or [^{3}H]METH (final concentration 100 nM plus 900 nM unlabelled METH). Assays continued for times ranging from 1 to 45 minutes. Assays were terminated by filtration through Wallac

Filtermat A filters presoaked in polyethyleneimine using a 96-well Tomtec cell harvester. Scintillation fluid (50 µl) was added to each filtered spot, and the radioactivity remaining on the filters was determined using a Wallac 1205 Betaplate scintillation counter. Specific uptake was calculated as the difference between uptake in the absence and presence of reserpine. Experiments were performed at least three times with duplicate determinations. Protein concentrations for this experiment were determined using a modified BCA protein assay.

Vesicular uptake in synaptic preparations from mouse striatum

Experiments were carried out as described for vesicular uptake in HEK-hVMAT2 cells with the following modifications. The striatum from ~140 day old mice was dissected and homogenized as described above. Following centrifugation at 60,000x g, the supernatant was again centrifuged at 100,000x g for 1 hour at 4°C. The resulting pellet was resuspended in 4 ml of VMAT2 uptake buffer and uptake assays were performed as described above. Protein concentrations were determined using a Coomassie protein assay.

Data analysis

Prism software (GraphPad Software, San Diego, CA) was used to analyze and graph all data. Data shown are mean ± range.

Results

[^{3}H]5-HT was used as a positive control in these experiments to demonstrate that the vesicular preparations contained VMAT2 protein that was functional and thus capable of transporting a substrate. In each type of tissue preparation, transfected mammalian cells, and striatal tissue, [^{3}H]5-HT was accumulated in a reserpine-sensitive fashion (Figures 6.1

& 6.2). Parallel experiments with [^{3}H]METH did not exhibit reserpine-sensitive uptake (Figs 6.1 & 6.2).

Discussion

The purpose of this study was to determine whether [^{3}H]METH is a substrate of the VMAT2 and whether it is accumulated and stored as a 'false transmitter'. Reserpine-sensitive uptake of [^{3}H]serotonin, an endogenous substrate of the VMAT2, demonstrated that the VMAT2 was functional following the extensive and harsh preparation and isolation of vesicular fractions. The lack or reserpine-sensitive uptake of [^{3}H]METH suggests that METH may not be a substrate of the VMAT2. Another possible hypothesis is that METH is transported and diffused out of the reconstituted vesicles so quickly that its uptake cannot be demonstrated in this preparation. Knoth et al. (1984) found that tyramine was transported by the highly homologous VMAT1 protein, but not effectively stored. They proposed that two aromatic hydroxyl groups were required for the proper storage of neurotransmitters by vesicles. This may hold true for METH, which has no aromatic hydroxyl groups.

To clearly define the interaction of METH with the VMAT2, electrophysiology studies similar to those of Sonders et al. (1997) on the cell surface dopamine transporter (DAT) should be performed on the VMAT2. These studies would compare the current-voltage plots of endogenous substrates like DA, 5-HT and histamine, with unknown compounds such as METH, amphetamine, parachloramphetamine, methylenedioxyamphetamine, with putative VMAT2 inhibitors such as tetrabenazine and reserpine. The difficulty with the VMAT2, however, is that it is not a cell surface protein, thus making electrophysiological studies much more difficult. Whitley et al. (2004)

Figure 6.1

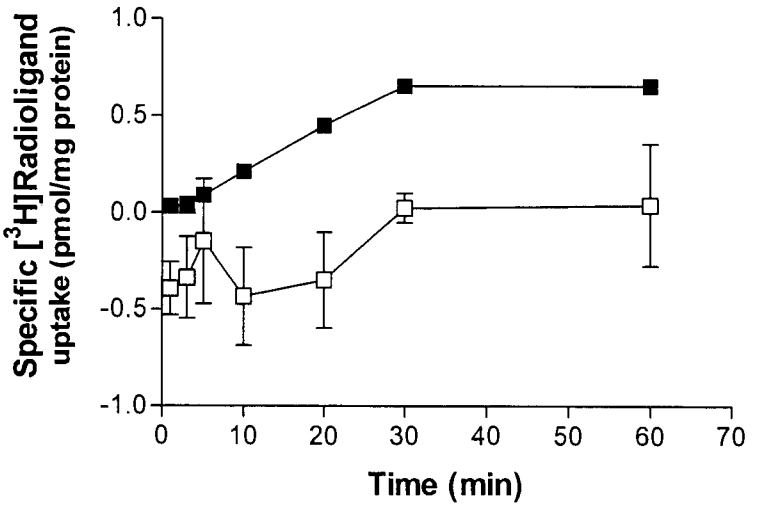

Figure 6.1. [^{3}H]Serotonin and [^{3}H]Methamphetamine uptake by vesicular preparations from HEK-hVMAT2 cells. hVMAT2 expressing cells were processed as described in the text. 40 nM [^{3}H]serotonin or 100 nM [^{3}H]methamphetamine plus 900 nM unlabelled methamphetamine were added to the VMAT2 tissue preparations and uptake was allowed to continue for the times noted. Nonspecific uptake was defined as the amount of radioligand accumulated in the presence of 1 μM reserpine. Closed squares (■) denote [^{3}H]serotonin uptake. Open squares (□) denote uptake of [^{3}H]methamphetamine. Data shown is a representative figure of an experiment repeated three times with similar results.

Figure 6.2

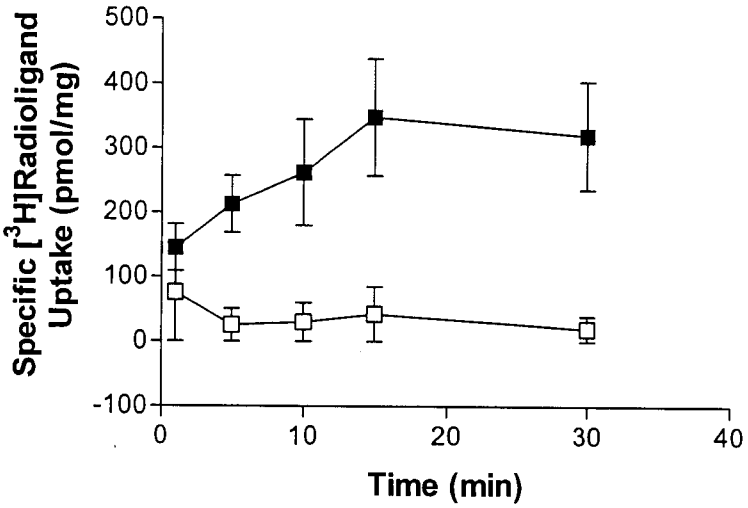

Figure 6.2. [^{3}H]Serotonin and [^{3}H]Methamphetamine uptake by vesicular preparations from mouse striatum. Striatal tissue was processed as described in the text. 40 nM [^{3}H]serotonin or 100 nM [^{3}H]methamphetamine plus 900 nM unlabelled methamphetamine were added to the tissue preparation and uptake was allowed to continue for the times noted. Nonspecific uptake was defined as the amount of radioligand accumulated in the presence of 1 μM reserpine. Closed squares (■) denote [^{3}H]serotonin uptake. Open squares (□) denote uptake of [^{3}H]methamphetamine. Data shown is the average of at least three independent experiments. Negative uptake values were defined as zero uptake.

explored the electrophysiological characteristics of a mutant VMAT2 protein that is retained on the cell surface following fusion with the plasma membrane. Two amino acids were mutated for this study, so it is not clear if the study identifies the true physiological currents of the VMAT2, or if these mutations had an impact on the function of the protein. Whether by using a mutated form of the VMAT2, or adding a leader sequence to the cDNA that codes for membrane insertion, electrophysiological study of the VMAT2 will provide highly important data on the function of the molecule, as well as to clearly identify substrates and non-substrates.

Some have suggested that not only does METH displace neurotransmitters from synaptic vesicles, but that METH is also concentrated, stored, and released by synaptic vesicles as a false transmitter (Kopin 1968). Our data clearly demonstrate in both transfected cells, and in mouse striatal tissue that [^{3}H]METH is not effectively accumulated. Previous data also suggests that in transfected DAT-VMAT2 cells, [^{3}H]METH is not effectively stored (Wilhelm et al. 2006). This data provides new insight into the mechanisms of METH action, but also bring to the forefront important questions about the interactions of METH will the VMAT2.

DISCUSSION

In this dissertation, I investigated the effect of coexpression of the hDAT and hVMAT2 on DA homeostasis. Techniques used include radioligand binding, uptake and release assays (both 'static' and superfusion), and fluorescence microscopy. The hDAT is a cell-surface protein that is responsible for reuptake of DA released from dopaminergic neurons (Jones et al. 1999). The hVMAT2 is an intracellular protein that is responsible for packaging DA (and other neurotransmitters) into vesicles in preparation for stimulated release (Fon et al. 1997, Fumagalli et al. 1999). HEK-293 cells expressing both the hDAT and hVMAT2 accumulated more [^{3}H]DA over time than cells expressing the hDAT alone. Likewise, a slight increase in the maximal rate (V_{max}) of [^{3}H]DA uptake was observed in cells that expressed both the hDAT and hVMAT2. Retention of [^{3}H]DA was also significantly increased in hDAT-hVMAT2 cells, as compared to cells expressing only the hDAT. Under the conditions tested, cells expressing only the hDAT did not exhibit drug-induced [^{3}H]DA release. In contrast, hDAT-hVMAT2 cells exhibited robust drug-induced [^{3}H]DA release following exposure to METH, DA, and tyramine, as well as the VMAT2 inhibitors DHTB and reserpine. Increased extracellular pH also elicited [^{3}H]DA release from both hDAT and hDAT-hVMAT2 cells.

The direct interactions of METH were also explored using hDAT and hDAT-hVMAT2 cells. [^{3}H]METH is accumulated in a mazindol-sensitive manner by cells expressing the hDAT. hDAT-hVMAT2 cells took up more [^{3}H]METH than hDAT cells. Despite the high degree of similarity between DA and METH, METH is not stored like the endogenous substrate DA. Following uptake, [^{3}H]METH is rapidly and completely lost from both hDAT and hDAT-hVMAT2 cells. In contrast to DA, increasing the extracellular

pH slowed the rate of [^{3}H]METH leakage. A pH-induced increase in [^{3}H]DA efflux, that was sensitive to the hDAT inhibitors GBR 12935 and cocaine, suggested the presence of a pH sensor within the hDAT.

Finally, DAT substrates, inhibitors and VMAT2 inhibitors were used to block both METH-induced [^{3}H]DA release and [^{3}H]METH accumulation. The most effective compound for blocking [^{3}H]METH uptake was lobeline, which blocked 60-70% of [^{3}H]METH accumulation. Lobeline decreased METH-induced [^{3}H]DA release to 77% of control. Nomifensine (blocked 30% of [^{3}H]METH uptake) was equally as effective as RTI-55 (blocked 45-50% of [^{3}H]METH uptake) at inhibiting METH-induced [^{3}H]DA release. Both nomifensine and RTI-55 decreased METH-induced [^{3}H]DA release to less than half of METH alone. RTI-55 and nomifensine may simply block efflux of [^{3}H]DA through the DAT. Lobeline itself induced release of [^{3}H]DA and therefore appeared to inhibit METH-induced [^{3}H]DA release via a mechanism distinct from that of RTI-55 and nomifensine. RTI-55, nomifensine and lobeline required significantly higher concentrations to inhibit METH-induced [^{3}H]DA release than [^{3}H]METH uptake, suggesting that transporter-mediated uptake of METH is not required to elicit [^{3}H]DA release.

Specific aim 1. Create and characterize an immortalized cell line expressing both the DAT and VMAT2.

The hVMAT2 cDNA was subcloned into the vector pcDNA3.1 (with G418 resistance). pcDNA 3.1 makes use of the cytomegalovirus promoter. The DNA complex was transfected into HEK-293 cells expressing the hDAT using lipofectamine. The

resulting clones were screened for hVMAT2 expression using the VMAT2 inhibitor DHTB. Saturation binding isotherms were carried out using [^{3}H]DHTB (Wilhelm et al. 2004). High affinity binding of [^{3}H]DHTB comparable to the reported affinity of DHTB for the hVMAT2 was found in two of the isolated clones (Thiriot and Ruoho, 2001). The clone with the highest expression level was selected and used for all subsequent experiments. The goal of this study was to isolate the transporters involved in DA homeostasis, specifically the DAT and VMAT2. To that end, HEK-293 cells were chosen because they are not neuronal and thus do not express synaptic vesicles that fuse with the plasma membrane, nor do they endogenously express the DAT, NET, or SERT. HEK-293 cells do not synthesize DA, norepinephrine, or monoamine oxidase (Vindis et al. 2000). Therefore, in this model system uptake of DA is simplified and can be attributed to the DAT using simple pharmacological techniques.

Saturation binding isotherms using [^{125}I]RTI-55 were performed to determine the relative levels of hDAT expression in hDAT and hDAT-hVMAT2 cells (Wilhelm et al. 2004). The results indicated that expression of the hDAT was unchanged between the parent hDAT cell line and the cotransfected hDAT-hVMAT2 cell line. Equal levels of hDAT expression meant that differences in uptake between hDAT and hDAT-hVMAT2 cells were the result of hVMAT2 expression.

Functional assays comparing [^{3}H]DA uptake time-courses and saturation curves in hDAT and hDAT-hVMAT2 cells were performed. Previous data had suggested that cells expressing both the hDAT and a rat isoform of the VMAT2 were capable of accumulating more [^{3}H]DA than cells that expressed only the hDAT (Pifl et al. 1995). It was unclear, however, whether the increased [^{3}H]DA uptake was the result of an increase in the affinity

(K_m), an increase in the maximal rate of transport (V_{max}), or an alteration in the time course of uptake. The affinity of DA was unchanged between hDAT and hDAT-hVMAT2 cells. Treatment with the VMAT2 inhibitor DHTB decreased the maximal rate of transport (V_{max}) of [^{3}H]DA uptake in hDAT-hVMAT2 cells, but did not affect the maximal rate of transport (V_{max}) in hDAT cells. Cells expressing only the hVMAT2 did not specifically accumulate [^{3}H]DA, indicating that the hVMAT2 does not contribute to surface transport. Functional coexpression of the hVMAT2 resulted in increased [^{3}H]DA uptake over time and concentration as indicated by time courses and saturation curves. An increase in the maximal rate of transport of [^{3}H]DA uptake without a change in the affinity suggests that the hVMAT2 improves the efficiency of the cell surface hDAT by sequestering intracellular [^{3}H]DA.

For the VMAT2 to function, it must be associated with an acidic intracellular compartment. HEK-293 cells are not neuronal and do not endogenously express synaptic vesicles. Eshleman et al. (2002) found that the hVMAT2 was associated with early endosomes. VMAT2 protein was also functionally expressed in transfected Cos-7 cells (Pifl et al. 1995 and 1999). The VMAT2 couples the transport of substrates to the counter transport of protons (Merickel et al 1995). Therefore, association of the hVMAT2 with an acidic intracellular compartment, such as the early endosome, provides the proper acidic environment for VMAT2 function.

Using immunolabelling, Haycock et al. (2003) measured the relative expression of numerous dopaminergic markers within the developing human brain. The ratio of hVMAT2:hDAT in the striatum varies throughout brain development, from about 1:1, to about 1:1.6 (Haycock et al. 2003). By comparison, the cotransfected model system used

here had an hVMAT2:hDAT ratio of 1:2.14 (Wilhelm et al. 2004). The hVMAT2:hDAT ratio in native tissue is largely dependent on the tissue chosen, for example, a section from the locus coeruleus, which contains noradrenergic projections would have high levels of hVMAT2 expression, but low levels of hDAT expression (Remy et al. 2005). hDAT-hVMAT2 cells have an hVMAT2:hDAT ratio that is comparable with the ratio in native dopaminergic tissue.

Further characterization of these cells could be carried out using confocal microscopy and cell surface biotinylation. First, confocal microscopy could be used to localize both the hDAT and hVMAT2 to specific cellular markers. Using colocalization studies with proteins that are known markers for the cell surface, early endosome, late endosomes, and other cellular compartments, could identify the precise cellular location of both the hDAT and hVMAT2. Cell surface biotinylation could also be used to verify that the hVMAT2 is not expressed on the cell surface. Despite the lack of [^{3}H]DA accumulation by cells expressing only the hVMAT2, it is possible that the hVMAT2 is expressed on the cell surface. As previously described, the VMAT2 requires a proton gradient for proper function; expression of the VMAT2 on the cell surface would not provide the required proton gradient and thus would not lead to functional expression of the VMAT2.

Specific aim 2. Test the hypothesis that DA and METH are stored similarly.

The primary function of the VMAT2 is to concentrate neurotransmitter into synaptic vesicles (Fon et al. 1997, Fumagalli et al. 1999). Upon stimulation, these vesicles fuse with the plasma membrane and spill their contents into the synapse (Fon and Edwards

2001). In DA neurons, released DA is recovered by the cell surface DAT and either degraded by enzymes, or recycled and repackaged by the VMAT2 into vesicles (Elsworth and Roth 1997, Jones et al. 1999). Not only is proper storage of DA important for efficiently conveying chemical messages, it is also essential to the health of dopaminergic neurons. High levels of DA exert oxidative stress on cells, which may result in cell death (Junn and Mouradian 2001). Oxidative stress caused by excessive levels of cytoplasmic DA is one possible explanation for the cause of Parkinson's disease, which is the degeneration of specific dopaminergic neurons (Fahn and Sulzer 2004). Thus, neurons have two important reasons for effectively storing DA. First, high concentrations of DA within synaptic vesicles provide for efficient signaling and second, excessive amounts of DA within the cytoplasm can be toxic.

The drug of abuse METH is structurally very similar to DA. Compared with DA, METH lacks two aromatic hydroxyl groups and possesses two methyl groups not present on DA. METH evokes current-voltage plots, as measured using electrophysiological techniques, which are similar to other DAT substrates such as DA, tyramine, and norepinephrine (Sonders et al. 1997). METH induces release of DA via the DAT (Eshleman et al. 1994). METH also displaces DHTB and reserpine from the VMAT2 (Erickson et al. 1996, Peter et al. 1994). Both DA and METH are weak bases, although METH has a higher pKa (METH pKa 9.9, DA pKa_1 8.9). Therefore, based on the similar structure and characteristics of METH and DA, it appears that these DAT substrates would be stored similarly within the cell. Sparse previous reports suggest that AMPH or METH are accumulated within striatal synaptosomes (Zaczek et al. 1991) or transfected cells (Pifl et al. 1999) expressing cell surface transporters. It is not clear, however, how retention of

AMPH-like compounds compares with retention of DA. The disposition of METH within the cell is important in order to identify appropriate sites for treatment of METH abuse.

A number of methods were used to study the retention of [^{3}H]METH and [^{3}H]DA. A "static" release system was employed, whereby cells are plated in 24-well plates. In these assays, cells expressing either the hDAT or both the hDAT and hVMAT2 were loaded with radioligand (DA, or METH), washed and the amount of labeled substrate remaining within the cells was measured over time. The caveat of this method is that any released radioligand remains in the extracellular milieu, where it can potentially be taken up again. The other system used to study substrate retention was a superfusion system. In this system, cells were loaded with radioligand, washed, and then placed into superfusion chambers. The superfusion apparatus provided a constant flow of buffer over the cells throughout the assay; therefore, as radioligand was released, it was promptly carried away in the assay buffer. Superfusion assays minimize reuptake of radioligand, but are more taxing on the cells.

In both "static" and superfusion release assays, the endogenous substrate DA was retained more effectively by cells expressing both the hDAT and hVMAT2 than cells expressing only the hDAT (Wilhelm et al. 2006). [^{3}H]DA uptake assays indicated that the hVMAT2 was sequestering the [^{3}H]DA, thereby, allowing hDAT-hVMAT2 cells to accumulate greater amounts of [^{3}H]DA than hDAT cells. The VMAT2 is a highly efficient molecule, with some studies suggesting that it is capable of maintaining a monoamine gradient of ~10^4 or greater, under physiological conditions (Schuldiner et al. 1995). Pharmacological blockade of hVMAT2 function by pretreating the cells (treatment prior to [^{3}H]DA uptake) with the hVMAT2 antagonist DHTB decreased retention of [^{3}H]DA at

both 22°C and 37°C in hDAT-hVMAT2 cells. At 37°C, there was no difference in [^{3}H]DA retention between hDAT-hVMAT2 cells pretreated with DHTB and hDAT cells. In hDAT-hVMAT2 cells, treatment with the VMAT2 inhibitors DHTB or reserpine resulted in drug-induced release of [^{3}H]DA. The question of whether VMAT2 inhibitors are capable of releasing DA *in vivo* is complicated. In the medial prefrontal cortex, Moghaddam et al. (1990), using *in vivo* microdialysis, found a decrease in extracellular DA in response to treatment with reserpine. Reserpine would redistribute vesicular DA to the cytosol where it could be released by the DAT (Jones et al. 1998). The net result of this may be a large decrease in vesicle-mediated DA release, but an increase in DAT-mediated DA release. Microdialysis does not differentiate between vesicle-mediated DA release and DAT-mediated DA release. Therefore, the *in vivo* effects of reserpine are not clear. Superfusion results clearly indicated, however, that both reserpine and DHTB induced [^{3}H]DA release from hDAT-hVMAT2 cells.

The importance of the VMAT2 is further underscored by studies of mice that do not express the VMAT2. VMAT2$^{-/-}$ mice do not eat well, exhibit severely limited locomotion and die just a few days after birth (Fon et al. 1997, Wang et al. 1997). In contrast, mice that are heterozygous VMAT2 knockouts can live into adulthood (Takahashi et al. 1997). Obviously, behavioral studies could not be conducted on VMAT2 knockout mice since they do not live very long. Heterozygous VMAT2 knockout mice exhibit reduced AMPH-induced conditioned place preference (Takahashi et al. 1997). Likewise, treatment with the neurotoxin MPTP caused greater dopaminergic cell death in VMAT2 heterozygous mice than in wild-type litter-mates (Takahashi et al. 1997). Thus, the VMAT2 is important in

mediating the drug effects of AMPH-like compounds, as well as scavenging, or protecting neurons from neurotoxic compounds like MPTP.

In 1968, Kopin et al. proposed the hypothesis that AMPH is a "false transmitter." This theory suggests that AMPH-like compounds, or their metabolites, can replace DA or other neurotransmitters within the secretory vesicles. Then, upon stimulation, the drug is released instead of the endogenous substrate. Previous studies have demonstrated this phenomenon for AMPH in noradrenergic systems (Pearl and Seiden 1976). To test the "false transmitter" hypothesis, as well as determine whether DA and METH are stored in a similar fashion, both "static" and superfusion [^{3}H]METH release experiments were performed. In "static" release experiments, [^{3}H]METH was rapidly lost from both hDAT and hDAT-hVMAT2 cells. 50% of preloaded [^{3}H]METH was lost in just 3 minutes at 37°C. Superfusion experiments showed similar results, with nearly all of the preloaded [^{3}H]METH being released from the cells after 10 minutes. Thus, [^{3}H]DA was retained much more effectively by hDAT-hVMAT2 cells than by hDAT cells, but [^{3}H]METH was not retained efficiently by either cell type. The lack of an effect of hVMAT2 expression on [^{3}H]METH retention suggests that [^{3}H]METH is not being sequestered by the hVMAT2. Thus, the retention experiments do not support the "false transmitter" hypothesis (Kopin 1968), nor do they support the hypothesis that DA and METH are stored in a similar fashion. METH may be taken up by the hVMAT2 and simply diffuse rapidly through the vesicular or associated organelle wall (as in the case with HEK-293 cells)(Mack and Bonisch 1979). The precise interaction of METH with the hVMAT2 is unclear.

The weak base hypothesis as proposed by Sulzer and Rayport (1995) suggests that AMPH-like compounds dissipate the acidic environment within the vesicles. The coupling

of substrate transport to the counter-transport of protons by the VMAT2 makes pH fundamentally important (Schuldiner et al. 1995). The effect of pH changes on substrate retention by the DAT and VMAT2 has not been explored. The hDAT contains a homologous amino acid identified as a pH sensor in a rat isoform of the SERT (Cao et al. 1998). Changes in extracellular pH affect the uptake affinity, but not the maximal rate of transport by the DAT (Berfield et al. 1999).

Increasing the extracellular pH above 7.4 increased retention of [^{3}H]METH (Wilhelm et al. 2006). Superfusion experiments with [^{3}H]METH agreed with the "static" release assays; increased extracellular pH led to an increase in the retention of [^{3}H]METH, although the amount of [^{3}H]METH recovered from cells at the end of the experiment remained minimal (1% at pH 7.4 versus ~2% at pH 8.6). In this case, increased retention of [^{3}H]METH translated into a decrease in the amount of [^{3}H]METH recovered from the first fraction at pH 8.6 versus pH 7.4, followed by increased recovery of [^{3}H]METH from the remaining fractions. As previously described, METH is a weak base and may exhibit ion trapping in acidic environments (Schepers et al. 2003). Increasing the extracellular pH above 7.4 makes the intracellular pH acidic relative to the extracellular environment. Thus, ion trapping could explain why [^{3}H]METH is better retained following exposure to increased extracellular pH. Furthermore, efflux of [^{3}H]METH was insensitive to either GBR 12935 or cocaine, further suggesting that this phenomenon was limited by diffusion and ion trapping (Wilhelm et al. 2006).

Knoth et al. (1984) explored transport of tyramine in chromaffin granule cells that express the VMAT1. Structurally, tyramine and DA are the same except tyramine has just one (as opposed to two for DA) aromatic hydroxyl group. Knoth et al. (1984) concluded

that two aromatic hydroxyl groups, though not required for transport by the VMAT1, were required for efficient storage and accumulation of phenethyleamines. METH does not possess any aromatic hydroxyl groups. The data presented here demonstrate that retention of [^{3}H]METH is not affected by expression of the VMAT2 and is poor in cells expressing only the DAT. This agrees with the hypothesis of Knoth et al. (1984). Although the precise nature of the interaction of METH with the VMAT2 is still unclear, the data strongly suggests that METH is not retained within vesicles and therefore cannot act as a "false transmitter".

Superfusion experiments demonstrated that retention of [^{3}H]DA was decreased in response to increased extracellular pH (Wilhelm et al. 2006). This effect was not observed in "static" release assays. The apparent disparity between "static" and superfusion results can be explained by the differences between the assays. In attached cell "static" release assays, released [^{3}H]DA remained in the extracellular milieu where it was available for reuptake. Robust reuptake of released [^{3}H]DA resulted in essentially no loss of [^{3}H]DA over the time course of the experiment in "static" release assays. In superfusion experiments, a constant flow of buffer was passed over the cells and carried away released [^{3}H]DA, thereby minimizing the possibility of reuptake. The decrease in [^{3}H]DA retention caused by increased extracellular pH could be attenuated in hDAT cells by the DAT antagonists GBR 12935 (30 nM) and cocaine (10 μM). This suggests that the extracellular pH is increasing the amount of [^{3}H]DA released through the DAT. One possible explanation for this is that the DAT may have a pH sensor that mediates release of intracellular DA in response to extracellular pH changes. Cao et al. (1997 and 1998) demonstrated that a rat (r) SERT, but not hSERT, has a pH-sensitive transport-associated

current. Using site-directed mutagenesis, they were able to disrupt this current in the rSERT (rT490K), and create a pH-sensitive transport current in the hSERT (hK490T). The hDAT shares this "pH-sensor" with the rSERT, thus the increase in [^{3}H]DA release in response to increased extracellular pH may be mediated by the corresponding amino acid in the DAT. Additional studies of a putative "pH sensor" on the DAT could use a similar site-directed mutagenesis scheme as incorporated by Cao et al. (1998) in the SERT. Instead of monitoring transport current, however, superfusion studies could monitor the efflux of [^{3}H]DA induced by increased extracellular pH. If this amino acid were a "pH-sensor", then the increased release of [^{3}H]DA following exposure to pH 8.6 may be attenuated or completely eliminated.

One drawback to this model system is that, although the hVMAT2 is functional in this system, it is not associated with an actual neuronal vesicle. Ion trapping may play a significant role for both DA and METH. This effect was most obvious for [^{3}H]METH, which was better retained at pH 8.6 than at pH 7.4. At pH 8.6, the intracellular pH (although it does increase in response to extracellular pH 8.6) is acidic relative to the extracellular environment. In this situation, a weak base such as METH, or DA will prefer the acidic environment and become "trapped" there. The same phenomenon would be true for vesicles, where the pH is far more acidic than the cytosol due to the activity of H^+-ATPases present on the vesicles (Cidon and Sihra 1989). These molecules pump protons into the lumen of the vesicle making it highly acidic relative to the cytosol of the cell. In this system, the hVMAT2 is associated with early endosomes (pH <6.2), which provide an environment similar to that of a synaptic vesicle (Clague et al. 1994, Schuldiner et al.

1995). Thus, although this model system does not contain native synaptic vesicles, it appears to be an accurate model of vesicular retention.

Substrates themselves can also be affected by pH. For DA, which exists in multiple ionic forms, the relationship is complex. The contribution of the second aromatic hydroxyl group is minimal near physiological pH so for the purpose of this discussion it will be ignored. This results in four possible ionic forms of DA: cation, neutral, zwitterions, and anion (Berfield et al. 1999). The relative prevalence of each of the isoforms can be calculated as defined in Wilhelm et al. (2006) and Berfield et al. (1999).

At pH 7.4, the relative abundances of DA are: 96.6% cation, 0.4% neutral, 2.9% zwitterion, and 0.1% anion. When the pH is increased to 8.6, the relative abundances of DA are: 64.2% cation, 4.5% neutral, 30.8% zwitterion, and 0.5% anion. The effect of pH on METH is less complicated than DA. METH exists in only two forms, neutral and cation. Therefore, the relative abundances at a given pH can be determined by the Henderson-Hasselbach equation ($pH = pK_a + \log (METH/METH^+)$). Using this equation, the relative abundances of METH at pH 7.4 are: 0.3% neutral and 99.7% cation. At pH 8.6, the relative abundances of METH are: 4.8% neutral and 95.2% cation. Increased prevalence of neutral forms of METH and DA increase the likelihood of diffusion. Thus, for release assays, where the substrates were predominantly stored intracellularly, it was important to determine the effect of changes in extracellular pH, on intracellular pH.

To determine the effect of altered extracellular pH on intracellular pH, a fluorescent assay was used. Specifically, the pH sensitive probe 5-and 6-carboxyseminapthorhodofluor-1 acetoxymethyl ester (carboxy-SNARF-1 AM; SNARF) was used to measure intracellular pH. Exposure of cells to extracellular pH 8.6 for 32

minutes (this was the length of superfusion assays) significantly increased the intracellular pH of both hDAT and hDAT-hVMAT2 cells. Curiously, under normal (extracellular pH 7.4) conditions, hDAT-hVMAT2 cells had a significantly higher pH than DAT cells. For release assays, the majority of the substrate was inside of the cells, therefore, an increase in the intracellular pH would change the abundance of the ionized forms of DA and METH. Berfield et al. (1999) proposed that the cationic and zwitterionic forms of DA were the forms of DA that are the substrate of the DAT. For DA, >94% of the molecules remain in these states between pH 7.4 and pH 8.6. Not determined, however, is the form of DA that is the substrate for reverse transport by the DAT, or the form of DA that is the substrate of conventional or reverse transport by the VMAT2.

Additional experiments could be performed both to confirm these findings and to provide further insight into the molecular mechanisms of AMPH-like compounds. To further support the *in vitro* findings, it would be useful to perform similar [^{3}H]DA and [^{3}H]METH efflux experiments on striatal synaptosomes from mice, rats, or other native animal tissue. These results should be similar to what was found using the hDAT-hVMAT2 model system. Striatal synaptosomes have a much higher degree of dopaminergic complexity, however, than HEK-293 cells do. For instance, synaptosomes contain synaptic vesicles capable of fusing with the plasma membrane. Synaptosomes also contain DA receptors as well as catabolic enzymes such as monoamine oxidase and catechol-o-methyltransferase. Also, striatal synaptosomes contain a heterogeneous mixture of cells, unlike the homogeneity provided by the HEK model system. Therefore, it is possible that the results may vary due to this increased complexity. There would not be striatal synaptosomal fractions without VMAT2, so experiments comparing retention of

[^{3}H]DA and [^{3}H]METH in the presence or absence of the VMAT2 could not be performed in this system. Reserpine or DHTB could be used to provide a pharmacological blockade of the VMAT2 in synaptosomes; however, these drugs may exert other unintended effects on other receptors or transporters. Endogenous DA and other neurotransmitters present in the tissue preparation may interfere with the results as well.

Perhaps the most important extension of this work is to gain a greater understanding of the interaction of METH with the VMAT2. METH displaces both reserpine and DHTB from the VMAT2, indicating METH interacts directly with the VMAT2 (Erickson et al. 1996, Peter et al. 1994). It is unclear, however, whether METH is a substrate of the VMAT2. The data presented here strongly suggests that METH is not effectively stored by the VMAT2. Uptake studies on attached cells, however, suggest that expression of the hVMAT2 increases [^{3}H]METH accumulation. In contrast, uptake by vesicle preparations suggests that [^{3}H]METH is not accumulated by the VMAT2. Since the VMAT2 is an intracellular protein localized to vesicles, direct electrophysiological studies have been impossible. As technology evolves, it may be possible to patch an electrode onto a neuronal vesicle and make recordings of the transport currents of the VMAT2. Until then, however, expression systems provide the only viable method for studying the VMAT2 using electrophysiological techniques. Whitley et al. (2004) used an rVMAT2 double mutant (I483A/L484A) that was retained on the cell surface, presumably following fusion with the plasma membrane, to electrically monitor efflux of DA by the VMAT2 in *Xenopus* oocytes. The rVMAT2 double mutant was expressed on the cell surface of *Xenopus* oocytes and released DA that was injected into the oocyte. This model system or perhaps a modified VMAT2 protein that contains a leader sequence coding for insertion into the

plasma membrane needs to be used to further explore the electrophysiological profile of the VMAT2, similar to the studies of Sonders et al. (1997) on the DAT. In particular, a comparison of the current-voltage plots elicited by endogenous VMAT2 substrates, such as DA, 5-HT, and histamine, as well as putative VMAT2 antagonists such as tetrabenazine, reserpine, and DHTB, should be compared with those of unknown compounds such as AMPH, METH, and MDMA to determine if AMPH-like compounds are substrates or inhibitors of the VMAT2.

Specific Aim 3. Identify compounds that effectively block METH-induced [^{3}H]DA release.

Perhaps the most rapid effect of METH is to release DA via interactions with the DAT and VMAT2 (Kuribara 1997, Sulzer and Rayport 1990). Therefore, blockade of METH-induced DA release is a reasonable goal for a pharmacotherapeutic. AMPH-like compounds cause reversal of transport by the cell surface DAT (Eshleman et al. 1994, Falkenburger et al. 2001). Studies using DAT knockout mice demonstrated that the VMAT2 is important, though not necessary, for mediating the DA releasing effects of METH (Jones et al. 1998 and 1999). The purpose of these studies was to identify compounds that are effective inhibitors of METH-induced [^{3}H]DA release. Additionally, I determined whether inhibition potency and/or maximal effect of METH-induced [^{3}H]DA release correlates with blockade of [^{3}H]METH accumulation. The effect of DAT substrates, antagonists, and VMAT2 antagonists on inhibition of the above-described phenomena was determined.

Some drugs actually increased METH-induced [^{3}H]DA release. The VMAT2 inhibitor reserpine blocked [^{3}H]METH accumulation at very high concentrations (>10 μM). When reserpine was coadministered with METH, [^{3}H]DA release was actually increased. This agrees with the effect of the VMAT2 inhibitor DHTB (Wilhelm et al. 2004), as well as previous studies by Pifl et al. (1995), which showed that expression of the VMAT2 decreased the potency of METH for inducing release of [^{3}H]DA in transfected cells also expressing the DAT. The potential use of VMAT2 inhibitors to treat METH abuse does not lie with simply coadministration of the compounds. Instead, VMAT2 inhibitors can effectively decrease the effects of METH, but only when given prior to administration of METH (Kuribara 1997). Mechanistically, VMAT2 inhibitors such as reserpine and DHTB deplete neurons of neurotransmitters, thereby decreasing the rewarding effects of drugs of abuse (Guo et al. 2003, Reches et al. 1983). Reserpine is used clinically to treat high blood pressure, but side effects include depression (Ganzini 1993, Lin et al. 1993, Skalisz et al. 2002). In contrast, tetrabenazine, which is metabolized to DHTB inside of the body, has been used clinically to effectively treat movement disorders (Paleacu et al. 2004). Side effects are rare as a result of low dose treatment with tetrabenazine. High doses of tetrabenazine, however, may result in undesired results such as neuroleptic malignant syndrome (NMS), which is characterized by muscular rigidity, fever, autonomic dysfunction, and altered mental status (Petzinger and Bressman 1997, Osseman et al. 1996). Additionally, studies exploring the toxicity of coadministration of tetrabenazine and METH should be performed to determine the safety of the two drugs used in combination. Depletion of neurotransmitters stores may be an effective treatment for METH abusers, however, the use of tetrabenazine, or any VMAT2 inhibitor, as a therapeutic for treatment

of METH abuse must be done very cautiously, due to the additive effects of these compounds *in vivo* (Kuribara 1997).

The most effective compound for blocking [^{3}H]METH accumulation was lobeline. Lobeline is a noncompetitive DAT inhibitor and also interacts with the VMAT2 (Teng et al. 1997). Lobeline decreased METH-induced [^{3}H]DA release by less than 25%, however, making it only partially effective compared with other compounds. Lobeline itself caused release of ~30% of preloaded [^{3}H]DA in "static" release experiments. This agrees with studies by Teng et al. (1997 and 1998), who found that lobeline increases [^{3}H]overflow from rat striatal slices and increases [^{3}H]DA release from rat striatal synaptic vesicles. Thus evidence from this study, as well as Teng et al. (1997), suggest that lobeline induces release of DA. This does not necessarily rule out lobeline as a treatment for METH abusers, however. One way to treat substance abuse disorders is to use a "partial agonist" to replace the drug of abuse with another drug that is less efficacious—using one drug to wean the patient off of the abused drug (Donny et al. 2005, Hallinan et al. 2005). Hence, lobeline may be a candidate if this type of treatment regimen is desired for METH. Using rats as a model, Harrod et al. (2003) found that lobeline was not self-administered, nor did it reinstate responding for METH. Harrod et al. (2003) also found that lobeline decreased METH self-administration. Further studies examining the toxicity of coadministration of both METH and lobeline would be important to insure that the combined effects of these drugs do not result in neurotoxicity. The half-life of lobeline in the human body would need to be determined to properly administer the drug and determine its feasibility as a pharmacotherapeutic. The findings of this study suggest that lobeline may be an effective therapeutic for treating METH abuse.

The DAT inhibitors nomifensine and RTI-55 decreased [^{3}H]DA retention by 10-15%, likely due to inhibition of reuptake. RTI-55 was an effective inhibitor of [^{3}H]METH accumulation, decreasing it to ~50% of control in DAT-VMAT2 cells. Nomifensine was less effective, decreasing [^{3}H]METH accumulation to only ~70% of control. Both compounds were effective inhibitors of METH-induced [^{3}H]DA release, decreasing it to less than 40% of METH alone. Nomifensine was ~30 times less potent than RTI-55 for inhibiting METH-induced [^{3}H]DA release. Both compounds required significantly greater concentrations to block METH-induced [^{3}H]DA release, than to inhibit [^{3}H]METH uptake (20-60 times less potent). This suggests that blockade of [^{3}H]METH accumulation does not directly translate into inhibition of METH-induced [^{3}H]DA release. It may be that RTI-55 and nomifensine are simply blocking the escape of [^{3}H]DA through the DAT. RTI-55 lacks therapeutic potential, regardless of its ability to inhibit METH-induced [^{3}H]DA release, because the drug itself is self-administered (Weed et al. 1995). Regardless, the disparity between the concentration of nomifensine or RTI-55 to block [^{3}H]METH uptake versus the concentration required to inhibit METH-induced [^{3}H]DA release suggests that uptake of METH via the DAT is not required to elicit DA release.

DA blocked [^{3}H]METH accumulation, but not METH-induced [^{3}H]DA release. Likewise, high concentrations of reserpine were able to inhibit [^{3}H]METH uptake, but coadministration of reserpine and METH resulted in increased drug-induced [^{3}H]DA release. Even the DAT antagonist lobeline, which blocked [^{3}H]METH accumulation very effectively, was less effective than both nomifensine, which was not a very effective inhibitor of [^{3}H]METH uptake, and RTI-55 for inhibiting METH-induced [^{3}H]DA release. As described above, RTI-55 and nomifensine may simply be blocking the release of

[^{3}H]DA from cells through inhibiting reverse transport by the DAT. The situation is more complex for lobeline. Lobeline itself induces the release of [^{3}H]DA (Wilhelm et al. 2004, Teng et al. 1997). Therefore, it is unlikely that lobeline is inhibiting release of [^{3}H]DA by the DAT. Thus, the ability of lobeline to inhibit METH-induced [^{3}H]DA release may be due to blockade of a direct interaction of METH with the DAT or VMAT2.

Further studies could be performed on additional compounds, comparing their ability to inhibit [^{3}H]METH accumulation and METH-induced [^{3}H]DA release. Lobeline stands out as a drug with therapeutic potential for treatment of METH abuse. Miller et al. (2004) identified a number of compounds analogous to lobeline that vary in their affinities for the DAT and VMAT2. Additional studies of [^{3}H]METH accumulation and METH-induced [^{3}H]DA release on these analogous lobeline compounds may reveal more about the underlying mechanisms of METH action, as well as identify compounds that may be equally as or more effective than lobeline at inhibiting METH-induced [^{3}H]DA release. Behavioral and biochemical studies to determine if lobeline is a suitable treatment for METH abuse have already begun. These studies have found that lobeline decreases the reinforcing properties of METH (Harrod et al. 2001), does not serve as a reinforcer in rats (Harrod et al. 2003), and blocks METH-induced changes in VMAT2 immunoreactivity and monamine depletion (Eyerman and Yamamoto 2005). The lab of Linda Dwoskin Ph.D. is in search of lobeline compounds with a high affinity at the VMAT2, hoping that these drugs will be effective for treatment of METH abuse (Miller et al. 2004). Their search for specificity may be wrong—it may be the combined effects of lobeline at the cell surface, as well as at the VMAT2 that acts to decreases the reinforcing and biochemical effects of

METH. Regardless, lobeline is an excellent starting point in the search for a therapeutic to treat METH abuse.

Summary of conclusions

The studies presented in this dissertation demonstrated that HEK-293 cells were capable of functionally expressing hVMAT2 molecules. Coexpression of the hVMAT2 with the hDAT resulted in cells that accumulate more [^{3}H]DA than cells expressing the hDAT alone, indicating that the hVMAT2 was sequestering intracellular [^{3}H]DA. Cells that coexpressed the hVMAT2 and hDAT also retained [^{3}H]DA more effectively than cells that expressed the hDAT alone. METH was not capable of inducing release from hDAT cells that were loaded with [^{3}H]DA to equilibrium, suggesting that the [^{3}H]DA was sequestered or trapped intracellularly and insensitive to METH treatment. In contrast cells expressing both the hDAT and hVMAT2 exhibited robust METH-induced [^{3}H]DA release, indicating that at the very least, the hVMAT2 provides a METH-sensitive pool of [^{3}H]DA. Coadministration of METH with a VMAT2 inhibitor (DHTB) shifted the dose-response curve for METH-induced [^{3}H]DA release to a higher affinity. This suggests that the interaction of METH with the VMAT2 is of lower affinity than the interaction of METH with the DAT.

[^{3}H]METH uptake time courses demonstrated that cells expressing both the hDAT and hVMAT2 accumulated more [^{3}H]METH over time than cells expressing the hDAT alone. This suggests that [^{3}H]METH was sequestered intracellularly by the hVMAT2 like [^{3}H]DA. Retention of [^{3}H]METH did not, however, resemble that of [^{3}H]DA. Both hDAT-hVMAT2 cells and hDAT cells retained [^{3}H]METH poorly in both static and superfusion release assays. Additionally, vesicular preparations from both hVMAT2-

transfected HEK cells or mouse striatum did not specifically accumulate [^{3}H]METH, but did exhibit accumulation of [^{3}H]serotonin. Hence, this data apparently conflicts with the [^{3}H]METH uptake data and suggests that [^{3}H]METH is not accumulated, or is poorly retained by vesicles, or cell membranes expressing the hVMAT2. It is unclear whether METH is a VMAT2 substrate. Thus, additional studies examining the interaction of METH with the VMAT2 need to be performed.

Retention of [^{3}H]METH increased in both hDAT and hDAT-hVMAT2 cells in response to elevated extracellular pH. Based on this finding, [^{3}H]METH appears to exhibit ion trapping, a process that is limited by diffusion. In contrast, elevated extracellular pH resulted in increased loss of [^{3}H]DA, which was attenuated by treatment with the DAT inhibitors cocaine and GBR 12935. This suggests that the hDAT may have a pH sensor. Additional studies would need to be performed, however, to confirm this hypothesis.

Appendix A: Drug Structures

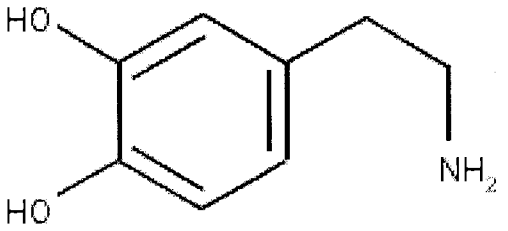

Dopamine

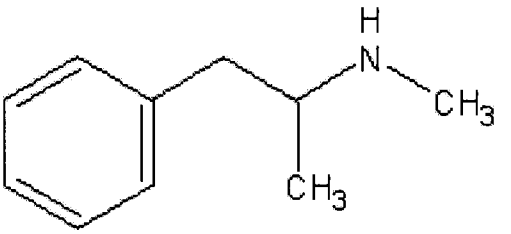

Methamphetamine

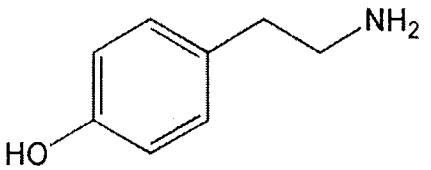

Tyramine

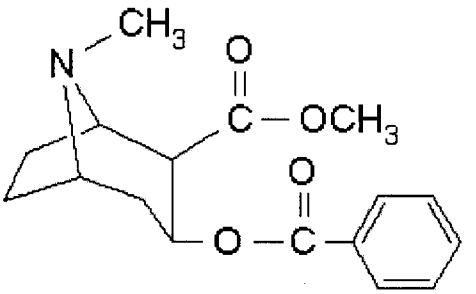

Cocaine

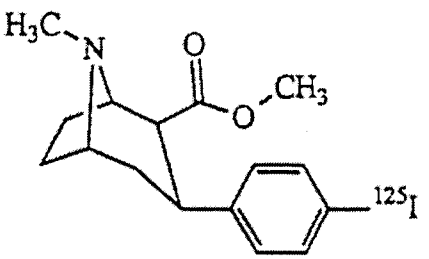

RTI-55 (β-CIT)

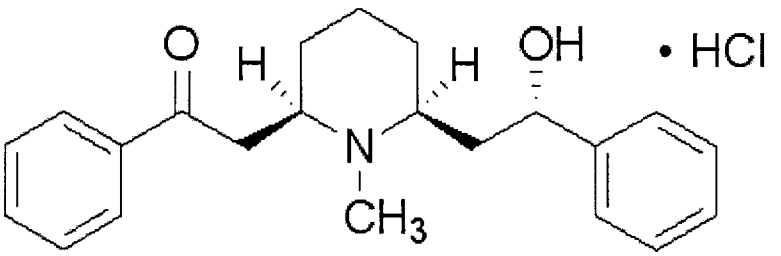

Lobeline

References

Alles GA (1933) The comparative physiological actions of the DL-β-phenylisopropylamines. I. Pressor Effects and toxicity. *J Pharamcol Exp Ther* **47:** 339-354.

Beckman ML and Quick MW (1998) Neurotransmitter transporters: regulators of function and functional regulation. *J Membr Biol* **164:** 1-10.

Berfield JL, Wang LC and Reith MEA (1999) Which form of dopamine is the substrate for the human dopamine transporter: the cationic or the uncharged species? *J Biol Chem* **274**:4876-4882.

Benoit-Marand M, Borrelli E and Gonon F (2001) Inhibition of dopamine release via presynaptic D2 receptors: time course and functional characteristics *in vivo*. *J Neurosci* **21:** 9134-9141.

Biel JH and Bopp BA (1978) Amphetamines: structure-activity relationships. In: Iversen LL, Iversen SD, Snyder SH (Eds.), Handbook of Psychopharmacology: Stimulants. Plenum New York, pp. 1-40.

Blaschko H, Richter D and Schlossmann H (1937) The inactivation of adrenaline, *J. Physiol.* **90:** 1–17.

Bower JF, Frame LY, Clausing P, Nagamoto-Combs K, Osterhout CA, Sterling CR and Tank AW (1998) Long-term effects of amphetamine neurotoxicity on tyrosine hydroxylase mRNA and protein in aged rats. *J Pharmacol Exp Ther* **286:** 1074-1085.

Bradberry CW and Roth RH (1989) Cocaine increases extracellular dopamine in rat nucleus accumbens and ventral tegmental area as shown by in vivo microdialysis. *Neurosci Lett* **103:** 97-102.

Brecht ML, Greenwell L and Anglin MD (2005) Methamphetamine treatment: trends and predictors of retention and completion in a large state treatment system (1992-2002). *J Subst Abuse Treat* **29:** 295-306.

Brown JM, Hanson GR and Fleckenstein AE (2000) Methamphetamine rapidly decreases vesicular dopamine uptake, *J Neurochem* **74:** 2221–2223.

Buck KJ and Amara SG (1994) Chimeric dopamine-norepinephrine transporters delineate structural domains influencing selectivity for catecholamines and 1-methyl-4-phenylpyridium. *Proc Natl Acad Sci* **91:** 12584-12588.

Buck KJ and Amara SG (1995) Structural domains of catecholamine transporter chimeras involved in selective inhibition by antidepressants and psychomotor stimulants. *Mol Pharmacol* **48:** 1030-1037.

Cao, Y., Mager, S., and Lester, H. A. (1997) H+ permeation and pH regulation at a mammalian serotonin transporter. *J. Neurosci.* **17:** 2257-2266.

Cao Y, Ming L, Mager S and Lester HA (1998) Amino acid residues that control pH modulation of transport-associated current in mammalian serotonin transporters. *J Neurosci* **18:** 7739-7749.

Chang MY, Lee SH, Kim JH, Lee KH, Kim YS, Son H, and Lee YS (2001) Protein kinase C-mediated functional regulation of dopamine transporter is not achieved by direct phosphorylation of the dopamine transporter protein. *J Neurochem* **77:** 754-761.

Chantry CJ, Seidler FJ and Slotkin TA (1982) Non-neurogenic mechanism for reserpine-induced release of catecholamines from the adrenal medulla of neonatal rats: possible modulation by opiate receptors. *Neuroscience* **7:** 673-678.

Cidon S and Sihra TS (1989) Characterization of a H+-ATPase in rat brain synaptic vesicles. Coupling to L-glutamate transport. *J Biol Chem* **264:** 8281-8288.

Ciliax BJ, Drash GW, Staley JK, Haber S, Mobley CJ, Miller GW, Mufson EJ, Mash DC and Levey AI (1999) Immunocytochemical localization of the dopamine transporter in human brain. *J Comp Neurol* **409:** 38-56.

Clague MJ, Urbe S, Aniento F and Gruenberg J (1994) Vacuolar ATPase activity is required for endosomal carrier vesicle formation. *J Biol Chem* **269:** 21-24.

Cretzmeyer M, Sarrazin MV, Huber DL, Block RI and Hall JA (2003) Treatment of methamphetamine abuse: research findings and clinical directions. *J Subst Abuse Treat* **24:** 267-277.

Crosby MJ, Hanson JE, Fleckenstein AE and Hanson GR (2002) Phencyclidine increases vesicular dopamine uptake. *Eur. J. Pharmacol.* **438:** 75–78.

Cubells JF, Rayport S, Rajendran G, Sulzer D (1994) Methamphetamine neurotoxicity involves vacuolation of endocytic organelles and dopamine-dependent intracellular oxidative stress. *J Neurosci* **14:** 2260–2271.

Dayan P and Balleine BW (2002) Reward, motivation and reinforcement learning. *Neuron* **36:** 285-298.

Di Chiara, G. (2002) Nucleus accumbens shell and core dopamine: differential role in behavior and addiction. *Behav Brain Res* **137**, 75-114.

Donny EC, Brasser SM, Bigelow GE, Stitzer ML and Walsh SL (2005) Methadone doses of 100 mg or greater are more effective than lower doses at suppressing heroin self-administration in opiod-dependent volunteers. *Addiction* **100:** 1496-1509.

Dwoskin, L. P. & Crooks, P. A. (2002) A novel mechanism of action and potential use for lobeline as a treatment for psychostimulant abuse. *Biochem Pharmacol* **63**, 89-98.

Edeleano L (1887) Über einige derivate der Phenylmethacrylsaure und der Phenylisobuttersaure. *Berl Dtsch Chem Ges* **20:** 616-622.

Edwards RH (1992) The transport of neurotransmitters into synaptic vesicles. *Curr Opin Neurobiol* **2:** 586-594.

Eiden LE, Schafer MK, Weihe E and Schutz B (2004) The vesicular amine transporter family (SLC18): amine/proton antiporters required for vesicular accumulation and regulated exocytotic secretion of monoamines and acetylcholine. *Pflugers Arch* **447:** 636-640.

Ellison G, Eison MS, Huberman HS and Daniel F (1978) Long-term changes in dopaminergic innervation of caudate nucleus after continuous amphetamine administration. *Science* **201:** 276-278.

Elsworth JD and Roth RH (1997) Dopamine synthesis, uptake, metabolism, and receptors: relevance to gene therapy of Parkinson's disease. *Exp Neurol* **144:** 4-9.

Erickson JD, Eiden LE, and Hoffman BJ (1992) Expression cloning of a reserpine-sensitive vesicular monoamine transporter. *Proc Natl Acad Sci USA* **89:** 10993-10997.

Erickson JD, Schafer MK, Bonner TI, Eiden LE and Weihe E (1996) Distinct pharmacological properties and distribution in neurons and endocrine cells of two isoforms of the human vesicular monoamine transporter, *Proc. Natl. Acad. Sci. U.S.A.* **93:** 5166–5171.

Eshleman AJ, Henningsen RA, Neve KA and Janowsky A (1994) Release of dopamine via the human transporter. *Mol Pharmacol* **45:** 312-316

Eshleman AJ, Neve RL, Janowsky A, and Neve KA (1995) Characterization of a recombinant human dopamine transporter in multiple cell lines. *J Pharmacol Exp Ther* **274**, 276-83.

Eshleman, A.J., Stewart, E., Evenson, A.K., Mason, J.N., Blakely, R.D., Janowsky, A., & Neve, K.A. (1997) Metabolism of catecholamines by catechol-O-methyltransferase in cells expressing recombinant catecholamine transporters. *J Neurochem* **69**(4), 1459-66.

Eshleman AJ, Carmolli M, Cumbay M, Martens CR, Neve KA, and Janowsky A (1999) Characteristics of drug interactions with recombinant biogenic amine transporters expressed in the same cell type. *J Pharmacol Exp Ther* **289:** 877-885.

Eshleman AJ, Wolfrum K, Johnson RA, Galey KM, and Janowsky A (2002) Expression of the vesicular monoamine transporter protein in transfected HEK cells: membrane fractions. Abstract No. 343.12. Society for Neuroscience, Washington, DC.

Eyerman DJ and Yamamoto BK (2005) Lobeline attenuates methamphetamine-induced changes in vesicular monoamine transporter 2 immunoreactivity and monoamine depletions in the striatum. *J Pharmacol Exp Ther* **312:** 160-169.

Fahn S and Sulzer D (2004) Neurodegeneration and neuroprotection in Parkinson disease. *NeuroRx* **1:** 139-154.

Falkenburger BH, Barstow KL and Mintz IM (2001) Dendrodendritic inhibition through reversal of dopamine transport. *Science* **293**, 2465–2470.

Fang Y, Rønnekleiv OK (1999) Cocaine upregulates the dopamine transporter in fetal rhesus monkey brain. J Neurosci 19:8966-8978.

Feany MB, Lee S, Edwards RH & Buckley KM The synaptic vesicle protein SV2 is a novel type of transmembrane transporter. *Cell* **70**, 861–867 (1992).

Filloux F and Townsend JJ (1993) Pre- and postsynaptic neurotoxic effects of dopamine demonstrated by intrastriatal injection. *Exp Neurology* **119:** 79-88.

Finn, J.P. and R.H. Edwards (1998) Multiple residues contribute independently to differences in ligand recognition between vesicular monoamine transporters 1 and 2. *J Biol Chem* **273:** 3943-3947.

Fleckenstein A, Metzger R, Wilkins D, Gibb J and Hanson G (1997) Rapid and reversible effects of methamphetamine on dopamine transporters, *J. Pharmacol. Exp. Ther.* **282:** 834–838.

Fon EA, Pothos EN, Sun BC, Killeen N, Sulzer D and Edwards RH (1997) Vesicular transport regulates monoamine storage and release but is not essential for amphetamine action. *Neuron* **19**:1271-1283.

Fon EA and Edwards RH (2001) Molecular mechanisms of neurotransmitter release. *Muscle Nerve* **24:** 581-601.

Fumagalli F, Gainetdinov RR, Wang YM, Valenzano KJ, Miller GW and Caron MG (1999) Increased methamphetamine neurotoxicity in heterozygous vesicular monoamine transporter 2 knock-out mice. *J Neurosci* **19:** 2424-2431.

Fung YK and Uretsky NJ (1982) The importance of calcium in the amphetamine-induced stimulation of dopamine synthesis in mouse striata in vivo, *J. Pharmacol. Exp. Ther.* **223:** 477–482.

Ganzini L, Walsh JR and Millar SB (1993) Drug-induced depression in the aged. What can be done? *Drugs Aging* **3:** 147-158.

Giros B, Jaber M, Jones SR, Wightman RM and Caron MG (1996) Hyperlocomotion and indifference to cocaine and amphetamine in mice lacking the dopamine transporter. *Nature* **379:** 606-612.

Giros B, Wang YM, Suter S, McLeskey SB, Pifl C and Caron MG (1994) Delineation of discrete domains for substrate, cocaine and tricyclic antidepressant interactions using chimeric dopamine-norepinephrine transporters. *J Biol Chem* **269:** 15985-15988.

Gonzalez AM, Walther D, Pazos A and Uhl G (1994) Synaptic vesicular monoamine transporter expression: distribution and pharmacologic profile. *Mol Brain Res* **22:** 219-226.

Grace, A. A. (2000) The tonic/phasic model of dopamine system regulation and its implications for understanding alcohol and psychostimulant craving. *Addiction* **95**, S119-28.

Gu H, Wall SC and Rudnick G (1994) Stable expression of biogenic amine transporters reveals differences in inhibitor sensitivity, kinetics, and ion dependence. *J Biol Chem* **269:** 7124-7130.

Gulley JM, Doolen S and Zahniser NR (2002) Brief, repeated exposure to substrates down-regulates dopamine transporter function in *Xenopus* oocytes in vitro and rat dorsal striatum in vivo. *J. Neurochem.* **83:** 400–411.

Guo N, Hwang DR, Lo ES, Huang YY, Laruelle M and Abi-Dargham A (2003) Dopamine deletion and in vivo binding of PET D1 receptor radioligands: implications for imaging studies in schizophrenia. *Neuropsychopharmacology* **28:** 1703-1711.

Guttman E and Sargeant W (1937) Observations on Benzedrine. *Br Med J* **1937:** 103-1015.

Hallinan R, Byrne A, Amin J and Dore GJ (2005) Hepatitis C virus prevalence and outcomes among injecting drug users on opiod replacement therapy. *J Gastroenterol Hepatol* **20:** 1082-1086.

Hansen JP, Riddle EL, Sandoval V, Brown JM, Gibb JW, Hanson GR and Fleckenstein AE (2002) Methylenedioxymethamphetamine decreases plasmalemmal and vesicular dopamine transport: mechanisms and implications for neurotoxicity. *J Pharmacol Exp Ther* **300:** 1093-1100.

Hanson GR, Sandoval V, Riddle E and Fleckenstein AE (2005) Psychostimulants and vesicle trafficking a novel mechanism and therapeutic implications. *Ann N Y Acad Sci* **1025:** 146-150.

Harrod SB, Dwoskin LP, Green TA, Gehrke BJ and Bardo MT (2003) Lobeline does not serve as a reinforcer in rats. *Psychopharmacology* **165:** 397-404.

Harrod SB, Dwoskin LP, Crooks PA, Klebaur JE and Bardo MT (2001) Lobeline attenuates d-methamphetamine self administration in rats. *J Pharmacol Exp Ther* **298:** 172-179.

Hastrup H, Karlin A and Javitch JA (2001) Symmetrical dimmer of the human dopamine transporter revealed by cross-linking Cys-306 at the extracellular end of the sixth transmembrane segment. *Proc Natl Acad Sci USA* **98:** 10055-10060.

Hastrup H, Sen N and Javitch JA (2003) The human dopamine transporter forms a tetramer in the plasma membrane: cross-linking of a cystein in the fourth transmembrane segment is sensitive to cocaine analogs. *J Biol Chem* **278:** 45045-45048.

Haycock JW (1993) Multiple signaling pathways in bovine chromaffin cells regulate tyrosine hydroxylase phosphorylation at Ser19, Ser31, and Ser40, *Neurochem. Res.* **18:** 15–26.

Haycock JW, Becker L, Ang L, Furukawa Y, Hornykiewicz O and Kish SJ (2003) Marked disparity between age-related changes in dopamine and other presynaptic dopaminergic markers in human striatum. *J Neurochem* **87:** 574-585.

Hersch SM, Yi H, Heilman CJ, Edwards RH and Levey AI (1997) Subecellular localization and molecular topology of the dopamine transporter in the striatum and substantia nigra. *J Comp Neurol* **388:** 211-227.

Hertting G, and Axelrod J (1961) Fate of tritiated noradrenaline at the sympathetic nerve endings. *Nature* **192:** 172-173.

Hoffman B, Mezey E, Brownstein M (1991) Cloning of a serotonin transporter affected by antidepressants. *Science* **254:**579-580.

Jaber M, Jones S, Giros B and Caron MG (1997) The dopamine transporter: a crucial component regulating dopamine transmission. *Mov Disord* **12:** 629-633.

Jones SR, Gainetdinov RR, Wightman RM and Caron MG (1998) Mechanisms of amphetamine action revealed in mice lacking the dopamine transporter. *J Neurochem* **18:** 1979-1986.

Jones SR, Joseph JD, Barak LS, Caron MG and Wightman RM (1999) Dopamine neuronal transport kinetics and effects of amphetamine. *J Neurosci* **73:** 2406-2414.

Johnson RA, Eshleman AJ, Meyers T, Neve KA, and Janowsky A (1998) [3H]substrate- and cell-specific effects of uptake inhibitors on human dopamine and serotonin transporter-mediated efflux. *Synapse* **30:** 97-106.

Junn E and Mouradian MM (2001) Apoptotic signaling in dopamine-induced cell death: the role of oxidative stress, p38 mitogen-activated protein kinase, cytochrome c and caspases. *J Neurochem* **78:** 374-383.

Kahlig KM, Binda F, Khoshbouei H, Blakely RD, McMahon DG, Javitch JA and Galli A (2005) Amphetamine induces dopamine efflux through a dopamine transporter channel. *Proc Natl Acad Sci USA* **102:** 3495-3500.

Kilbourn MR, Kuszpit K and Sherman P (2000) Rapid and differential losses of in vivo dopamine transporter (DAT) and vesicular monoamine transporter (VMAT2) radioligand binding in MPTP-treated mice. *Synapse* **35:** 250-255.

Kilty J, Lorang D, and Amara SG (1991) Cloning and expression of a cocaine-sensitive rat dopamine transporter. *Science* **254**, 578-579.

Kittner B, Brautigam M and Herken H (1987) PC12 cells: a model system for studying drug effects on dopamine synthesis and release. *Arch Int Pharmacodyn Ther* **286:** 181-194.

Knoth J, Zallakian M, Njus D (1981) Stoichiometry of H^+-linked dopamine transport in chromaffin granule ghosts. *Biochemistry* 20:6625–29

Knoth J, Peabody JO, Huettl P, and Njus D (1984) Kinetics of tyramine transport and permeation across chromaffin-vesicle membranes. *Biochemistry* **23**:2011-6.

Kopin IJ (1968) False adrenergic transmitters. *Annu Rev Pharmacol* **8:**377-394.

Krueger BK (1990) Kinetics and block of dopamine uptake in synaptosomes from rat caudate nucleus. *J Neurochem* **55:** 260-267.

Kuczenski R (1975) Effects of catecholamine releasing agents on synaptosomal dopamine biosynthesis: multiple pools of dopamine or multiple forms of tyrosine hydroxylase. *Neuropharmacology* **14:** 1–10.

Kuribara H (1997) Effects of tetrabenazine on methamphetamine-induced hyperactivity in mice are dependent on order and time-course of administration. *Pharmacol Biochem Behav* **56:** 9-14.

LaVoie MJ and Hastings TG (1999) Dopamine quinine formation and protein modification associated with striatal neurotoxicity of methamphetamine: evidence against a role for extracellular dopamine. *J Neurosci* **19:** 1484-1491.

Leitz FH and Stefano FJ (1971) The effect of tyramine, amphetamine and metaraminol on the metabolic disposition of ^{3}H-norepinephrine released from the adrenergic neuron. *J Pharmacol Exp Ther* **178:** 464–473.

Lin HC, Yu PC, Lee SD, Tsai YT, Kuo JS and Yang MC (1993) Effects of reserpine administration in two models of portal hypertension in rats. *J Hepatol* **19:** 413-417.

Lineberry TW and Bostwick JM (2006) Methamphetamine abuse: a perfect storm of complications. *Mayo Clin Proc* **81:** 77-84.

Liu Y, Peter D, Roghani A, Schuldiner S, Prive GG, Eisenberg D, Brecha N and Edwards RH (1992) A cDNA that supresses MPP^{+} toxicity encodes a vesicular amine transporter. *Cell* **70:** 539–51.

Liu, Y. & Edwards, R.H. (1997) Differential Localization of Vesicular Acetylcholine and monoamine transporters in PC12 cells, but not CHO cells. *J Cell Bio* **139,** 907-16.

Lysko, P. G., Weinstock, J., Webb, C. L., Brawner, M. E. & Elshourbagy, N. A. (1999) Identification of a small-molecule, nonpeptide macrophage scavenger receptor antagonist. *J Pharm Exp Ther* **289**, 1277-1285.

Mack F and Bonisch H (1979) Dissociation constants and lipophilicity of catecholamines and related compounds. *Naunyn Schmiedebergs Arch Pharmacol* **310:** 1-9.

Mayfield RD, Maiya R, Keller D, and Zahnizer NR (2001) Ethanol potentiates the function of the human dopamine transporter expressed in Xenopus oocytes. *J. Neurochem.* **79**, 1070-1079.

Melikian HE and Buckley KM (1999) Membrane trafficking regulates the activity of the human dopamine transporter. *J Neurosci* **19:** 7699-7710.

Menniti FS and Diliberto EJ Jr (1989) Newly synthesized dopamine as the precursor for norepinephrine synthesis in bovine adrenomedullary chromaffin cells. *J Neurochem* **53:** 890-897.

Meredith CW, Jaffe C, Ang-Lee K and Saxon AJ (2005) Implication of chronic methamphetamine use: a literature review. *Harv Rev Psychiatry* **13:** 141-154.

Merickel A, Rosandich P, Peter D and Edwards, RH (1995) Identification of residues involved in substrate recognition by a vesicular monoamine transporter. *J Biol Chem* **270:** 25798-25804.

Miller DK, Crooks PA, Zheng G, Grinevich VP, Norrholm SD and Dwoskin LP (2004) Lobeline analogs with enhanced affinity and selectivity for plasmalemma and vesicular monoamine transporters. *J Pharmacol Exp Ther* **310:** 1035-1045.

Miller, D. K., Crooks, P.A., Teng, L., Witkin, J.M., Munzar, P., Goldberg, S.R., Acri, J.B. & Dwoskin, L.P. (2001) Lobeline inhibits the neurochemical and behavioral effects of amphetamine. *J Pharmacol Exp Ther* **296**, 1023-34.

Miller GW, Gainetdinov RR, Levey AI and Caron MG (1999) Dopamine transporters and neuronal injury. *Trends Pharmacol Sci* **20:** 424-429.

Moghaddam B, Roth RH and Bunney BS (1990) Characterization of dopamine release in the rat medial prefrontal cortex as assessed by in vivo microdialysis: comparison to the striatum. *Neuroscience* **36:** 669-676.

Moriyama Y, Amakatsu K and Futai M (1993) Uptake of the neurotoxin, 4-methylphenylpyridinium, into chromaffin granules and synaptic vesicles: A proton gradient drives its uptake through monoamine transporter. *Arch Biochem Biophys* **305:** 271-277.

Mueller RA, Thoenen H and Axelrod J (1969) Increase in tyrosine hydroxylase activity after reserpine administration. *J Pharmacol Exp Ther* **169:** 74-79.

Nass R and Blakely RD (2003) The Caenorhabditis elegans dopaminergic system: opportunities for insights into dopamine transport and neurodegeneration. *Annu Rev Pharmacol Toxicol* **43:** 521-544.

Nelson N (1998) The family of Na+/Cl- neurotransmitter transporters. *J Neurochem* **71:** 1785-1803.

Nirenberg MJ, Vaughan RA, Uhl GR, Kuhar MJ and Pickel VM (1996) The dopamine transporter is localized to dendritic and axonal plasma membranes of nigrostriatal dopaminergic neurons. *J Neurosci* **16:** 436-447.

Nordahl TE, Salo R and Leamon M (2003) Neuropsychological effects of chronic methamphetamine use on neurotransmitters and cognition: a review. *J Neuropsychiatry Clin Neurosci* **15:** 317-325.

Ondo WG, Hanna PA and Jankovic J (1999) Tetrabenazine treatment for Tardive Dyskinesia: assessment by randomized videotape protocol. *Am J Psychiatry* **156:** 1279-1281.

Ossemann M, Sindic CJ and Laterre C (1996) Tetrabenazine as a cause of neuroleptic malignant syndrome. *Mov Disord* **11:** 95.

Pacholczyk T, Blakey RD and Amara SG (1991) Expression cloning of a cocaine- and antidepressant-sensitive human noradrenaline transporter. *Nature* **350:** 350-354

Paleacu D, Giladi N, Moore O, Stern A, Honigman S and Badarny S (2004) Tetrabenazine treatment in movement disorders. *Clin Neuropharmacol* **27:** 230-233.

Partilla, J.S., Dersch, C.M., Yu, H., Rice, K.R. & Rothman, R.B. (2000) Neurochemical neutralization of amphetamine-type stimulants in rat by the indatraline analog (-)-HY038. *Brain Res Bull* **53,** 821-826.

Pearl RG and Seiden LS (1976) The existence of tolerance to and cross-tolerance between d-amphetamine and methylphenidate for their effects on milk consumption and on differential-reinforcement-of-low-rate performance in the rat. *J Pharm Exp Ther* **198:** 635-647.

Peter D, Jimenez J, Liu Y, Kim J and Edwards RH (1994) The chromaffin granule and synaptic vesicle amine transporters differ in substrate recognition and sensitivity to inhibitors. *J Biol Chem* **269**:7231-7237.

Peter D, Liu Y, Sternini C, de Giorgio R, Brecha N and Edwards RH (1995) Differential expression of two vesicular monoamine transporters. *J Neurosci* **15:** 6179-88.

Peter D, Vu T and Edwards RH (1996) Chimeric vesicular monoamine transporters identify structural domains that influence substrate affinity and sensitivity to tetrabenazine. *J Biol Chem* **271:** 2979-2986.

Petzinger GM and Bressman SB (1997) A case of tetrabenazine-induced neuroleptic malignant syndrome after prolonged treatment. *Mov Disord* **12:** 246-248.

Pifl C, Drobny H, Reither H, Hornykiewicz O, and Singer EA (1995) Mechanism of dopamine-releasing actions of amphetamine and cocaine: plasmalemmal dopamine transporter versus vesicular monoamine transporter. *Mol Pharmacol* **47**, 368-73.

Pifl C and Singer EA (1999) Ion dependence of carrier-mediated release in dopamine or norepinephrine transporter-transfected cells questions the hypothesis of facilitated exchange diffusion. *Mol Pharmacol* **56:** 1047–1054.

Rao, T.S., Correa, L.D., Adams, P., Santori, E.M. & Sacaan A.I. (2003) Pharmacological characterization of dopamine, norepinephrine and serotonin release in the rat prefrontal cortex by neuronal nicotinic acetylcholine receptor agonists. *Brain Res* **990**, 203-208

Reches A, Hassan MN, Jackson V and Fahn S (1983) Lithium interferes with reserpine-induced dopamine depletion. *Ann Neurol* **13:** 671-673.

Reis DJ, Joh TH and Ross RA (1975) Effects of reserpine on activities and amounts of tyrosine hydroxylase and dopamine-beta-hydroxylase in catecholamine neuronal systems in rat brain. *J Pharmacol Exp Ther* **193:** 775-784.

Remy P, Doder M, Lees A, Turjanski N and Brooks D (2005) Depression in Parkinson's disease: loss of dopamine and noradrenaline innervation in the limbic system. *Brain* **128:** 1314-1322.

Riddle EL, Topham MK, Haycock JW, Hanson GR and Fleckenstein AE (2002) Differential trafficking of the vesicular monoamine transporter-2 by methamphetamine and cocaine. *Eur J Pharmacol* **449:** 71–74.

Robbins, A. K. & Horlick, R. A. (1998) Macrophage scavenger receptor confers an adherent phenotype to cells in culture. *Biotechniques* **25**, 240-4.

Rothman, R.B., Partilla, J.S., Baumann M.H., Dersch C.M., Carroll, F.I. & Rice, K.C. (2000) Neurochemical neutralization of methamphetamine with high-affinity nonselective inhibitors of biogenic amine transporters: a pharamcological strategy for treating stimulant abuse. *Synapse* **35,** 222-7.

Rush RA and Geffen LB (1980) Dopamine beta-hydroxylase in health and disease. *Crit Rev Clin Lab Sci* **12:** 241-277.

Sabol, K. E. & Seiden, L. S. (1998) Reserpine attenuates D-amphetamine and MDMA-induced transmitter release in vivo: a consideration of dose, core temperature and dopamine synthesis. *Brain Res* **806**, 69-78.

Saunders C, Ferrer JV, Shi L, Chen J, Merril G, Lamb ME, Leeb-Lundberg LM, Carvelli L, Javitch JA, and Galli A (2000) Amphetamine-induced loss of human dopamine transporter activity: an internalization-dependent and cocaine-sensitive mechanism. *Proc Natl Acad Sci USA* **97,** 6850-55.

Sandoval V, Riddle EL, Hanson GR and Fleckenstein AE (2003) Methylphenidate alters vesicular monoamine transport and prevents methamphetamine-induced dopaminergic deficits. *J Pharmacol Exp Ther* **304:** 1181-1187.

Scarponi M, Bernardi G and Mercuri NB (1999) Electrophysiological evidence for a reciprocal interaction between amphetamine and cocaine-related drugs on rat midbrain dopamineric neurons. *Eur J Neurosci* **11:** 593-598.

Schepers RJF, Oyler JM, Joseph JR RE, Cone EJ, Moolchan ET and Huestis MA (2003) Methamphetamine and amphetamine pharmacokinetics in oral fluid and plasma after controlled oral methamphetamine administration to human volunteers. *Clinical Chemistry* **49:** 121-132.

Scherman D and Henry JP (1984) Reserpine binding to bovine chromaffin granule membranes. Characterization and comparison with dihycrotetrabenazine binding. *Mol Pharmacol* **25:** 113-122.

Schmid JA, Schloze P, Kudlacek O, Freissmuth M, Singer EA and Sitte HH (2001) Oligomerization of the human serotonin transporter and of the rat GABA transporter 1 visualized by fluorescence resonance energy transfer microscopy in living cells. *J Biol Chem* **276:** 3805-3810.

Schmidt CJ & Gibb JW (1985) Role of dopamine uptake carrier in the neurochemical response to methamphetamine: effects of amfonelic acid. *Eur J Pharmacol* **109**, 73-80.

Schmitz, Y., Lee, C. J., Schmauss, C., Gonon, F. & Sulzer, D. (2001) Amphetamine distorts stimulation-dependent dopamine overflow: effects on D2 autoreceptors, transporters, and synaptic vesicle stores. *J Neurosci* **21**, 5916-24.

Schuldiner S, Shrivan A and Linial M (1995) Vesicular neurotransmitter transporters: from bacteria to humans. *Physiol Rev* **75:** 369-392.

Schuldiner S, Steiner-Mordoch S, Rodrigo Y, Wall SC and Rudnick G (1993) Amphetamine derivatives interact with both plasma membrane and secretory vesicle biogenic amine transporters. *Mol Pharmacol* **44**:1227-1231.

Schwartz K, Weizman A and Rehavi M (2005) The effect of psychostimulants on [(3)H]dopamine uptake and release in rat brain synaptic vesicles. *J Neural Transm* Dec. 2005 Epub.

Sesack SR, Aoki C and Pickel VM (1994) Ultrastructural localization of D2 receptor-like immunoreactivity in midbrain dopamine neurons and their striatal targets. *J Neurosci* **14:** 88-106.

Sheff, D.R., Daro, E.A., Hull, M., & Mellman, I. (1999) The receptor recycling pathway contains two distinct populations of early endosomes with different sorting functions. *J Cell Bio* **145,** 123-39.

Sievert, M. K., Thiriot, D. S., Edwards, R. H. & Ruoho, A. E. (1998) High-efficiency expression and characterization of the synaptic-vesicle monoamine transporter from baculovirus-infected insect cells. *Biochem J* **330**, 959-66.

Sitte HH, Huck S, Reither H, Boehm S, Singer E A, and Pifl C (1998) Carrier-mediated release, transport rates, and charge transfer induced by amphetamine, tyramine, and dopamine in mammalian cells transfected with the human dopamine transporter. *J Neurochem* **71**, 1289-1297.

Skalisz LL, Beijamini V, Joca SL, Vital MA, Da Cunha C and Andreatini R (2002) Evaluation of the face validity of reserpine administration as an animal model of depression—Parkinson's disease association. *Prog Neuropsychopharmacol Biol Psychiatry* **26:** 879-883.

Sonders MS, Zhu SJ, Zahniser NR, Kavanaugh MP and Amara SG (1997) Multiple ionic conductances of the human dopamine transporter: the actions of dopamine and psychostimulants. *J Neurosci* **17**:960-974.

Sulzer D, and Rayport S (1990) Amphetamine and other psychostimulants reduce pH gradients in midbrain dopaminergic neurons and chromaffin granules: a mechanism of action. *Neuron* **5**:797-808

Sulzer D, Chen TK, Lau YY, Kristensen H, Rayport S and Ewing A (1995) Amphetamine redistributes dopamine from synaptic vesicles to the cytosol and promotes reverse transport. *J Neurosci* **15**:4102-4108.

Sulzer D, Sonders MS, Poulsen NW and Galli A (2005) Mechanisms of neurotransmitter release by amphetamines: a review. *Prog Neurobiol* **75:**406-433.

Takahashi N, Miner LL, Sora I, Ujike H, Revay RS, Kostic V, Jackson-Lewis V, Przedborski S and Uhl GR (1997) VMAT2 knockout mice: heterozygotes display reduced amphetamine-conditioned reward, enhanced amphetamine locomotion, and enhanced MPTP toxicity. *Proc Natl Acad Sci USA* **94:**9938-9943.

Teng L, Crooks PA, Sonsalla PK and Dwoskin LP (1997) Lobeline and nicotine evoke [3H] overflow from rat striatal slices preloaded with [3H]dopamine: differential inihibition of synaptosomal and vesicular [3H]dopamine uptake. *J Pharmacol Exp Ther* **280:** 1432-1444.

Teng L, Crooks PA and Dwoskin LP (1998) Lobeline displaces [3H]dihydrotetrabenazine binding and releases [3H]dopamine from rat striatal synaptic vesicles: comparison with d-amphetamine. *J Neurochem* **71:** 258-265.

Thiriot DS and Ruoho AE (2001) Mutagenesis and derivation of human vesicle monoamine transporter 2 (VMAT2) cysteines identifies transporter domains involved in tetrabenazine binding and substrate transport. *J Biol Chem* **29:** 27304-27315.

Torres GE, Gainetdinov RR and Caron MG (2003) Plasma membrane monoamine transporters: structure, regulation and function. *Nature Rev Neurosci* **4:** 13-25.

Ugarte, Y. V., Rau, K. S., Riddle, E. L., Hanson, G. R. & Fleckenstein, A. E. (2003) Methamphetamine rapidly decreases mouse vesicular dopamine uptake: role of hyperthermia and dopamine D2 receptors. *Eur J Pharmacol* **472**, 165-71.

Uhl GR, (2003) Dopamine transporter: Basic science and human variation of a key molecule for dopaminergic function, locomotion, and parkinsonism. *Movement Disorders* **18:** 71-80.

Vaughn RA and Kuhar MJ (1996) Dopamine transporter ligand binding domains. Structural and functional properties revealed by limited proteolysis. *J Biol Chem* **271:** 21672-21680.

Vindis C, Seguelas MH, Bianchi P, Parini A and Cambon C (2000) Monoamine oxidase B induces ERK-dependent cell mitogenesis by hydrogen peroxide generation. *Biochem Biophys Res Commun* **271:** 181-185.

Vizi, E. S. (1998) Different temperature dependence of carrier-mediated (cytoplasmic) and stimulus-evoked (exocytotic) release of transmitter: a simple method to separate the two types of release. *Neurochem Int* **33**, 359-366.

Volz TJ and Schenk JO (2005) A comprehensive atlas of the topography of functional groups of the dopamine transporter. *Synapse* **58:** 72-94.

Von Gersdorff H and Mathews G (1994) Dynamics of synaptic vesicle fusion and membrane retrieval in synaptic terminals. *Nature* **367:** 735-739.

Wang YM, Gainetdinov RR, Fumagalli F, Xu F, Jones SR, Bock CB, Miller GW, Wightman RM and Caron MG (1997) Knockout of the vesicular monoamine transporter 2 gene results in neonatal death and supersensitivity to cocaine and amphetamine. *Neuron* **19:** 1285-1296.

Weed MR, Mackevicius AS, Kebabian J and Woolverton WL (1995) Reinforcing and discriminative stimulus effects of beta-CIT in rhesus monkeys. *Pharmacol Biochem Behav* **51:** 953-956.

Whitley J, Parsons J, Freeman J, Liu Y, Edwards RH and Near JA (2004) Electrochemical monitoring of transport by a vesicular monoamine transporter expressed in *Xenopus* oocytes. *J Neurosci Methods* **133:** 191-199.

Wilhelm CJ, Johnson RA, Lysko PG, Eshleman AJ and Janowsky A (2004) Effects of methamphetamine and lobeline on vesicular monoamine and dopamine transporter-mediated dopamine release in a cotransfected model system. *J Pharm Exp Ther* **310:** 1142-51.

Wilhelm CJ, Johnson RA, Eshleman AJ and Janowsky A (2006) Hydrogen ion concentration differentiates effects of methamphetamine and dopamine on transporter-mediated efflux. *J Neurochem* **96:** 1149-1159.

Xie T, McGann UD, Kim S, Yuan J and Ricaurte GA (2000) Effect of temperature on dopamine transporter function and intracellular accumulation of methamphetamine: implications for methamphetamine-induced dopaminergic neurotoxicity. *J Neurosci* **20**: 7838-7845.

Yamamoto B.K. & Zhu W. (1998) The effects of methamphetamine on the production of free radicals and oxidative stress. *J. Pharmacol. Exp. Ther.* **287:** 107–114.

Yang J, Hodel A and Holman GD (2002) Insulin and isoproterenol have opposing roles in the maintenance of cytosol pH and optimal fusion of GLUT4 vesicles with the plasma membrane. *J Biol Chem* **277**: 6559–6566.

Zaczek R, Culp S and De SE (1991a) Interactions of [3H]amphetamine with rat brain synaptosomes. II. Active transport. *J Pharmacol Exp Ther* **257**: 830-835.

Zaczek R, Culp S, Goldberg H, McCann DJ, De SE (1991b) Interactions of [^{3}H]amphetamine with rat brain synaptosomes. I. Saturable sequestration. *J Pharmacol Exp Ther* **257**: 820-829.

Zahniser NR and Doolen S (2001) Chronic and acute regulation of Na+/Cl- -dependent neurotransmitter transporters: drugs, substrates, presynaptic receptors, and signaling systems. *Pharmacol Ther* **92:** 21-55.